

Developmental basis of primate mandibular molar crown patterning: an endostructural perspective

by Simon Chapple

A Dissertation submitted to

The School of Anthropology and Conservation at The University of Kent, Canterbury in Partial
Fulfilment of the Requirements of the degree of Doctor of Philosophy

December 11, 2022

41,907 words, 205 pages

Dissertation Supervised By

Professor Matthew M. Skinner

and Professor Tracy Kivell

This thesis is dedicated to the memory of Jess Small

Acknowledgements

First and foremost, I would like to thank my advisor, Matt Skinner, for his unwavering support, guidance and friendship throughout my doctoral studies. Matt has supported me professionally and personally, and provided me with a wealth of opportunities to learn, grow and participate in a wide range of academic and non-academic opportunities. I would also like to thank my co-supervisor, Tracy Kivell for her support throughout this project. For access to specimens, I thank Steffen Bock and Christiane Funk of the Museum für Naturkunde, Berlin, and Tanya Smith of Griffith University, Australia. For fruitful discussions and help during the course of my doctoral studies I thank Tanya Smith, Bill Plummer, Tom Davies, Mykolas Imbrasas, and Chris Dunmore. I would like to thank Heiko Temming, Tom Davies, and all the staff at Max Planck Institute for Evolutionary Anthropology, Leipzig, Germany for their participation in the computed tomography scanning of specimens for this project. Finally, I would like to thank my family for their continued support throughout my academic and educational journey.

Abstract of Dissertation

Developmental basis of primate mandibular molar crown patterning: an endostructural perspective

As a growing number of studies have recently implicated important developmental models and mechanisms in the cusp patterning and overall crown morphology of certain mammal taxa, it was essential to assess the relevance of these processes to the primate dentition, and their potential implications to studies of primate crown morphology. In doing so, this also allowed for the assessment of current primate crown nomenclature schemes, which growing evidence has suggested may be critically flawed. This thesis focused on an examination of the enamel-dentine junction (EDJ) of lower molars in a taxonomically broad sample of primate taxa to address these two concerns. This work represents the first attempt to gain a broad perspective of crown patterning across all primates at the EDJ surface, and from this, present a more appropriate and unified assessment of cusp patterning and nomenclature that acknowledges the important developmental processes responsible for cusp expression.

The first chapter of the thesis reviewed the literature associated with studies of EDJ morphology, the recent advances in developmental biology relevant to the mammalian dentition, and the current state of the tooth crown nomenclature. Chapter 3 assessed the multiple phylogenetic and developmental components that appear to be responsible for crown patterning in mammals, and considered their application and consequence to the study of primate crown morphology. Important examples of previously unrecognized

aspects of growth are introduced here, and considered within the context of these developmental models. Chapter 4 employed geometric morphometrics to examine the covariation between accessory cusp presence and other aspects of molar crown shape in a population of macaque lower second molars, and demonstrates that while current development models used to interpret variation in cusp patterning are broadly appropriate in macaque molars, they do not explain all manifestations of accessory cusp expression. Chapter 5 focused on the first comprehensive analysis of variation in cusp patterning on mandibular molars within the major primate clades and from this assessed the applicability of the current nomenclature schemes to each clade. Results reveal numerous new patterns of lower molar accessory cusp expression in primates, and highlight the frequent discrepancies between the expected patterns of variation inferred from the current literature and the new patterns of expected variation discovered in this study. Chapter 6 provides a discussion of the broader results of this dissertation within the context of our current understanding of primate tooth crown development.

Structure of the dissertation

This thesis has been structured and designed around three distinct projects that have been prepared and organized as independent manuscripts. As such, Chapters 1-2 provide a literature review and description of the materials and methods for the thesis as a whole; acknowledging that the chapters representing manuscripts also contain specific (and overlapping) information about the study background, literature, materials and methods. Each of the manuscript chapters (i.e., Chapters 3-5) have been submitted to international journals and as of the date of submission of this dissertation are in various stages of publication/preparation. Chapter 3 is accepted with **minor revisions** at *Evolutionary Anthropology* and the revised manuscript is under review. Chapter 4 was rejected for publication at *Journal of Anatomy* due to concerns over sample size, and the manuscript is currently being supplemented with additional molars and prepared for re-submission. Chapter 5 is published in *PeerJ*. As there are discussion sections in each of the respective manuscript chapters, Chapter 6 provides a broader discussion of the dissertation as a whole.

Table of Contents

Acknowledgments	iii
Abstract	iv
Structure of the dissertation	vi
Table of Contents	vii
Chapter 1. Introduction and Literature Review	
1.1 Introduction	1
1.2. The Importance of Studying Enamel-Dentine Junction Morphology	3
1.3. Odontogenesis	5
1.4. Dental Developmental Genetics and the Role of Enamel Knots in Tooth Morphogenesis	9
1.5 The Patterning Cascade Model of Cusp Development	13
1.6. The History and Current State of Primate Tooth Crown Nomenclature	16
1.7 Concepts of Homology	21
Chapter 2: Materials and Methods	
2.1. Materials	22
2.2. Methods	24
CHAPTER 3: A Tooth Crown Morphology framework (TCMF) for interpreting the diversity of primate dentitions	
3.1. Introduction	30
3.2. Clade and region-specific tooth form	33
3.3. Relative tooth size	35
3.4. Cusp development	38
3.5. Crest formation	43
3.5.1. <i>Primary crest patterning is independent of cusp patterning</i>	44
3.5.2. <i>Trigonid and talonid crest patterning in hominoids</i>	45
3.5.3. <i>Secondary crest patterning</i>	47
3.6. Growth processes of the inner enamel epithelium	48
3.7. Amelogenesis	49
3.8. Discussion	53

3.8.1. <i>The TCMF and crown nomenclature</i>	53
3.8.2. <i>Discrete dental traits under the TCMF</i>	56
3.8.3. <i>Relevance of TCMF to other tooth types</i>	58
3.8.4. <i>Relevance of the TCMF beyond primates</i>	59
3.8.5. <i>Spatial constraints on the tooth germ</i>	60
3.9. Conclusion	61

CHAPTER 4: Testing the Patterning Cascade Model of Cusp Development in *Macaca fascicularis* mandibular molars

4.1. Introduction	72
4.2. Material and Methods	75
4.2.1. <i>Study sample</i>	75
4.2.2. <i>Scoring procedures</i>	75
4.2.3. <i>MicroCT, image filtering and tissue segmentation</i>	76
4.2.4. <i>Landmark collection and derivation of homologous landmark sets</i>	77
4.2.5. <i>Geometric morphometric analysis and visualisation of shape variation</i>	77
4.3. Results	78
4.3.1. <i>Lingual accessory cusp analysis</i>	78
4.3.2. <i>Distal accessory cusp analysis</i>	80
4.4. Discussion	81

CHAPTER 5: Primate Tooth Crown Nomenclature Revisited

5.1. Introduction	100
5.2. Materials	107
5.3. Methods	108
5.4. Results	109
5.4.1. <i>Strepsirrhini</i>	109
5.4.2. <i>Tarsiidae</i>	115
5.4.3. <i>Ceboidea</i>	116
5.4.4. <i>Cercopithecidae</i>	120
5.4.5. <i>Hominoidea</i>	124
5.5. Discussion	131

5.6. Conclusions	131
CHAPTER 6. Conclusions and Future Directions	
6.1 Thesis summary	150
6.2 Discussion	152
Bibliography	156
Appendix A. Study sample	182
Appendix B. Example of the R code used in Chapter 4	183

CHAPTER 1: Introduction, Literature Review, Materials, and Methods

1.1 Introduction

Teeth are the most durable part of the skeletal system and therefore represent a significant portion of the primate fossil record. As such, primate dental morphology plays a critical role in reconstructing the phylogenetic relationships (Wood and Abbott, 1983; Bailey, 2000; Pilbrow, 2003; Skinner et al., 2009; Singleton et al., 2011), diet (Kay, 1977; Bunn et al., 2011; Cooke, 2011), and ethology of mammalian taxa (Ungar, 2004; Seiffert et al., 2005). The occlusal surface of tooth crowns in particular often exhibits a complex and variable suite of morphological features that are extensively used in systematics, functional and comparative morphology, and the reconstruction of the evolutionary history of the primate clade. However, the use of tooth shape variability in studies of primate systematics and taxonomy deserves renewed consideration as a growing number of studies have shed light on important *developmental* mechanisms (not just phylogenetic and evolutionary trends), that contribute to the diversity seen in mammalian crown (Jernvall, Keränen and Thesleff, 2000; Jernvall and Thesleff, 2000; Salazar Ciudad and Jernvall, 2002, 2010; Järvinen et al., 2006; Renvoise et al., 2009; Tummers and Thesleff, 2009; Morita et al., 2022). While these studies provide new and revised ways to interpret morphological variation in mammals, the role of development on the morphological diversity in the primate dentition has generally been overlooked. Although this partially reflects an inability to conduct similar experimental research on human and non-human primates, issues have often been confounded by observations that are limited to the outer enamel surface (OES) of the tooth crown. Recent advances in high-resolution imaging, however, have made it possible to study the primary developmental structures of tooth crowns in sufficient detail to extract novel morphological data that can be used to answer some of these questions. Observations of enamel-dentine

junction (EDJ) crown patterning in hominoid molars have already demonstrated an added level of developmental complexity not yet widely acknowledged (Skinner et al. 2008; Martin et al. 2017), but it is not clear whether similar patterns of developmental complexity exist in other primate taxa. Currently, an incomplete understanding of the phylogenetic and developmental processes underlying dental morphology leads to ambiguity regarding the interpretation of dental variation in primate systematics. More fundamentally, it challenges the presumed homology of crown traits among primates, and raises concerns regarding the suitability of the current nomenclature system used to identify and name these dental features.

Utilising a vast database of micro-CT scanned primate dentitions, this thesis conducts qualitative and quantitative analyses of the enamel-dentine junction (or dentine surface) from a taxonomically broad sample of primate lower molars to assess the suitability of the current phylogenetic and developmental processes traditionally implicated as being responsible for tooth crown patterning. Can diversity in primate tooth morphology be confidently attributed solely to phylogenetic inheritance? Are the current developmental models responsible for crown variation in mouse molars also applicable to primate teeth, and can they explain all the types of variation present? These observations also allow for testing of the suitability of the current nomenclature system used to identify and name dental features in primates. For over a century, the study of the occlusal surface of tooth crowns has required a system of nomenclature that identifies various structures such as cusps and crests. However, over this time the current system of nomenclature has become beset by a number of problems regarding definitions of named structures, multiple names

for the same structure, and systems of terminology that attempt to broadly categorise all mammalian dentitions within one system of nomenclature. This component of the thesis has three main objectives. First, to document variation in cusp patterning within major clades of Primates. Second, to assess the applicability of the current nomenclature to each clade and to propose clade specific nomenclatures when appropriate. Third, to present an updated approach to the use of nomenclature schemes for the purpose of primate systematics.

1.2 The Importance of Studying Enamel-Dentine Junction Morphology

Despite a growing understanding of the developmental mechanisms underlying tooth formation in mammalian molars, it has been difficult to confidently attribute these same processes to the growth and development of a diverse primate tooth crown. In part, this is because many studies have been restricted to observations at the outer enamel surface, which are limited in their ability to determine the precise morphology and developmental origin of many dental crown structures. While the study of tooth germs is an invaluable way to examine the processes and stages of tooth morphogenesis (Butler, 1967), this form of experimental research is no longer possible in primates due to ethical reasons. However, as tooth shape is largely determined by the growth and folding of the inner enamel epithelium and underlying basement membrane, which is preserved as the EDJ surface thanks to the subsequent calcification of the tooth above and below the basement membrane, the EDJ conserves the original configuration of the membrane in fully developed teeth and can be considered a 'blueprint' for final crown shape. Crown novelties in mammals are thought to develop primarily from modifications that alter the shape of the oral epithelium and

mesenchyme interface (Jernvall, 2000; Butler, 1956). This suggests that any given OES phenotype is likely driven primarily by modifications at the EDJ surface. Numerous studies have provided evidence to support this statement, demonstrating that the OES is largely a reflection of the EDJ (Butler, 1956; Nager, 1960; Skinner et al. 2008, 2009). These studies also emphasise however, that variation in enamel thickness may impact the way the OES echoes the EDJ. As EDJ shape is responsible for the majority of OES shape and patterning, it is the established shape of this tissue interface that ensures functional occlusion by establishing the necessary topographical properties associated with shape, orientation, elevation, and incline etc. These properties are particularly important for primates that display a varied selection of dental form that are optimised for processing of a wide array of diets composed of differing types of materials. While the precise shape of the unworn OES reflects obvious selective dietary adaptation, the precise shape of the tooth established by the EDJ also impacts the 'secondary morphology' of tooth (Forteluis, 1985). A secondary morphology is attained through wear (i.e., 'dental sculpting'), and is considered a considerable modification to the original primary morphology. Generally, for any given diet, this secondary morphology should provide a functional improvement over the primary morphology (Ungar, 2015), but is achieved through selection acting on the primary morphology the and topographical properties previously mentioned. As such, the precise shape and patterning of the EDJ acts as the primary source of selection during *both* development and subsequent wear.

Many early attempts to conduct three-dimensional analyses of EDJ morphology employed techniques that attempted chemically remove the enamel cap (Kraus, 1952; Nager, 1960;

Corruccini, 1987; Corruccini and Holt 1989), but often suffered from potential damage to the dentine surface during the removal of adhering enamel. In a series of publications by Korenhof (1960, 1961, 1978, 1982), plaster endocasts were produced from a collection of naturally preserved enamel caps that revealed notable information regarding the correspondence between the outer enamel surface and EDJ surface. Unfortunately, this collection was the result of an extremely rare set of taphonomic processes and is not available for any other primate samples. Recent advances in high-resolution imaging techniques have, however, facilitated the non-destructive analysis of the EDJ, making it possible to study EDJ morphology in sufficient detail to extract novel morphological data in studies of human and non-human primate dentitions (Skinner, 2008; Skinner and Gunz, 2010; Skinner et al, 2010; Bailey et al., 2011; Anemone et al., 2012; Ortiz et al., 2018; Davies et al. 2019, 2021). Utilising these same methods of high-resolution micro-CT and imaging, this thesis produces three-dimensional models of the EDJ surface from a broad sample of primate lower molars. These three-dimensional images are used for the basis of qualitative and quantitative analyses conducted in Chapters 3 to 5.

1.3 Odontogenesis

While the primary focus of this thesis is on the morphology of fully formed primate molars, this section provides a review of the various stages of tooth development. It is during these latter stages of development that the folding of the inner enamel epithelium occurs, and much of the crown pattern of the tooth is established. The development of individual teeth is the result of a series of reciprocal interactions between two adjacent tissues of different embryonic origin; ectodermally-derived oral epithelium and neural crest-derived

mesenchyme (Thesleff, 2003; Tucker and Sharpe, 2004; Jernvall and Thesleff, 2012). The ectoderm is one of three primary germ layers that is formed in early embryonic development. In vertebrates, ectoderm is divided into two parts; *surface ectoderm* and the *neural crest*. Surface ectoderm gives rise to most epithelial tissue, including the skin, glands, hair, and nails. Surface ectoderm also gives rise to epithelium-derived ameloblasts, that go on to produce enamel. The vertebrate neural crest is transient population of specialized cells that also arise during the early stages of embryogenesis. Neural crest cells are multipotent mesenchymal cells that differentiate into a wide variety of cell types including neurons, glial cells, and melanocytes (Noden, 1983; Hall, 1999). Importantly, neural crest cells also have the unique ability to produce mesenchymal cells that give rise not only to most of the dental tissues, but also the periodontium. Interestingly, recombination experiments have demonstrated that other sources of epithelium and mesenchyme are unable to sustain tooth formation (Mina and Kollar, 1987; Lumsden, 1988). While the formation of the tooth is a continuous process, it is commonly divided into five stages; initiation, cap, bud, bell, and the later crown stage associated with amelogenesis and dentinogenesis. The review below briefly describes these five stages as understood through the histological analysis of human tooth germs by Ten Cate (1998) (Figure 1).

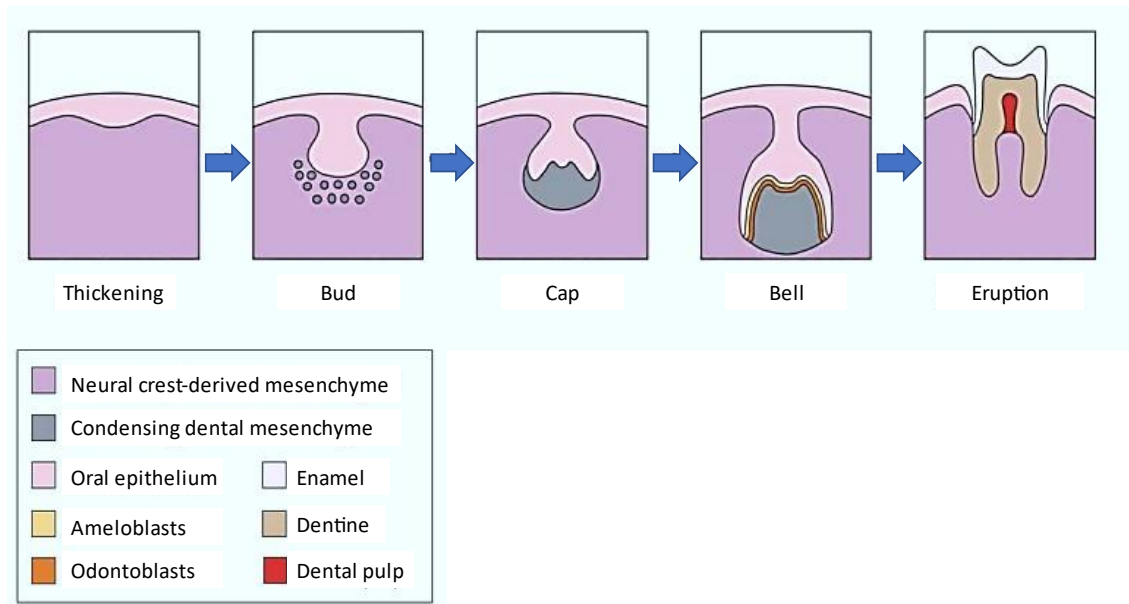


Figure 1. Stages of tooth development from the first signs of thickening during the initiation stage to tooth eruption. Adapted from Tucker and Sharpe (2004).

The initiation stage begins with the appearance of two arc-shaped epithelial thickenings, called the dental lamina, in positions that correspond to the curve and positioning of the future dental arches of the upper and lower jaws. Continued epithelial cell proliferations in the dental lamina produce localised thickenings known as dental placodes, which mark the locations of future teeth. The bud stage is a period of rapid cell proliferation that causes the oral epithelium to swell and invaginate into the underlying mesenchyme. As the mesenchyme condenses around the invaginating epithelium, a bud-like structure is formed.

In the cap stage, the epithelial tissue extends further into the mesenchyme and becomes invaginated by a condensation of mesenchymal cells. As the epithelial tissue extends

downwards, it wraps itself around the condensed mesenchyme, forming a cap-like structure. The mesenchyme cells inside the cap-shaped structure form the dental papilla, which eventually gives rise to the dentine and dental pulp of the tooth. Above this, the dental organ (or enamel organ) is formed from the dental epithelium. The dental follicle, which later gives rise to the cementum and periodontal ligament, is also comprised of peripheral mesenchymal cells and surround the dental organ and dental papilla. Collectively, these three structures constitute the tooth germ.

The early bell stage is characterised by the histodifferentiation and morphodifferentiation of the epithelial cells within the dental organ. During this stage, these epithelium cells differentiate into morphologically and functionally distinct forms: the outer enamel epithelium (located along the peripheral surface of the dental organ); the inner enamel epithelium (located over the dental papilla), the stellate reticulum (located within the dental organ and surrounded by outer and inner enamel epithelium); and the stratum intermedium (located between the stellate reticulum and the surrounding epithelium). The inner and outer enamel epithelium are continuous as the cervical loop, which marks the edge of the bell-shaped structure. It is the continued growth and folding of the inner enamel epithelium at the sites of the future cusp tips that define the overall crown pattern of the tooth (Jernvall and Thesleff, 2012).

The crown stage is characterised by the continued mineralisation of hard tissue that initiated at the end of the bell stage. This process is initiated when the mesenchymal cells of the dental papilla directly beneath the inner enamel epithelium differentiate into

odontoblasts. After the odontoblasts have begun depositing pre-dentine and dentine begins to form, the columnar cells of the inner enamel epithelium adjacent to the dentine differentiate into ameloblasts, which deposit enamel matrix over the dentine surface. Both secretion processes begin at the tip of a future cusp and progress down the cusp walls towards the future tooth root. Ameloblast differentiation ends at the tooth cervix, while the odontoblasts continue to proliferate apically to form the roots. Cementoblasts deposit cementum over the dentine of the roots, meeting the enamel at the cemento-enamel junction.

After the crown stage, the inner and outer enamel epithelium continue to grow around the dental papilla. However, they are no longer separated by stellate reticulum, and as the cervical loop continues to grow, forms the Hertwig's epithelial root sheath (HERS). The sheath grows in an apical direction and determines the final shape of the root(s). The dental papilla cells adjacent to the inner enamel epithelium and basement membrane are then induced to become odontoblasts, and subsequently form root dentine. After root dentine formation, the HERS enveloping the root become perforated, and allows dental follicle cells to contact the newly formed root dentin surface through the epithelial root sheath. The dental follicle cells subsequently differentiate into cementoblasts and form cementum. Dental follicle cells also secrete collagen fibres that are fixed into the cementum matrix and fasten the root to the surrounding jaw. As the root continues to grow, the tooth crown gradually erupts into the oral cavity to establish occlusal contact.

1.4 Dental Developmental Genetics and the Role of Enamel Knots in Tooth Morphogenesis

Advances in developmental biology and genetics have facilitated the understanding of the molecular mechanisms, genetic markers, and signalling pathways underlying tooth development in vertebrates (Jernvall and Thesleff, 2000, 2012; Tucker and Sharpe, 2004). The development of all mammalian teeth involves sequential and reciprocal interactions between the oral epithelium and the neural crest-derived mesenchyme (Soukup et al., 2008). These interactions are regulated by signalling molecules that determine when and where a tooth will form, as well as what tooth type will grow (Tucker et al., 1998; Tucker and Sharpe, 2004). Interestingly, tissue recombination, in situ hybridization, and gene knockout experiments have shown that the various stages of odontogenesis described in section 1.2 are largely mediated by many of the same molecular pathways (Jernvall and Thesleff, 2000; Tummers and Thesleff, 2009). Members of four families of signaling proteins are iteratively and reciprocally expressed in interactions between the oral epithelium and crest-derived mesenchyme; transforming growth factor (TGF), fibroblast growth factor (FGF), sonic hedgehog (Shh), ectodysplasin (Edar) and wingless-integrated (Wnt) signaling pathways. Also, many of the same transcription factors and signal receptors are repeatedly present in these interactions, including Msx1, Msx2, p21, Lef1, Pax9, Dlx2, Gli2 and Gli3 (Jernvall and Thesleff, 2000, 2012; Thesleff, 2003; Tucker and Sharpe, 2004).

While the precise molecular mechanisms associated with the earliest stages of tooth development are unclear, several studies have identified sonic hedgehog (Shh) and pituitary homeobox 2 (Pitx2) expression in the formation of dental lamina in several taxa (Keränen et al., 1999; Fraser et al., 2006; Jernvall and Thesleff, 2012). In relation to the early determination of tooth identity in the developing oral epithelium, antagonistic signalling

between FGF and BMP appear to control the expression of homeobox genes in the underlying neural-crest-derived mesenchyme that set up the presumptive incisor and molar fields of the tooth row. Discussion of presumptive tooth fields follow the proposed gradient model of Butler (1956) that suggests that concentration gradients of unspecified molecules determine the separate fields in which incisors and molars develop. This also provides evidence supporting Osborn's (1978) clone model that suggests that different populations of mesenchymal cells populated the first branchial arch give rise to incisor and molar specific mesenchymal cells. The determination of the size of these tooth fields (and therefore the number of teeth that will form in each region) involve the ectodysplasin (EDA) family of signalling molecules. When EDA receptors are disrupted in mouse embryos, the number of teeth that are formed is affected. When EDA signalling is increased, the size of the molar field expands, and a supernumerary tooth develops distal to the first molar (although it displays a reduced cusp pattern best resembling a premolar)(Tucker and Sharpe, 2004). The nested expression of FGF8, and BMP2 and BMP4, are thought to control the spatial pattern of Pax9 expression associated with the formation of the tooth bud. SHH also seems to regulate the proliferation of dental epithelial cells to produce the tooth bud, as it can be found in the tip of the epithelium that invaginates into the mesenchyme (Hardcastle et al. 1998). The dental placodes themselves express several BMP, FGF, Wnt and Shh signalling molecules, as well as the Edar receptor, which control their growth into the bud stage (Mustonen et al., 2004)

The late bud stage and early cap stage of odontogenesis is a key step in tooth development and involves several processes that are critical to defining the overall pattern of the tooth

crown. Most importantly and specifically, this involves the differential proliferation of epithelial and mesenchymal cells by epithelial signalling centres, known as enamel knots. These enamel knots are formed by non-proliferative epithelial cells and coordinate the differential growth and folding of the dental epithelium, thereby making a significant contribution to both the shape of the tooth crown base and the size and relative positioning of the individual cusps. Unsurprisingly, these signalling centres express a wealth of signalling factors, including SHH and members of the BMP, FGF and Wnt families (Tucker and Sharpe, 2004). In particular, the expression of FGFs is thought to play a critical role in the growth and folding of the enamel epithelium. In unicuspid teeth (e.g. the incisors and canines of primates), the primary enamel knot (PEK) forms at the tip of the tooth germ and gives rise to the single cusp. While high levels of apoptosis eventually cause enamel knots to disappear, in multi-cusped teeth, secondary (SEK) and tertiary (TEK) enamel knots arise shortly after the apoptotic loss of the PEK and lead to further infolding of the dental epithelium, resulting in the formation of extra cusps (Jernvall, 2000). The order of appearance of SEK is thought to closely correspond to the relative height of the individual cusps and the order in which they begin to mineralize (Jernvall and Thesleff, 2012). SEK and TEK form in a predictable sequence during the bell stage, shortly after the apoptotic removal of the PEK. While there appear to be some differences in signalling expression between PEK and SEK (including the strong expression of BMP2 during the early bell stage in PEK), both PEK and SEK express many of the same signals (Keränen et al., 1998). Interestingly, one study has shown that PEK cell movement may occur in the tooth germ and that SEK form from the non-proliferative or slowly cycling cells belonging to the PEK (Coin et al., 1999). While this suggests that not all the cells of the PEK are removed apototically, it

also poses fascinating questions for those interested in the development of these features and proper terminology used to describe them.

In multi-cusped teeth, cusp spacing appears to be controlled by the nested expression of FGF4 and BMP4. While the former acts as a cusp activator, the latter inhibits the FGF4 signal, thereby regulating the space between neighbouring cusps (Jernvall and Thesleff, 2000). *Edar* has also been implicated in the determination of cusp number in mice (Tucker and Sharpe, 2004), and in the regulation of enamel knot size. Increasing *Edar* expression levels in mouse molars has been shown to result in notable changes in cusp number, shape, and spacing (Kangas et al., 2004). In summary, tooth morphogenesis occurs through sequential and reciprocal signalling within the oral epithelium, and between the oral epithelium and underlying crest-derived mesenchyme. Many of the same transcription factors and signal receptors are repeatedly present in these interactions, and are primarily regulated by enamel knots. In signalling expression and function, these signalling centres express many of the same signals and play a key role in the final shape and patterning of the tooth crown (Jernvall and Thesleff, 2012). Collectively, these studies suggest that the cusps of a tooth crown may not be that developmentally different from each other. Subsequently, there may not be a specific gene or genetic package that is responsible for the development of each cusp (Jernvall and Jung, 2000).

1.5 The Patterning Cascade Model of Cusp Development

Inspired by some of the genetic research discussed above, Jernvall and colleagues proposed a developmental model to explain variation in cusp patterning in multi-cuspid teeth (Jernvall, 1995, 2000; Salazar-Ciudad and Jernvall, 2002). The model, known as the patterning cascade model of cusp development (PCM), argues that cusp patterning on the tooth crown is the result of a morphodynamic program regulated by the punctuated and iterative appearance of the enamel knots. Enamel knots are thought to be equivalent to the signalling centres responsible for the epithelial appendage patterning of scales, feathers, limb buds and hair follicles (Niswander and Martin 1992; Thesleff, Vaahtokari, and Partanen 1995; Thesleff and Nieminen 1996). In these examples, pattern formation is regulated and controlled by the spatial distribution of signalling centres, and a Turing-type reaction-diffusion system that involves the interaction between differentially diffusing activatory and inhibitory morphogens. While morphogens are signalling molecules, in developmental biology the term often refers to mechanisms that operate directly on cells to produce a specific cellular response that depend on morphogen concentrations. While enamel knots are critical in the cell proliferation and folding of the inner enamel epithelium, they similarly produce inhibitory proteins that prevent the formation of new enamel knots nearby, creating a spatiotemporal zone of inhibition. As such, new signalling centres can only form outside the zones of inhibition of previously formed enamel knots. Hypothetically, as enamel knots appear along the inner enamel epithelium at the sites of the future cusps, they in turn influence the potential expression of further cusps through an interplay between the timing and spacing of enamel knot initiation, and the duration of growth before mineralisation. Importantly, this suggests that the patterning of cusps is not predetermined. Instead, the size, spacing, and timing of initiation of previously-formed cusps influences the presence of later-forming cusps. This also suggests that small

perturbations in the spatiotemporal pattern of cusp formation or parameters of growth can be expected to have a potential cumulative effect on the size, shape and location of later developing cusps (Jernvall, 2000; Jernvall and Jung, 2000; Salazar-Ciudad and Jernvall, 2002).

Originally, the PCM was used to examine variation in cusp number and patterning among Lake Ladoga ringed seals (Jernvall, 2000), and as developmental programs associated with tooth formation are likely to have evolved early in mammalian evolutionary history, it can be expected that it may also explain cusp patterning in other mammal clades. In primates, the vast majority of work has been conducted on Hominidae molars, and the findings are generally consistent with the predictions made by the PCM. For example, both Kondo and Townsend (2006) and Harris (2007) showed that an accessory cusp was more likely to be present on larger molars of humans. The PCM would suggest this was due to reduced spatial constraint on SEK formation within the tooth germ. Similarly, Skinner and Gunz (2010) reported the presence of dentine horns on the distal margin of the enamel-dentine junction (EDJ) of chimpanzee mandibular molars that were consistent with PCM predictions. More recently, Ortiz et al., (2018) examined 17 living and fossil hominoid species and reported that while the majority of accessory cusp expression could be explained by the PCM, some accessory cusps pointed to potential deviations from the developmental model. Extensive research in other primate clades however, is currently lacking. Monson (2012) and Winchester (2016) noted some discordance between certain aspects of their observed morphology and a PCM-predicted morphology in Cercopithecine molars, but this has yet to be formally and extensively studied.

1.6 The History and Current State of Primate Tooth Crown Nomenclature

The current dental nomenclature used in mammalian dental morphology attempts to broadly recognise and describe features of the tooth crown based on interpretations of dental homologies and evolutionary relationships. The most widely used system of nomenclature was initially developed from Edward Drinker Cope's work on the evolution of mammalian tooth form, and Henry Fairfield Osborn's elaboration of these ideas into a functional nomenclature (Cope, 1883; Osborn, 1888). Cope described a model for the evolution and development of tribosphenic, multicuspid molars from the primitive cone-shaped teeth of mammalian ancestors. According to the model, the ancestral condition was haplodonty; a single, cone-shaped structure that Osborn (1888, 1907) called the protocone for the upper dentition, and protoconid for the lower dentition (Figure 2). Two additional cusps then developed from this cone, initially in mesial and distal orientation to the protocone(id), and were named the paracone(-id) and metacone(-id), respectively. From this triconodont configuration, Cope believed the paracone and metacone of the upper teeth migrated in a buccal direction, while the protocone moved lingually, creating a V-shaped symmetrodont configuration. In the lower molars, a similar migration of cusps was thought to have occurred. However, in this case the paraconid and metaconid rotated lingually relative to the protoconid, creating a reversed triangle configuration between upper and lower dentitions. In the quadritubercular upper molar, a fourth cusp distal to the protocone later formed on a low shelf and was named the hypocone. In the lower molars, a low shelf also formed distal to the symmetrodont triangle, from which developed the entoconid on the lingual margin, the hypoconid on the buccal margin, and the hypoconulid on the distal margin. In addition to the primary cusps of the mammalian molar, secondary features of upper and lower molars were named using the prefixes associated with their

neighbouring primary cusps, along with an appropriate suffix to denote the type of feature in question (conules or conulids for cusps, and crista or cristid for crests). An ending with -a or -id was also included in the name to denote the maxilla or mandibular arcade respectively. For crests, these names were further preceded with a pre- or post- connotation to indicate the location or 'direction' of the crest relative to the mesial-distal orientation of the tooth and associated cusp.

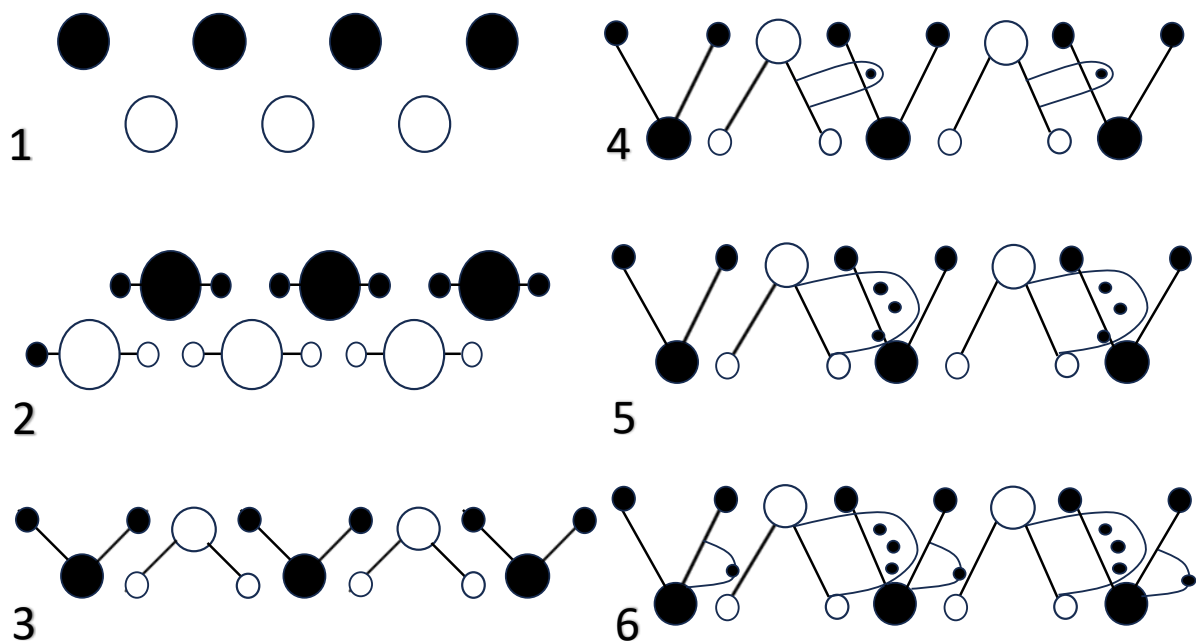


Figure 2. The Cope-Osborn model for the development of the tribosphenic molar. Adapted from Osborn (1907). Black circles represent cusps of the upper molar, and white circles represent cusps of the lower molars. The lines depict the crests connecting the primary cusps. This figure shows the transition from single cone-like structures (1), to triconodonty (2), and symmetrodonty (3). The cusps of the talonid then arrive and develop (4-5), followed by the talon (6).

Unfortunately, as researchers began to identify and study new fossil species, it became clear that some stages of evolution described by Cope and Osborn's model did not form a strict phylogenetic sequence as they had assumed. Furthermore, it is now known that multicuspid configurations developed independently in several therapsid groups, and that the cheek teeth of the earliest known mammals were not haplodont (Patterson, 1956; Butler, 1978). Ultimately, Cope and Osborn had misinterpreted cusp homologies and got the order of cusp appearance wrong. As a consequence, Osborn's nomenclature, which was originally intended to denote evolutionary processes and historical homology, was found to be flawed. Palaeontological evidence now indicates that the primitive cusp of early upper and lower molars is the mesio-buccal cone, or the paracone and protoconid of Osborn's nomenclature (Butler, 1978). Furthermore, the mesial cusp of the triconodont configuration is not the paracone seen in extant taxa, but is now recognised as the stylocone (Butler, 1978). While the metacone is still homologous with the metaconid, the other upper and lower primary cusps of the same prefix are no longer considered homologous. Such fundamental flaws in nomenclature resulted in what Hershkovitz (1971, p.95) described as the "corruption of dental evolutionary thought through use of similar terms for non-homologous upper and lower dental elements, and dissimilar terms for the homologous element(s)".

Since the introduction of Osborn's nomenclature, numerous alternative systems and names have been devised and adopted, either to address some of the known issues of homology that had been recognised in Osborn's terminology, due to a perceived better representation and corresponding description of the feature in question, or in an attempt to communicate

a structure in a way that is free of developmental implication. In some cases, this involved a substantial revision and a proposal of a new system (Vandebroek, 1961), while in other cases it simply involved the introduction of new terms as they were recognised and studied (Dalberg, 1945). In 1961, Vandebroek proposed a new system of nomenclature for tribosphenic molars that attempted to address some of the issues in Osborn's terminology (e.g., suggesting the term 'eocone' for the 'paracone', and 'epicone' for the 'protocone'). However, despite some support and use of this system in the academic literature, it was not widely accepted. A decade later, Hershkovitz (1971) proposed his revision of the nomenclature that suggested to serve as a "master plan of coronal pattern of upper and lower eutherian molars" (p. 135). This system maintained some of Osborn's terms, adopted the eocone and epicone of Vandebroek (1961), and introduced several new terms and previously unstudied dental elements. This resulted in a nomenclature that acknowledged 92 different features on the upper and lower molar crown. While several aspects of this amalgamated nomenclature were adopted, many previously proposed terms were preferred and maintained, resulting in a mosaic, interchangeable, and highly inconsistent nomenclature that varies in its use of the many positional, Osbornian, numerical, Latin, and clinical terms that currently exist.

Due to the convoluted history of the current nomenclature, the aforementioned proliferation, mixing, and multiplication of terms, and the influence that individual researchers working on particular mammalian groups has had on the current nomenclature, a number of issues should be acknowledged and addressed. First, early systems only described the basic morphologies, did so with simple descriptions or diagrams, and the

original description is often difficult to reconcile with more recent systems. Second, many nomenclatures attempt to apply their systems to taxonomically broad groups (e.g., all primates/mammals). However, while these, in principal, can allow for discourse on the evolution and homology of dental crown features across wide groups, in reality they become burdened by inconsistencies or inapplicability to the variation that is present in the groups they are applied to. For example, terminologies initially created based on observations of crown morphology of a specific clade of mammal (e.g., Gregory, 1916), may be unsuitable for all primates. Third, many of the current systems do not provide enough topographical information (both directional and positional) to ensure their accurate use (e.g., the interconulid and the varied use of this term for different morphological structures). Similarly, some systems are very complex and require the identification of a single and specific term from a diagram with many closely-positioned but distinct features (e.g., Hershkovitz's many ectostylid forms). Additionally, some terms reflect assumptions about the developmental origin of the feature and/or their association with adjacent features, when we lack direct evidence of an actual developmental link. Fourth, some systems still maintain names for features that are associated with an extinct nomenclature, such as the inappropriate use of the term eoconulid if one is not using the term eoconid for the mesio-buccal primary cusp (e.g., Vandebroek, 1961). Finally, as new terms were often introduced as direct equivalents to previously named features, authors have attempted to provide lists of current terms and synonyms that are considered equivalent. However, due to many of the factors discussed above, these synonyms are not always accurate and therefore introduce further error into the system (Swindler, 2002).

1.6 Concepts of Homology

While the current systems of nomenclature appear to be flawed, in that they were originally intended to denote evolutionary processes and historical homology, it is necessary here to discuss the concepts of homology and what is meant by 'historical homology'. While evolutionary biologists and anthropologists do not entirely agree on how to define the concept of homology, in its broadest sense, homology is a hypothesis about similarity. However, as phenotypic similarities can be the result of several related and/or unrelated events or mechanisms, there are numerous approaches to identifying and defining homology. Perhaps the most common and broadly described concept of homology is the historical approach (also known as phylogenetic homology) that adopts an explicit and simple phylogenetic definition of homology that recognises similarities that derive from common ancestry (Lieberman, 1999). Unfortunately, identifying true historical homology can be problematic if homologous features have not already been recognized and phylogenetic relationships among taxa established. An alternative approach is to integrate phylogenetic analyses with a developmental concept of homology. Developmental homology is defined as similarity through the same proximate mechanisms that generate it (Roth, 1984). As Lieberman (1999) suggests "things that resemble each other (morphological homology) because they result from common ancestry (phylogenetic homology) are likely to be similar because they grew through the same inherited processes (developmental homology)" (p.146). This approach can be problematic as it is well known that similar developmental signals and mechanisms can lead to contrasting morphological outcomes (Muller and Wagner, 1996). Furthermore, as patterns of development tend to be conserved among closely related taxa, morphological similarities can arise that are developmentally, but not phylogenetically, homologous (Shubin and Wake, 1996).

Further refining the concept of developmental homology, Lieberman (1999) suggests that one can either adopt an ontogenetic or mechanistic approach to the problem. By adopting an ontogenetic approach, the focus is on examining the ontogenetic stages associated with any given morphological similarity. If traits do not change in the same way between two or more organisms through the ontogenetic sequence, they may not be strictly homologous in a developmental sense. Unfortunately, “the sequences of developmental processes that generate morphological integration tend to be highly labile” (Lieberman, 1999, p.147), creating difficulties in confidently applying this approach. Furthermore, for studies of primate evolution, there is rarely a sufficiently complete fossil record that can document ontogenetic sequences of growth. Mechanistic homology recognises homology as morphological traits that are similar in the specific proximate developmental processes by which they grow and change. This involves studying morphological traits in terms of the specific intermediate mechanisms and processes that create phenotypic outcomes. However, as developmental similarities are likely to arise from similar processes and therefore evolve independently in more than one clade, confidently identifying mechanistic homology without prior information on phylogeny is problematic. While it is beyond the scope of this thesis to discuss in further detail which concept of homology is most appropriate for studies of primate dental morphology, it was important to describe the concept of historical homology as it is mentioned throughout.

CHAPTER 2: Materials and Methods

2.1 Materials

The complete sample of specimens used in this thesis is provided in Appendix A. The sample consists of mandibular first and second molars from 479 specimens, representing 72 primate species. These consist of 1) specimens selected, micro-CT scanned, and digitally processed specifically for this project, 2) specimens scanned for previous research projects and provided in raw tiff stack form for processing and analysis, 4) specimens that had been previously scanned and processed for previous projects but were subject to reprocessing and analysis, 5) and previously scanned and processed specimens that had adequate surface models for immediate analysis. Importantly, a number of teeth are used in multiple analyses. Many further specimens were subject to processing and analysis, but do not feature in the chapters. The study sample was selected to include species from all major clades. Sex was not considered as there is no evidence that it impacts the presence of crown morphology. Sample sizes for some species are low due to difficulties in identifying and micro-CT scanning specimens with unworn mandibular molars (this is particularly challenging as most primate species are relatively thin-enamelled). Specimens with low to moderate attrition were included as it did not impact the ability to identify particular crown features with confidence.

The majority of specimens were derived from the Museum für Naturkunde (denoted as ZMB) in Berlin, Germany and were collected during several visits. The *Pan* sample also includes a large skeletal collection housed at the Max Planck Institute for Evolutionary Anthropology in Leipzig, Germany (MPI-EVA). This collection derives from naturally deceased individuals collected within the research mandate of the Tai Chimpanzee Project based in the Tai National Park, Republic of Côte d'Ivoire. Four molars belonging to *Homo*

neanderthalensis used in the study derive from the site of El Sidron, Spain (Rosas et al., 2006) and are curated at the Museo Nacional de Ciencias Naturales (MNCN), Madrid, Spain. For Chapter 3, the sample consists of lower second molars of *Macaca fascicularis* (n=13) from the Wake Forest University Primate Centre (Winston-Salem, NC). The majority of individuals from this facility were captive, and those with signs of dental or skeletal pathology were excluded. Specimens were chosen to have relatively equal numbers of accessory cusp expression, while also restricting the sample to those individuals with relatively unworn or undamaged mandibular second molars.

2.2 Methods

As the chapters of this thesis are written in manuscript format, the methodology associated with Chapter 3 and Chapter 4 is briefly discussed under the relevant heading, including mention of any specific scoring procedures and definitions used. As Chapter 2 largely represents a more theoretically-driven article in which the specimens serve to compliment the overall discussion, there is no standalone methods section. This section of the thesis allows for detailed discussion of the methods and protocols associated with the processing of all specimens, including those utilised in Chapter 2. This involves discussion regarding the processes associated with EDJ imaging, including micro-computed tomography, image filtering, and tissue segmentation. This section also provides a more detailed discussion of the geometric morphometric analysis conducted in Chapter 3.

Micro-computed Tomography

Specimens were scanned by colleagues and technicians on a number of different microCT systems. These include the beamline ID 19 at the European Synchrotron Radiation Facility (ESRF, Grenoble, France), a BIR ACTIS 225/300 or SkyScan 1172 microtomographic scanner at the Department of Human Evolution, Max Planck Institute for Evolutionary Anthropology, and a X-Tek HMXST 225 CT or Nikon Corporation X-Tek XT H225 CT at the Harvard University Centre for Nanoscale Systems, US. Scanning was conducted under standard operating conditions (current, energy, and metallic filters) following established protocols (Olejniczak et al. 2007; Feeney et al. 2010; Smith et al. 2012; Kato et al. 2004). Due to the significant cranial and mandibular size differences across all specimens, scan resolution varied between 10 and 60 microns. The choice of scan resolution was dictated by overall tooth size with the teeth of smaller primates being scanned at <20 microns, medium-sized primates at 20-35 microns and only the largest teeth (e.g., *Gorilla*) scanned at 35-60 microns. For the very smallest of crown features insufficient scan resolution can make it difficult to assess their presence and morphology. In such instances, these teeth were excluded from analysis. Voxel sizes for the *Macaca fascicularis* mandibles associated with chapter 2 ranged between 17 and 28 cubic microns.

Image filtering and Tissue Segmentation

After individual molars of interest had been identified and cropped, image stacks were then filtered using a 3D mean-of-least-variance filter. This process sharpens the boundaries between tissue types by assigning pixels at intermediate gray-scale values present at tissue interfaces to the appropriate tissue. For the focus of this study, sharpening the boundaries between tissue types allows for a clearer segmentation of enamel and dentine (Schulze and

Pearce, 1994). While filtering image stacks technically alters the original data, Skinner (2008) demonstrated that this process has minimal influence on EDJ shape as captured by landmark data and qualitative observation. All dentitions scanned for this project, specimens scanned at the European Synchrotron Radiation Facility, and all *Macaca fascicularis* molars were filtered with a kernel size of 1 using MIA open source software (Wollny et al. 2013). Molars that had previously been processed and were considered suitable for this project were filtered using a kernel size between 1 and 3. Using a kernel size of 3 is necessary to reduce the need for significant amounts of manual segmentation where the contrast between tissue types is low.

Filtered image stacks were imported into Avizo 6.3 for segmentation. Enamel and dentine was segmented using a seed growing watershed algorithm employed via a custom Avizo plugin that separates voxels based on grayscale values. After segmentation, the EDJ was reconstructed as a triangle-based surface model. After segmentation, triangle-based surface models of the EDJ were produced using the generate surface module and then saved in polygon file format (.ply), using the unconstrained smoothing parameter in Avizo. For the qualitative analysis of EDJ shape and patterning in Chapter 2 and 4, specimens with significant damage or missing areas were included if they nevertheless demonstrated features or regions of the tooth that were of particular interest to the project. In other cases, where specimens exhibited cracks or were missing small portions of the EDJ, these defects were digitally corrected using the software Geomagic Studio 2014 (www.geomagic.com). For the *Macaca fascicularis* specimens used in Chapter 3, the accurate placement of primary dentine horn tips and marginal ridge for landmarking was

essential. As such, specimens were only included that exhibited minimal wear that could be accurately reconstructed in Geomagic Studio. This software was also used to crop the *Macaca fascicularis* accessory cusps from EDJ surface models in Chapter 3. This allowed for the complete placement of landmarks around the marginal ridge of the tooth without the influence of potentially confounding dentine horn-line features. All of the surface models used for Chapter 4 can be viewed online via the Human-Fossil-Record.org online archive (<https://human-fossil-record.org>).

Geometric Morphometric Analysis

In chapter 3, geometric morphometrics were employed to examine whether shape variation in the EDJ of *Macaca fascicularis* mandibular second molars correlated with accessory cusp presence. Initially this involved importing EDJ surface models into Avizo 6.3 to gather Cartesian coordinates for three sets of anatomical landmarks. The first set (referred to as 'EDJ_MAIN') were placed at the tips of the dentine horn for each primary cusp in order of protoconid (1), metaconid (2), entoconid (3), and hypoconid (4) (see Chapter 3, Fig.2). The second set (referred to as 'EDJ_RIDGE') were placed along the top of the marginal ridge running between each of the four primary dentine horns, creating a continuous set of landmarks around the basin of the tooth. The third set of landmarks (referred to as 'CEJ_RIDGE') were placed along the cementum-enamel junction (CEJ). The first landmark in this set began directly below dentine horn tip of the protoconid and proceeding towards the metaconid and around the cervix, also creating a continuous set of landmarks around the tooth. In specimens where portions of the CEJ were missing due to cervical enamel fracture,

the location of these landmarks were estimated. Landmark datasets were then exported from Avizo as text documents (.txt).

Geometrically homologous semi-landmarks (Bookstein, 1997; Gunz et al., 2005) for the EDJ_RIDGE and CEJ_RIDGE were then derived in R from the three landmark files. This process first involves the fitting of a smooth curve through the landmarks of the EDJ and CEJ ridge using a cubic-spline function. This function ensures that the curve passes through each measured coordinate. For the EDJ_RIDGE curve, the four EDJ_MAIN landmarks were projected onto the curve, dividing it into mesial, distal, lingual, and buccal sections. From there, a fixed number of equally spaced semilandmarks were placed along the curve. Along the buccal and lingual ridges of the EDJ_RIDGE curve 18 landmarks were placed, while 12 landmarks were placed along the shorter mesial and distal ridges. The CEJ_RIDGE had a single set of 30 landmarks that surrounded the CEJ. The number of semilandmarks along each curve was chosen to reflect the general length of each section, and ensure that shape variation was fully captured. While the EDJ_MAIN landmarks remain fixed, the landmarks attributed to the EDJ_RIDGE and CEJ_RIDGE were allowed to slide along their respective curves to minimise the bending energy of the thin-plate spline interpolation function calculated between each molar and the Procrustes average for the sample (Gunz et al., 2005, Gunz and Mitteroecker, 2013). It is this sliding process that renders the landmarks geometrically homologous.

The homologous set of landmarks and semilandmarks were then converted into shape coordinates by Generalized Least Squares Procrustes superimposition (Gower, 1975; Rohlf

and Slice, 1990). This eliminates information about the location and orientation of the raw coordinates and standardizes each specimen to unit centroid size; a size-measure computed as the square root of the sum of squared Euclidean distances from each landmark to the specimen's centroid (Dryden and Mardia, 1998). A principle components analysis (PCA) was conducted using the Procrustes coordinates of each specimen in shape space. This creates a set of hypothetical variables (known as principal components) that are linear combinations of the original variables. Beginning with the first component, it produces orthogonal axes which represent the primary components of shape variation (Hammer and Harper, 2006). This was conducted on three different sets of EDJ landmarks for both the LAC and DAC: a complete analysis including the EDJ and CEJ landmarks, a marginal ridge analysis that excluded the CEJ and only consisted of EDJ_MAIN and EDJ_RIDGE landmarks, and an isolated ridge analysis that only included the ridge landmarks between the two dentine horns where the accessory cusp is found (isolated distal ridge between the hypoconid and entoconid for the DAC analysis, and isolated lingual ridge between the metaconid and entoconid for the LAC analysis). 2D and 3D PCA plots (whole tooth, marginal ridge, and isolated ridge) were generated to visualize variation in EDJ shape between the 'Present' and 'Absent' groups. Wireframe models were then used to visualise the shape changes along the first two principle components. Shape changes in the wireframes provided were exaggerated to display the shape of a hypothetical specimen occupying the extreme ends of each principle component, and were depicted as two standard deviations from the mean. The size of specimens was analysed using the natural logarithm of centroid size and visualised through boxplots.

CHAPTER 3: A Tooth Crown Morphology framework (TCMF) for interpreting the diversity of primate dentitions

Abstract

Variation in tooth crown morphology plays a crucial role in species diagnoses, phylogenetic inference, and the reconstruction of the evolutionary history of the primate clade. While a growing number of studies have identified developmental mechanisms linked to tooth size and cusp patterning in mammalian crown morphology, it is unclear 1) to what degree these are applicable across primates and 2) which additional developmental mechanisms should be recognized as playing important roles in odontogenesis. From detailed observations of lower molar enamel-dentine junction morphology from taxa representing the major primate clades, I outline multiple phylogenetic and developmental components responsible for crown patterning, and formulate a Tooth Crown Morphology Framework (TCMF) for the holistic interpretation of primate crown morphology. I suggest that considering this framework is crucial for the characterization of tooth morphology in studies of dental development, discrete trait analysis, and systematics.

3.1 Introduction

Teeth are the most durable part of the skeletal system and therefore represent a significant portion of the primate fossil record. As such, variation in tooth crown morphology plays a crucial role in species diagnoses, phylogenetic inference, and in the reconstruction of the evolutionary history of the primate clade. However, the use of tooth shape variability in studies of primate systematics and taxonomy deserves renewed consideration as a growing number of studies have shed light on important developmental mechanisms (not just

phylogenetic and evolutionary trends), that contribute to the diversity seen in mammalian crown morphology (Jernvall, Keränen and Thesleff, 2000; Jernvall and Thesleff, 2000; Salazar Ciudad and Jernvall, 2002, 2010; Järvinen et al., 2006; Renvoise et al., 2009; Tummers and Thesleff, 2009; Morita et al., 2022). These various studies have highlighted a complex relationship between the genotype and phenotype of the mammalian dentition (Hall, 2003; Polly, 2008), and provide new and revised ways to interpret morphological variation. In particular, these studies have demonstrated how small changes in the developmental parameters of growth can have a significant impact on variation in the morphology of molars (Jernvall, 2000; Plikus et al., 2005; Kavanagh, Evans and Jernvall, 2007; Salazar-Ciudad and Jernvall, 2010).

The two most recognized developmental models that have arisen from evolutionary developmental studies of murine dentitions and comparative studies of mammalian dentitions are the patterning cascade model of cusp development (Jernvall, 2000; Jernvall and Thesleff, 2000; Salazar-Ciudad and Jernvall, 2002, 2010; Kangas et al., 2004; Kassai et al., 2005) and the inhibitory cascade model of tooth size variation (Kavanagh, Evans and Jernvall, 2007). While a number of studies have found support for these models to explain variation in primate tooth crown morphology and metamerism size variation, they cannot account for a number of aspects of primate tooth crown morphology. For example, there are several patterns of cusp expression in primates that appear to suggest an added level of developmental complexity not yet widely acknowledged (Skinner et al., 2008; Martin et al., 2017). Additionally, these studies provide little insight into the complex patterning of *crest* morphology present among primate molar crowns. Thus, our understanding of the phylogenetic and developmental processes underlying the dental morphology used in

primate systematics is incomplete and leads to ambiguity regarding the interpretation of dental variation in primate systematics. More fundamentally, it challenges the presumed homology of crown traits among primates, and raises concerns regarding the suitability of the current nomenclature system used to identify and name these dental features.

Despite a growing understanding of the developmental mechanisms underlying tooth formation in mouse molars, it has been difficult to confidently attribute these same mechanisms to the growth and development of primate teeth. While this partially reflects an inability to conduct experimental research on human and non-human primates, this issue has often been confounded by observations of final tooth form that are limited to the outer enamel surface (OES). In part, this is because such studies are limited in their ability to determine the precise morphology and developmental origin of many dental crown structures. High-resolution imaging of the dentine surface (or enamel-dentine junction) has made it possible to study the primary developmental structures of tooth crowns in sufficient detail to extract novel morphological data that can be used to resolve some of these issues. The dentine surface preserves the morphology of the basement membrane of the developing tooth germ prior to mineralization (Nager, 1960; Krause and Jordan, 1965), and therefore represents the first stage of crown development in which many morphological features of the tooth crown appear. The value of the dentine surface for understanding the developmental basis of crown morphology has already been demonstrated by a number of previous studies (Kraus, 1952; Nager, 1960; Korenhof, 1961, 1982; Kraus and Jordan, 1965; Corruccini, 1987; Schwartz et al., 1998; Olejniczak, Martin and Ulhaas, 2004; Macchiarelli et al., 2006; Skinner et al., 2008). Utilising a vast database of micro-CT scanned primate dentitions, I conduct qualitative observations of the dentine surface from a taxonomically broad sample of primate

lower molars to assess the suitability of the current phylogenetic and developmental processes traditionally implicated as being responsible for tooth crown patterning. Can diversity in primate tooth morphology be confidently attributed solely to phylogenetic inheritance? Are the current developmental models responsible for crown variation in mouse molars also applicable to primate teeth, and can they explain all the types of variation present? From these extensive observations, and a review of the current anthropological and developmental literature, I address these concerns and introduce a new developmental framework termed the 'Tooth Crown Morphology Framework' (TCMF) for the holistic interpretation and application of tooth crown diversity in primates (Figure 1). Below I introduce each component of the framework, including some previously unrecognized aspects of growth, and provide examples of how they manifest themselves in various primate dentitions and how collectively, they are responsible for the ontogenetic process of tooth crown growth and patterning.

3.2 Clade and region-specific tooth form

The first component of the framework is the genetic base that is responsible for the clade-specific morphologies seen in the primate dentition. While clearly an important source of variation for the patterning of primate teeth itself, this combined package of genetic mechanisms establishes the region-specific (e.g., incisors, canines, premolars and molars), and clade-specific tooth shape that many of the other components of the framework are linked to. By understanding the mechanisms responsible for dental variation at this genetic level, the timing of these events relative to the other components of the framework, and the perceived limitations or constraints of these processes, considerations of other elements of

the framework can be made and deviations from expected morphologies appropriately considered.

Early theories for interpreting dental diversity and the underlying mechanisms involved in the development of specific tooth types focused on explaining the graded sequence of tooth shape in mammals. Based on early observed correlations between tooth position and shape across a wide range of mammals, Butler (1939) proposed the 'regional field' theory to explain the development of different tooth types along the dental axis. This theory suggested that all tooth primordia were initially equivalent and that tooth shape was controlled by varying gradients of signalling molecules along the first branchial arch. This model therefore suggested that tooth type was determined by extrinsic factors. Much later, Osborn (1978) proposed the 'dental clone' theory to explain serial differences in tooth patterning, suggesting that teeth develop from a single clone of cranial neural crest-derived mesenchymal cells. As these initial cells were non-equivalent for incisor, canine and molar tooth categories, they were able to form these different shaped dental series. Unlike the 'regional field' model, the clone theory suggested that tooth type was intrinsically determined. More recent progress on the mechanisms responsible for tooth patterning at the genetic level have shown temporal and spatial patterns of region-specific gene expression in the branchial arch mesenchyme that appear to specify tooth type (Sharpe, 1995; Cobourne and Mitsiadis, 2006). These genes are activated and inhibited by gradients of morphogenetic protein (BMP) and fibroblast growth factor (FGF) signalling molecules along the antero-posterior axis of the epithelium. The expression of these genes in the neural crest-derived cells are thought to define different dental clone cell populations, which contribute to the formation of new group-specific tooth types (Tucker, Matthews and Sharpe, 1998; Wakamatsu et al., 2019).

The implications of this for the dental morphologist are that we should expect to see, within a particular clade, similar crown morphology from one tooth to the next in the same regional zone, with the potential for slight variation as the 'clone signalling' is passed along the tooth row. Importantly, when we observe significant deviations from the morphologies predicted by the field and clone theories, this allows us to either return to and perhaps challenge the suitability of these models for primate dentitions, or allows us to hypothesise how other developmental factors or components of the framework may interact with these basic morphologies to create the variation observed. For the sake of simplicity here, I focus on the four patterns of morphology seen in primate lower molars (Fig. 2). While this clearly represents an incomplete representation of the diversity of basic crown morphology in primates, particularly when considering the variation in tooth form within the strepsirrhine clade, this does provide the basic expectation of tooth shape and patterning for each group that later components of the TCMF framework can interact with to create the variation we see in each taxon.

3.3 Relative tooth size

The second component of the framework is tooth size. Overall size of the mammalian dentition is undoubtedly maintained by a relatively stable genetic/phylogenetic program. Numerous studies of non-human primate dentitions have yielded estimates of heritability and genetic pleiotropy for various odontometric variables (Hlusko, Do and Mahaney, 2007; Hlusko and Mahaney, 2007, 2009; Koh et al., 2010; Hlusko, Sage and Mahaney, 2011), as well as patterns of genetic integration between antimeres, isomers, metameris, and among tooth classes (Hlusko, 2016; Hlusko et al., 2016). At the same time, developmental models have

been proposed for how the modification of dynamic developmental pathways may have influenced the evolutionary trends in postcanine tooth size seen within the mammalian dentition. In 2007, Kavanagh, Evans, and Jernvall proposed an inhibitory cascade model of tooth development based on experimental studies of mouse molars in culture. During these experiments, they found that when mouse molars were isolated from their posterior tail in vitro, the rate of initiation of the succeeding molars in the sequence was increased and resulted in larger teeth. From this, Kavanagh, Evans, and Jernvall (2007) hypothesised that relative dental proportions in mammals are established by the net balance between the level of genetic activation signalling from the mesenchyme, and molar-derived inhibitory signalling from the previously formed tooth. A key feature of the inhibitory cascade is that the changes in these competing activator/inhibitor signals should be cumulative. The model therefore predicts that the size of the second molar should account for approximately one third of the area of the molar row, and that the size of the first and third molar should follow a predictable relationship that results in either a small-to-large gradient, large-to-small pattern, or a sequence of molars of equal size. Billet and Bardin (2021) recently demonstrated in a large sample of placental species that the directionality of these molar size proportions covary with the absolute size of the molar field; large-sized species follow a small-to-large gradient from anterior to posterior, while small-sized species follow a large-to-small gradient from anterior to posterior.

In general, observations of relative molar proportions in mammalian tooth rows tend match the predictions of the inhibitory cascade model. In an analysis of 35 mammals, including several marsupials and extinct taxa, the model matched the predictions for all but a few outliers (Polly, 2007). These predictions have also been matched in a sample of Rodentia

(Labonne et al., 2012), a sample of South American ungulates (Wilson et al., 2012) and a large sample of Mesozoic and Cenozoic mammaliaforms (Halliday and Goswami, 2013). In primates specifically, studies show that most taxa conform to the inhibitory cascade model (Polly, 2007; Halliday and Goswami, 2013), and demonstrate a linear change in size with tooth position. In platyrrhines, Bernal, Gonzalez, and Perez (2013) demonstrated that relative occlusal areas were not significantly different from the size gradients predicted by the model when phylogeny was taken into account, while Schoer and Wood (2015) report similar findings among all but *Papio* from their cercopithecoid sample. Figure 3 provides examples of contrasting size gradients that are consistent with the inhibitory cascade in the lower molars of *Macaca mulatta* (cercopithecoid) and *Chiropotes satanas* (platyrrhine).

While observations of relative molar proportions in mammalian teeth tend to match the predictions of the inhibitory cascade model, it should be noted that some studies have reported strong deviations from the predictions of the model. For example, while Roseman and Delezene (2019) found that molar proportions in a sample of anthropoid primates were generally consistent with the inhibitory cascade, their hominoid and cercopithecine sample showed a significant divergence from the predictions of the model. By considering deciduous premolars however, Evans et al., (2016) showed that hominoids do actually meet the expectations of the ICM. The lower deciduous premolars showed a linear increase in size from tdp3–dp4–m1, while the permanent molars also followed the inhibitory cascade pattern, but with size decreases linearly from M1–M3. As the first molar is the largest in the row, teeth increase and decrease around this central tooth position. As such, the pattern of dp4–m1–m2 did not follow the linear pattern predicted by the inhibitory cascade. Bernal, Gonzalez, and Perez (2013) point out that while their platyrrhine molars were generally consistent with

the model, it could not explain the loss of the third molar in callitrichines. Finally, studies have suggested that the inhibitory cascade model may be limited in its ability to predict intraspecies molar size variation (Vitek, Roseman and Bloch, 2020), over-predicting aspects of within-species covariation by substantial margins (Carter and Worthington, 2016, Bermúdez de Castro et al., 2021). Boughner, Marchiori, and Packota (2021) also found no predictable patterns of molar size ratios among a sample of human molars. Whether these specific deviations relate to modifications in the ratios of activator/inhibitor signals at certain stages of growth, or represent a unique and independent contribution to molar size covariation, the model appears to be relevant for the majority of studied mammalian groups and therefore is likely to be a fundamental developmental process in the development of primate dentitions. A more recent study has also demonstrated in a sample of extant euarchontans that molar complexity may also conform to the ICM, following a linear, morphogenetic gradient along the molar row (Selig, Khalid and Silcox, 2021). As such, inclusion of these processes and concepts are a key component of the Tooth Crown Morphology Framework (TCMF), and the proper description and interpretation of primate crown size and patterning.

3.4 Cusp development

Much of what is known about the development of multicuspid teeth comes from research in experimental genetics, evolutionary morphology, and embryology, and has led to the development of models through which variability in tooth crown morphology can be interpreted. In particular, studies of developing murine teeth (Jernvall, 2000; Jernvall and Thesleff, 2000; Salazar-Ciudad and Jernvall, 2002; Kangas et al., 2004; Kassai et al., 2005), and computational modelling of mammalian tooth germs (Salazar-Ciudad and Jernvall, 2002,

2010), have shown that the mechanisms responsible for the patterning of multicuspid tooth crowns involve the punctuated and iterative appearance of embryonic signalling centres known as enamel knots. These enamel knots are thought to be equivalent to the signalling centres responsible for the epithelial appendage patterning of scales, feathers, limb buds and hair follicles (Niswander and Martin, 1992; Thesleff, Vaahtokari and Partanen, 1995; Thesleff and Nieminen, 1996).

In these examples, pattern formation is regulated and controlled by the spatial distribution of the signalling centres, and a Turing-type reaction-diffusion system that involves the interaction between differentially diffusing activatory and inhibitory morphogens. While these signalling centres have been implicated in the control of cell proliferation and folding of the inner enamel epithelium, which determines the shape and size of the tooth, they also produce proteins that inhibit the formation of new enamel knots nearby, creating a temporospatial zone of inhibition. As such, new signalling centres can only form outside the zones of inhibition of previously formed enamel knots. The primary enamel knot appears in the tooth germ at the tip of the first cusp and induces the appearance of secondary enamel knots. These secondary enamel knots appear along the inner enamel epithelium at the sites of the future cusps and, in turn, influence the potential expression of further cusps through an interplay between the timing and spacing of enamel knot initiation, and the duration of growth before the late bell stage of odontogenesis where appositional growth begins. This morphodynamic iterative process, which has been called the patterning cascade model (PCM) of cusp development, suggests that the patterning of cusps is not predetermined. Instead, the size, spacing, and timing of initiation of previously-formed cusps influences the potential presence of later-forming cusps.

Originally, the PCM was used to examine variation in cusp number and patterning among Lake Ladoga ringed seals (Jernvall, 2000), and as developmental programs associated with tooth formation are likely to have evolved early in mammalian evolutionary history, this model may also explain cusp patterning in other mammal clades. In primates, the vast majority of work has been conducted on hominid molars, and in general report findings consistent with predictions made by the PCM. In humans, Kondo and Townsend (2006) and Harris (2007) showed that the presence of an accessory cusp on the mesio-lingual aspect of the upper molars was more likely to be present on larger molars, presumably due to the reduced spatial constraint of the secondary enamel knots. Similarly, studying the dentine surface of chimpanzee lower molars, Skinner and Gunz (2010) report the presence of accessory cusps on the distal margin of the tooth crown that were generally consistent with PCM predictions. More recently, Ortiz et al. (2018) conducted similar research at the dentine surface of 17 living and fossil hominoid species, and reported that most of the diversity in accessory cusp expression in this sample could be explained by the PCM. Monson (2012) and Winchester (2016) noted some discordance between certain aspects of their observed morphology and a PCM-predicted morphology in cercopithecine molars, but this has yet to be formally and extensively studied. Extensive research in other primate clades is currently lacking.

Figure 4 provides examples of accessory dentine horns at the dentine surface from a variety of primate taxa whose presence and size could be consistent with the iterative patterning inherent in the PCM. In these examples, the positioning of the taller accessory dentine horn tip corresponds to the location of a previously present enamel knot and subsequent temporospatial zone of inhibition. Due to the size of the cusp, and the relative position on the

marginal ridge, this allows the initiation of a new enamel knot on the marginal ridge, and subsequent dentine horn. Despite these observations, support for the PCM explaining variation in accessory cusp presence in primates tends to continuously focus on particular regions of the tooth crown. For example, the distal marginal ridge of mandibular molars (i.e., the location of a cusp 6) or the mesiolingual corner of maxillary molars (i.e., the location of Carabelli's trait). Significantly less attention has been drawn to the *lack* of accessory cusp presence in other regions of the tooth crown. Recently, Bermudez de Castro et al., (2022) demonstrated that while molar size decreases in *Homo sapiens* from anterior to posterior, the absolute and relative size of the protoconid (the first cusp to appear in the developmental sequence) increases from M1 to M3. They suggest that the comparatively large zones of inhibition associated with the protoconid on the M3 may be responsible for the common reduction or disappearance of the cusps of the talonid in humans. How this interaction relates to the size and placement of the other principle cusps, remains to be determined.

While studies provide evidence in primates for how the components of the PCM may restrict or inhibit cusp formation, there are several examples of morphological patterns of expression where dentine horns are almost never observed. In 2008, Skinner et al., described variation in the position of dentine horns on the distal and lingual ridge of extant and fossil hominoid molars, and identified several distinct patterns of expression. On the distal margin, accessory dentine horns were found on the distal slope of the hypoconulid, the distal slope of the entoconid and/or in the fovea between the hypoconulid and entoconid. Similarly, on the lingual margin, Skinner et al., (2008) report the variable presence of accessory dentine horns both within the fovea between the metaconid and entoconid, and on the distal slope of the metaconid. However, accessory dentine horns are rarely seen on the mesial and distal slopes

of other primary dentine horns as might be predicted under the PCM. For example, from our extensive observations conducted on hundreds of molars representing almost all primate genera, accessory dentine horns on the mesial slope of the entoconid, the mesial slope of the hypoconid, or the distal slope of the protoconid are extremely rare. These observations remain consistent across the primate taxa in our sample despite significant variation in the height, shape, and position of the relevant primary dentine horn, and overall tooth size. Whether this relates to the impact these morphologies would have on occlusal dynamics, remains to be tested.

More generally, based on the assumption that secondary enamel knot zones of inhibition are the only constraining factor in cusp formation, it should be expected that cusps would form in the wide occlusal space of the trigonid and talonid basins. However, cusps are almost never observed in these locations in primates. Thus, there must be additional, currently unidentified, factors present in the developing tooth germ that influence where cusps (and particularly small accessory cusps) can form. I suggest that one of these factors is a developmental link between what manifests as the marginal ridge at the dentine surface and iteratively initiated enamel knots. While the marginal ridge of a tooth may display multiple closely spaced accessory cusps between two primary cusps, only a few observations of dentine horns within the occlusal basin have been made (and crucially these are often associated with abnormalities in crest patterning). Skinner et al., (2008) suggest this could be related to a highly conserved pattern of expression of inhibitory proteins such as *Sostdc1* (ectodin), which have been implicated in cusp patterning in mice (Kassai et al., 2005). Another influencing factor in accessory cusp expression that warrants further research relates to the shape of individual cusps. Evans et al., (2021) recently proposed the ‘power cascade model’

to explain the growth and shape of unicuspid teeth and individual cusps. As individual cusp shape varies significantly between primate groups, cusp shape may have some influence on the variable presence of accessory cusps in these taxa. A developmental link between cusps and crests (see also crest section below) also needs further testing in primates. It is crucial to acknowledge the hypothesized constraint on where cusps can form on the tooth crown when assessing cusp number variation linked to taxonomy, discrete dental trait variation (e.g., the concept of a 'double' cusp also discussed below), and patterns of cusp variation that could provide a functional advantage during mastication and confer fitness advantages.

3.5 Crest formation

While the mechanisms responsible for overall tooth shape and cusp formation have received considerable attention from developmental biologists and anthropologists, the mechanisms driving crest formation have received comparatively little attention. I expect that this has been due to a focus on the enamel surface, in which enamel deposition often removes or minimizes the expression of crests, and the associated difficulty in imaging the dentine surface, where crests are predominant. Current genetic research has implicated Ectodysplasin (Eda) signalling in the regulation of crests in mouse dentitions (Rodrigues et al. 2013). The vast majority of work from dental morphologists and anthropologists has focused on specific, prominent, and often unique crest morphologies in certain primate groups that were thought to convey phylogenetic information. This includes variation in the positioning and direction of the cristid obliqua in some platyrrhine and strepsirrhine clades (Swindler, 2002), the presence or absence of a lingual marginal ridge connecting the metaconid and entoconid in some strepsirrhine groups (Schwartz and Tattersall, 1985), and the presence, expression and variation seen in trigonid crest morphology in hominoids (Swindler, 2002) and middle

Pleistocene hominins (e.g. Bailey, Skinner and Hublin, 2011; Martínez de Pinillos et al., 2015). Unfortunately, while these observations at the enamel surface have been useful in gathering a broad understanding of crest morphology in primates, they are limited in their ability to assess subtle morphological variation in these features and develop hypotheses on how developmental processes or patterns of covariation may also influence the expression of these features in some clades. Based on my examination of mandibular molar dentine surface morphology I suggest that 1) primary crest patterning does not necessitate the presence of cusps and that 2) there is a meaningful developmental distinction between primary crests (those that form the marginal ridge of the crown) and secondary crest patterning (those found within the occlusal basin or beyond the marginal ridge) during odontogenesis.

3.5.1 Primary crest patterning does not necessitate the presence of cusps

Historically, the study of crests on molar crowns was based on observations at the enamel surface. In the case of thick-enamelled primates, such as humans and all fossil hominins, the marginal ridge crest that runs between dentine horns is all but invisible. This has resulted in a focus on cusps and cusp patterning. Examination of the dentine surface reveals that in all primate clades there is a primary pattern of crests on the molar crown (although it is of course, visible in the many thin-enamelled primates). Our examination across a broad sample of primate taxa demonstrates that crest patterning may not require the presence of cusps, such that within a species there can be instances of primary crests that are (and are not) interrupted, or associated with a primary cusp. Figure 5 presents molar rows of a fossil *H. sapiens* individual (Sidi Abderrahman 2) and a *Cheirogaleus major* individual (MfN 35352). In the human, the first and second molar have entoconid dentine horns on the distolingual crest, while the third molar of this individual has the crest but no entoconid. Similarly, the *C. major*

molars have a prominent marginal crest that circumscribes the crown, but no distal dentine horns. I suggest this is clear evidence that the processes of primary crest and secondary enamel knot development are somewhat independent (acknowledging the constraint the former may have on the latter discussed above). This is a similar phenomenon to the expanded talonid on, for example, hominoid mandibular fourth premolars that present a prominent distal marginal ridge at the dentine surface but no distal dentine horns.

Marginal ridge crest formation in primate molars is, I suggest, an unrecognized, but important developmental process that can interact with other components of the framework to create variation in crown morphology. I find further evidence of this in the case of incompletely formed marginal crests (Figure 6). This concept would also be consistent with incompletely formed marginal ridges on mandibular premolars (Davies et al., 2019). In addition to the marginal crests that circumscribe the crown, I also recognise the trigonid crest connecting the two mesial cusps as the result of the same primary crest patterning mechanism in most primate groups (see below for discussion of exceptions). As seen in the *Chiropotes* specimen in figure 7, a prominent middle trigonid crest separates the trigonid and talonid basin despite the comparatively small size of the mesial dentine horns. I consider it extremely unlikely that such a well-pronounced ridge represents a passive structure produced simply by cusp-induced tensions of the epithelium. Furthermore, the trigonid crest of the *Chiropotes* specimen appears to join the buccal marginal ridge distal to the protoconid, further suggesting the independent nature of these features.

3.5.2 Trigonid and talonid crest patterning in hominoids

While generally categorising trigonid crest expression in primates to what I have termed ‘primary crest patterning’, specific mention needs to be made of the variable expression of these features in hominoids. Unlike the stable expression of trigonid crests seen in the previous examples, extant hominoids such as *Pan* (Skinner et al., 2008) and middle Pleistocene hominins (Bailey, 2002; Bailey, Skinner and Hublin, 2011; Martínez de Pinillos et al., 2015) can exhibit complex and variable patterns of trigonid crest expression that have been discussed in relation to their potential taxonomic and phylogenetic significance. Some of these studies have established graded scales or typologies of observed variation to allow for the comparison of trait frequency among groups. In some cases, these have resulted in the description of up to 14 different morphological crest variants in the mesial half of *Homo* mandibular molars (e.g., Martínez de Pinillos et al., 2015). These vary from well-pronounced and continuous single crests, to specimens with weakly pronounced, incomplete, and/or multiple ridge patterned morphologies. While some of these may represent ‘true’ trigonid crests, I encourage the consideration of other developmental factors in the variable expression of these features. For example, in the trigonid crest variants presented there was also significant variation in cusp arrangement, tooth size, and tooth shape within their sample. As I have discussed previously, cusp patterning and tooth size appears to have a significant influence on discrete dental trait expression, and I suggest the same for trigonid crest patterning in hominoids. Furthermore, it is also possible that some variants of this trait may represent or be further influenced by the growth processes of the IEE discussed below. Importantly however, these features appear to be highly variable and their taxonomic and phylogenetic, and/or functional significance remain to be tested. I thus recommend exercising caution when using these features for phylogenetic analysis until an improved understanding of their developmental origin is discovered.

3.5.3 Secondary crest patterning

In addition to what I identify above as the primary crests that form the marginal ridge at the dentine surface, there are numerous examples of secondary crests that develop inside, but also outside, the occlusal basin. The most commonly cited example of these secondary crests in primate dental morphology is the protostylid (Wood and Abbott, 1983; Suwa, Wood and White, 1994; Irish and Guatelli-Steinberg, 2003; Hlusko, 2004; Guatelli-Steinberg and Irish, 2005). The protostylid has traditionally been viewed as an accessory cusp or crest on the buccal surface of the protoconid, and a remnant of the primitive buccal cingulum (Dahlberg, 1950; Turner et al., 1991). In Skinner, Wood, and Hublin's (2009) analysis of protostylid expression in early hominin taxa, they expanded this definition to include the presence of crest features along the anterior, middle, and distal portion of the buccal face of the tooth, arguing that they appear to be the result of the same developmental process. In this study, I extend these observations to non-hominoid primate molars, and report findings that agree with those of Skinner, Wood, and Hublin (2009). While in many strepsirrhine clades, a complete cingulum crest is observed along the buccal surface of the tooth, variably expressed and often incomplete crests were observed in several Old World and New World monkey taxa. Skinner et al., (2008) suggested that the presence and expression of protostylid crests in hominoids is influenced by the size, shape, and spacing of the dentine horns, and the overall size of the tooth. Additionally, it is also possible that the size of the tooth germ, the slope of the cusp surface, and direction of the dentine horn tip play a role in producing secondary crest variation. Our observations of protostylid expression in non-hominoid primates are consistent with this suggestion, and thus I distinguish these features from the primary crest patterning discussed above. Unlike the developmental mechanisms responsible for primary crest

patterning, secondary crest formation appear to reflect many of the same constraints as those imposed by secondary cusp development.

3.6 Growth processes of the inner enamel epithelium

A final point of discussion regarding crown complexity at the dentine surface points to the phenomenon of wrinkling within the occlusal basin (as seen in figure 8). Unlike the primary and secondary crest patterning described in the previous sections, this form of occlusal complexity is exclusively found in extant and fossil hominoid molars, and varies significantly in presence and patterning both within and between species. Currently it is unknown what developmental processes are responsible for this phenomenon. Kraus and Oka (1967) observed wrinkles on the dentine surface of fetal molars germs in a small sample of hominoids and suggested that they may result from rapid cell division in the inner enamel epithelium. Why rapid cell division would occur only in the occlusal basin and not on the outer surfaces of the crown is a problem worthy of consideration. It is also conceivable that the mineralisation of enamel and dentine could influence the IEE and introduce the subtle wrinkling seen in some hominoid molars, however this hypothesis may also struggle to account for the localisation of wrinkling within the occlusal basin. Butler (1956) suggested that ridges were “produced by tensions set up in the epithelium by the relative movement of cusps, owing to unequal growth or to changes in the shape of the follicle”. While this theory may account for the localisation of wrinkling within the occlusal basin, as tensions could only be established between cusps, it struggles to account for why this phenomenon is only observed in some hominoid molars and no other primate clades. While it is still unclear how these features occur, it is important to differentiate them from the primary and secondary crest patterning discussed above.

3.7 Amelogenesis

The majority of studies that have examined both the dentine surface and enamel crown of the same teeth have concluded that occlusal crown features at the OES are visible at the dentine surface (Kraus, 1952; Nager, 1960; Korenhof, 1961, 1982; Kraus and Jordan, 1965; Corruccini 1987; Schwartz et al., 1998), and that the process of enamel deposition appears to only modify the expression of crown features, instead of eliminating or producing them (Skinner et al., 2008). In 2010, Skinner et al. identified several different patterns (similar to those first identified by Nager, 1960) of contribution from dentine surface shape and enamel deposition to final external morphology. In the first pattern, enamel disposition did not appear to add or remove features observed at the dentine surface. Enamel deposition did, however, alter the surface slope of certain traits, creating broad convex cusps from much thinner dentine horns. In the second pattern, enamel deposition appeared to accentuate features already present at the dentine surface, although new features were not observed along areas of the OES that corresponded with smooth, low-complexity locations of dentine surface. The third pattern, initially reported in one *Chiropotes* specimen but since commonly observed in this study in several species of *Pithecia*, demonstrated a crenulated OES that was independent of the comparatively smooth underlying dentine surface. Importantly, Skinner et al., (2010) considered this third observation to represent a developmentally distinct process from the enamel contributions of the previous patterns.

More recently, Häkkinen et al., (2019) explored the mechanisms that could be responsible for the uneven enamel distributions overlying smooth dentine surfaces. Using horizontal micro-CT sections of pig molar as the starting point of their simulations, Häkkinen et al., (2019)

modelled enamel matrix secretion on to reconstructed dentine surface outlines as a diffusion-limited free boundary problem and as a simple geometric extrapolation. While the geometric extrapolation model assumes an excess availability of nutrients along the advancing ameloblast layer during the secretory stage of amelogenesis, a diffusion-limited secretion process model assumes an environment in which concave surfaces become increasingly exaggerated as these features extending into the nutrient-rich domain receive progressively more nutrients than the concavities. These simulations showed that diffusion-limited processes of matrix secretion accurately predicted the enamel deposition patterns observed in real pig molars, successfully reproducing the thickened enamel observed above dentine surface ridges and the deep enamel fissures on the concave sides of the cusps. In contrast, these features were lost when enamel deposition was geometrically extrapolated. Importantly, similar results were also found when simulating enamel deposition in *Homo* and *Pongo* molars, and showed how subtle features present at the dentine surface in hominoids could translate into exaggerated forms at the OES. In relation to the crenulated enamel pattern observed in several Pitheciidae species, Häkkinen et al., (2019) showed that reducing interfacial tension in their simulations increased small undulations in the ameloblast moving front, suggesting that lowered stiffness of the ameloblast layer may be responsible for the crenulated enamel seen in some taxa. While further research is needed to uncover the precise mechanisms responsible for producing crenulated enamel in certain primate taxa, the results of this simulation are consistent with previous suggestions that crenulated enamel is the result of a distinct developmental process (Figure 9).

Currently, the model of diffusion-limited enamel deposition proposed by Häkkinen et al., (2019) represents the best mechanical explanation for how small features observed at the

dentine surface in primates can transform into the altered, and often exaggerated, traits observed at the OES in primates. Collectively, both the observations made from this study and from computational modelling demonstrate that the OES is not simply an extrapolation of the dentine surface, and that the process of amelogenesis can significantly enhance, and in rare cases introduce, variation in final tooth form. This has important implications for the identification and scoring of discrete dental traits at the OES, and the homology of tooth crown features across primates. For example, our observations show that in some cases, crest features present at the dentine surface may resemble cusp-like structures at the OES due to corresponding localised thickening of enamel above these crests.

While these studies further our understanding of the potential mechanisms responsible for morphological alterations and exaggerations of the dentine surface at the OES, one final observation that deserves discussion in this section is the presence of uneven enamel deposition and subsequent cuspal growth in the *absence* of a discernible corresponding dentine horn. As seen on the distal marginal ridge of the *P. robustus* specimen in figure 9, cuspules may appear at the OES without an obvious corresponding dentine horn at the dentine surface. Although it is possible that the scan resolution of these images may hinder the visualisation of very small, but present, dentine horns in these examples, it is also worth considering whether other anatomical or developmental mechanisms may be responsible for this phenomenon. Studies examining the gross anatomy and microstructure of tooth enamel using scanning electron microscopy and histology have demonstrated numerous differences in the orientation of the enamel rods between the enamel deposited over the dentine horn and the surrounding cervical enamel (Macho, Jiang and Spears, 2003; Dean, 2004). Such variation suggests the potential for differences in localised ameloblast signalling, and as the

enamel knot is the primary signalling centre of dental development, may indicate that ameloblasts over the location of previously formed enamel knots are receiving specific growth instructions relative to the surrounding tissue. If enamel knots are responsible for variation in ameloblast behaviour along the EDJ, it may be possible that they also have the potential to provide unique cuspal growth instructions that are capable of creating cuspules at the OES without a dentine component in the form of a horn. While this provides a tentative hypothesis for the presence of OES cuspules in these specimens, a further requirement of this suggestion would be evidence of a lack of IEE folding in the presence of an enamel knot. Although many of these suggestions remain to be tested, recognition of these features in some primate taxa does provide early insights into the complex relationship between enamel knot signalling and cusp expression in the primate dentition.

In summary, I am proposing the TCMF as a means to understand and interpret crown variation based on six components: clade-specific tooth form, relative tooth size, cusp patterning, crest patterning, growth processes of the IEE, and amelogenesis. Importantly, while the framework currently acknowledges the six components described, I consider it possible that an increased understanding of the processes responsible for tooth development may reveal factors that warrant the inclusion of additional components within the framework. Currently however, I consider the components of the framework useful in understanding and describing the morphological diversity seen in primates. I suggest that adopting this framework is crucial for the proper interpretation of tooth crown morphology in studies of dental development, discrete trait analysis, odontometrics, and systematics. Furthermore, the framework contributes to a recent focus on understanding some of the developmental processes that natural selection can act upon to create the phenotypic variation seen in mammals (Gould,

1977; Oster and Alberch, 1982; Hendrikse, Parsons and Hallgrímsson, 2007). While the components of TCMF likely represent a strong constraint on crown form among mammals, it is important to acknowledge that other sources of variation may exist that allow selection to drive tooth forms to evolve into morphospaces not yet predicted by the TCMF. For example, while Navarro and Maga (2018) successfully mapped quantitative trait locus (QTL) in mice associated with the predictions of the ICM, another single QTL was found that only influenced the M3. In addition to discussions regarding the presence of morphological features at the crown surface, the current developmental hypotheses for their variable expression, and how these match with current observations at the dentine surface, the TCMF also formally acknowledges distinctive patterns of morphological *absence* in primates; the lack of morphological features where they should be expected based on the current theories of development. The TCMF has a number of implications for important aspects of dental morphology that are discussed below.

3.8 Discussion

3.8.1 The TCMF and crown nomenclature

The TCMF contributes to an understanding of how phylogenetic and developmental mechanisms, and the interplay between these factors, contribute to tooth crown patterning in primates. Despite studies highlighting the important influence of signalling interactions and developmental processes on tooth size along the tooth row, overall crown size is expected to reflect genetically determined processes and thus carry a strong phylogenetic signal. This is likewise true of the presence and topography of primary cusps, which are likely to be constrained by the sequence of cusp formation. Unlike these components of the framework, growing evidence suggests that accessory cusp expression is based on a morphodynamic

process related to the timing, spacing and size of earlier forming cusps. Thus, it is unlikely that the expression of accessory cusps in primates relates to the phylogenetic inheritance and conservation of a specific ancestral gene coded for a particular cuspule. The relatively predictable presence and expression of accessory cusps in certain primate clades likely reflects the phylogenetic influence of some of the contributory factors responsible for accessory cusp expression (i.e., tooth size and primary cusp size and position relative to the overall tooth germ). As patterning of these genetically determined contributory factors are shared among closely related primate clades, they also then share similar constraints on accessory cusp formation, resulting in predictable trends of accessory cusp expression both within and between species.

Recognizing that accessory cusps may be of limited phylogenetic value raises important considerations regarding the suitability of the current nomenclature system used to identify these dental structures (including small crests). The most widely used and established system of nomenclature for studying mammalian molars was introduced by Cope (1888) and Osborn (1888), and was based on interpretations of the origins of tritubercular mammalian molar patterns. This involved modelling the evolution of the mammalian dentition from a simple cone-shaped tooth, through the more complex forms that involved the budding and rotation of several structures along the crown surface over time. Individual cusps and associated structures were thus named in this system based on their presumed origins and relations to the original primitive tooth cone. Unfortunately, despite being intended to denote evolutionary processes and historical homology, fundamental errors associated implicit in this terminology have since been recognised, resulting in what Hershkovitz (1971) describes as the “corruption of dental evolutionary thought through use of similar terms for non-

homologous upper and lower dental elements, and dissimilar terms for the homologous element(s)". Despite the early realisation of fundamental flaws in this system, the majority of these terms are still widely used today.

Other researchers have proposed alternative systems of nomenclature, such as those of Vandebroek (1961) and Gregory (1916). The benefits associated with using these alternative terms may have related to a perceived better representation and corresponding description of the feature in question, a perceived form of homology associated with that term, or represented an attempt to communicate a structure in a way that is free of any developmental implication. However, rarely are the systems of nomenclature from which they are borrowed used in their entirety, resulting in a mosaic, interchangeable and highly inconsistent nomenclature. While I agree that the names for the primary cusps of mammalian molars are likely too entrenched in the discipline to change (Butler 1978), I suggest caution in naming accessory cusps and using them for systematics wherein there is an implicit assumption of homology between distantly related taxa. As Skinner and Gunz (2010) have previously suggested, the commonly used terms 'double C6' and 'double C7' to describe the presence of two cusps on the distal or lingual marginal ridges of lower molars also appear to be invalid and misrepresent the developmental processes that underlie the formation of these cusps. That is, under an iterative pattern it is not correct to consider additional accessory dentine horns as being a 'double' of the previously formed dentine horn (nb. I do acknowledge the formation of 'twinned' dentine horns as noted by Martin et al., 2017 whose aetiology remains poorly understood).

While Skinner and Gunz (2010) drew their conclusions from observations of hominoid molars (and specifically *Pan troglodytes*), I extend these concerns to several new primate groups, and to other examples of ‘double’ and ‘triple’ cusp expression in the literature (Hlusko, 2002; Martin et al., 2017). Of equal importance is the acknowledgement that in some primate clades, accessory cusps are extremely stable in their expression and thus appear developmentally distinct from cusps found in the same location of the crown in other primate groups. For example, while the majority of cusps found on the mesial marginal ridge of primate lower molars represent true accessory cusps (in that they are variable within species and reflect differences in primary cusp patterning and tooth germ size), the presence of a cusp mesial to the protoconid in Pitheciinae was consistently expressed in this clade in our sample. This may warrant the introduction of new terms for these features that distinguish them from traditional accessory cusps found in other taxa. Overall, I believe the TCMF is ideally suited to readdressing the issues of nomenclature that are clearly present in the discipline.

3.8.2 Discrete dental traits under the TCMF

Discrete dental trait analysis is a longstanding and useful tool for assessing evolutionary relationships among modern humans (Scott and Turner, 1997, and references therein), fossil hominins (e.g. Wood and Abbott, 1983; Bailey, 2002; Hlusko, 2004; Bailey and Lynch, 2005; Guatelli-Steinberg and Irish, 2005; Bailey and Wood, 2007), and living nonhuman primates (Johanson, 1974; Uchida, 1996; Pilbrow, 2006). Skinner et al., (2008) previously highlighted the importance of using dentine surface morphology to elucidate developmental processes responsible for the presence and variable manifestation of dental traits. I would suggest that the TCMF is also crucial to properly defining discrete dental traits, creating appropriate

scoring procedures, and using them in systematics. As noted previously, Skinner and Gunz (2010) highlighted the likely link between the patterning cascade model and cusp 6 expression in chimpanzee and bonobo molars. Similarly, Skinner, Wood, and Hublin (2009) noted that variation in protostylid expression between *Australopithecus africanus* and *Paranthropus robustus* was related to a) the relative placement of the protoconid (cusp patterning) and b) the expression and location of buccal crests (crest patterning). Shovel-shaped incisors are clearly associated with variation in crest development, while the Carabelli's cusp trait appears to be linked to placement of the protocone (cusp spacing) relative to the crown base (tooth size).

Importantly, while I aim to draw attention to the developmental factors responsible for discrete dental trait expression in primates, I am not suggesting that these features carry no heritable or genetic component, or are of no use for inferring genetic relatedness within or between closely related species. Numerous studies have successfully used discrete dental traits as a means of documenting biological relationships among human populations (Scott and Dahlberg, 1982; Scott and Turner, 1997; Durand et al., 2010), demonstrating some level of genetic influence in their expression. Rather than these features simply representing the phenotypic expression of a specific gene however, it is likely that, for many dental traits, population trends may also reflect regional differences in cusp patterning and tooth size, which themselves carry some genetic component. As such, while some phylogenetic signal may still be present within each of those variables in some form, it may not be comparable to the development of a genetically programmed cusp. This is a challenging problem as each dental feature within each species and/or population may have a differing contribution of genetic and non-genetic factors responsible for its presence and expression. Ultimately, I

emphasise that traits should be carefully considered within the components of this framework, and that caution is advised when interpreting trait expression patterns at higher taxonomic levels. Acknowledging the developmental factors responsible for discrete dental trait expression will improve the identification and scoring of these features in many cases, while in others may inform their incorporation into future phylogenetic investigations.

3.8.3 Relevance of TCMF to other tooth types

While I have formulated and presented this framework with a focus on mandibular molars, I would suggest that it is also consistent with the developmental mechanisms responsible for all other tooth types of the primate dentition. For example, at the dentine surface, incisor morphology is created by a strong single crest and often a varying number of mamelons, which I would suggest are more accurately described as dentine horns or primary and secondary enamel knots. Canines tend to be formed by a large primary cusp with mesial and distal crests, although in some taxa (e.g, lemurs) they have been incorporated into the incisor row and are incisor-like in shape. Premolars are particularly relevant for evaluating the applicability of the framework as they can be both canine-like and molar-like in their morphology. Indeed, phenotypic similarity between the premolars and molars of some primate clades suggest similarities in genetic control (perhaps due to overlapping/extending gradient fields in the dental arch) and thus similarities in the contributions of various components in the framework. Examples of this include transverse crests between mesial cusps of mandibular premolars that are likely developmentally similar to trigonid crests in mandibular molars, or distal accessory cusps on the talonid that are similar to distal dentine horns of mandibular molars. Additionally, evidence of integrative modules in dentitions of hominoids (Gomez-Robles and Polly, 2012) and baboons (Koh et al., 2010) suggests links

between premolar and molar development. It is appropriate to consider variations in morphology of each tooth type and similarities in morphology between tooth types within the context of the TCMF we have outlined.

3.8.4 Relevance of the TCMF beyond primates

It is worth considering the degree to which many (if not all) aspects of this framework are relevant to the study of non-primate mammalian dentitions. Multicuspid teeth have evolved in many vertebrate species, and although their morphological patterning may not share a strict phylogenetic relationship, the processes responsible for the development of tooth patterning appear to be highly conserved. For example, a defining feature of tooth crown patterning in mammalian dentitions appears to be the presence and expression of secondary enamel knots, and these molecular structures have been reported in mouse, vole, shrew, and ferret dentitions (Jernvall, Keränen and Thesleff 2000; Miyado et al., 2007; Järvinen et al., 2008; Järvinen, Tummars and Thesleff, 2009). Perhaps most significantly however, observations of secondary enamel knots in a species of marsupial (*Monodelphis domestica*) (Moustakas, Smith and Hlusko, 2011), suggest that all mammalian dentitions may share the same regulatory mechanisms. Furthermore, as previously discussed, the inhibitory cascade model has been generally supported in widely disparate phylogenetic clades, as well as a phylogenetically broad sample of extant and extinct mammals, suggesting that this developmental mechanism may have been established early in mammalian evolution. Importantly though, many of the studies that investigated the predictions of the patterning cascade model in tribosphenic molars also report that the model did not *consistently* explain accessory cusp expression in their entire sample, suggesting slightly different developmental pathways or additional unknown parameters in these taxa (Kozitzky and Bailey, 2019).

Whether these developmental deviations relate to the similar unknown factors responsible for unpredictable cusp expression in primate molars (and in particular the lack of accessory cusps surrounding the entoconid), remains to be determined.

3.8.5 Spatial constraints on the tooth germ

One developmental phenomenon that is not currently included in the framework is physical pressure that can be put on the developing tooth germ to influence its morphological development. It is possible that pressure could be applied by a number of anatomical structures such as large blood vessels, the cortical bone of the mandible or maxilla, or an adjacent developing tooth crown. Previous authors have hypothesised how the amount of available space in a jaw may contribute to increased tooth crown variability in third molars (Morita, Morimoto and Ohshima, 2016; Marchiori, Packota and Boughner, 2016). Skinner et al., (2017) hypothesized that a defect on the maxillary lateral incisor of an orangutang was caused by direct contact, via a fenestration in the tooth crypt, with the maxillary central incisor. The much larger and more developmentally advanced central incisor creates an indentation on the lateral incisor crown and that this close-packing of tooth germs could be caused by undergrowth of the face in orangutans. In 2017, Renvoisé et al., demonstrated from both computational modelling and cultured tooth explants that cusp positioning in mouse and vole molars may be significantly dependent on the support of the developing jaw. The vole molars in culture, which would normally display an offset cusp pattern in vivo, lost their offset arrangement. Conversely, in the mouse molars, an unnatural cusp offset pattern was achieved in the cultured molars when attached with artificial lateral constraints. While these findings have yet to be tested in primate dentitions, these studies do point to the role of surrounding tissue in the regulation of tooth shape and patterning.

3.9 Conclusion

From extensive qualitative observations from a broad sample of primate lower molars I assessed developmental processes that underlie tooth crown patterning. In addition to currently recognized processes I identify additional aspects of dental tissue development and formalize the Tooth Crown Morphology Framework (TCMF). I recommend this framework be used to understand and interpret variation in primate tooth crown morphology. As the precise developmental mechanisms responsible for several components of the framework are still unknown, it is not possible at this time to provide a strict guide on how to directly implement all these findings into studies of dental development. This was a concern addressed by several reviewers during a recent journal submission of this manuscript, but has been more recently redacted. Collective efforts need to be made into investigating and developing a better understanding of these processes, so they can be used with more confidence in the future. In the next chapter, I contribute to these collective efforts, by testing the predictions of an important component of the framework; the patterning cascade model of cusp development. Importantly, I suggest that the acknowledgement of these components and their phylogenetic and developmental basis is crucial for the holistic and cautious interpretation of tooth crown morphology in future studies of dental development, discrete trait analysis, odontometrics, and systematics. Additionally, these components, and the underlying mechanisms that have been described here, impact future considerations of crown nomenclature within this thesis.

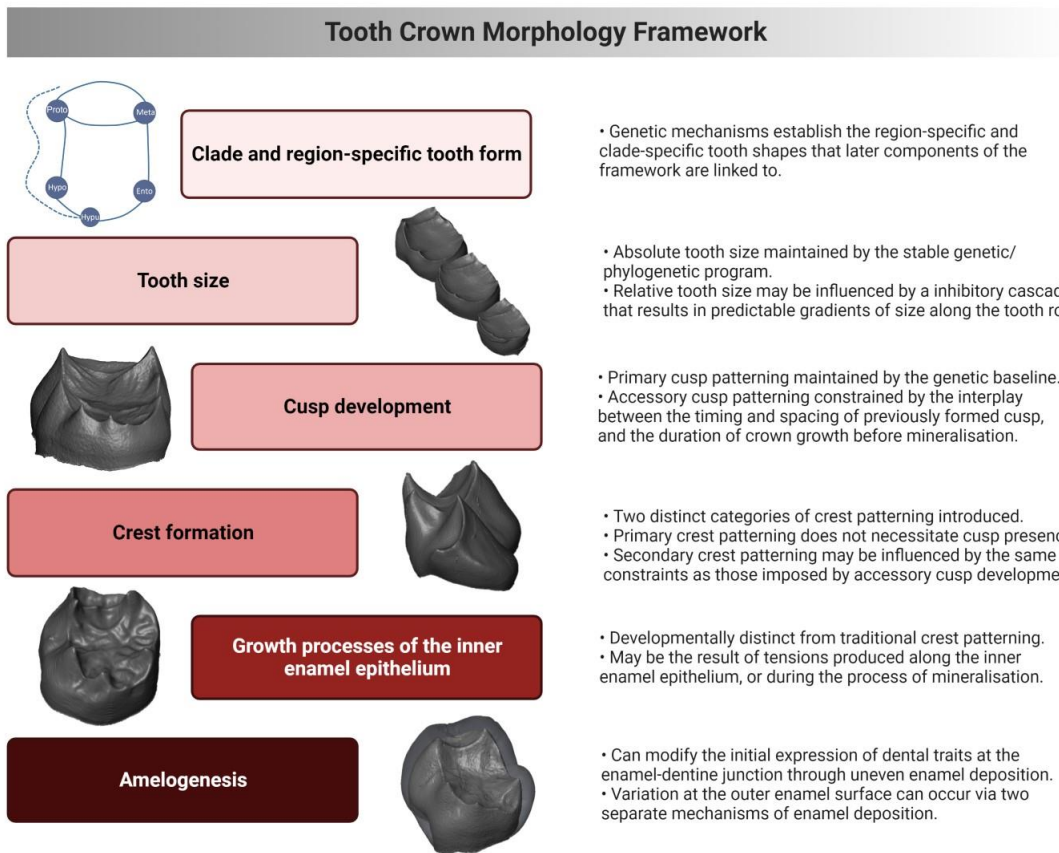


Figure 1. Schematic diagram summarizing the main components of the proposed Tooth Crown Morphology Framework (TCMF). Created with BioRender.com.

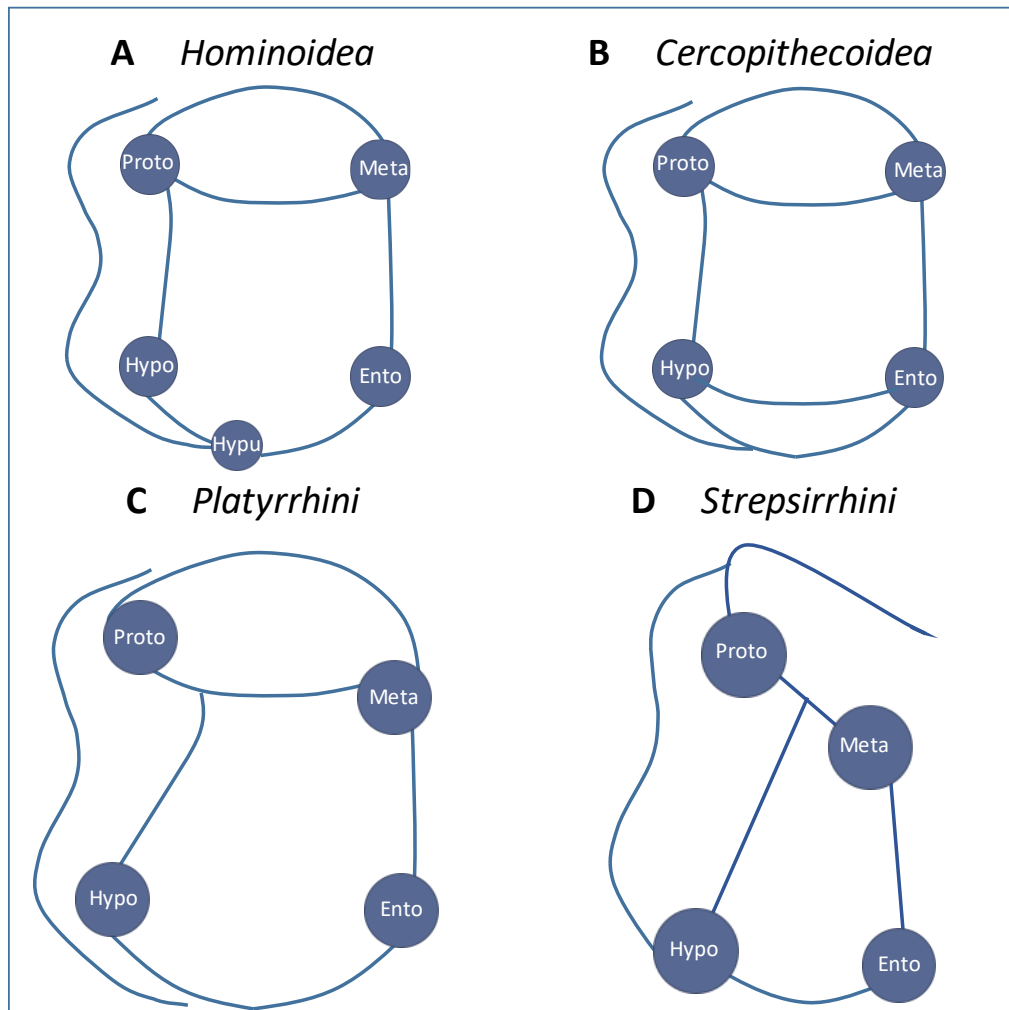


Figure 2. The basic form of molar in each clade; (A) the Y-5 molar pattern of hominoids, (B) the bilophodont pattern of cercopithecoids, (C) the 4-cusped pattern of platyrrhines, (D) and the tribosphenic pattern of the strepsirrhines.

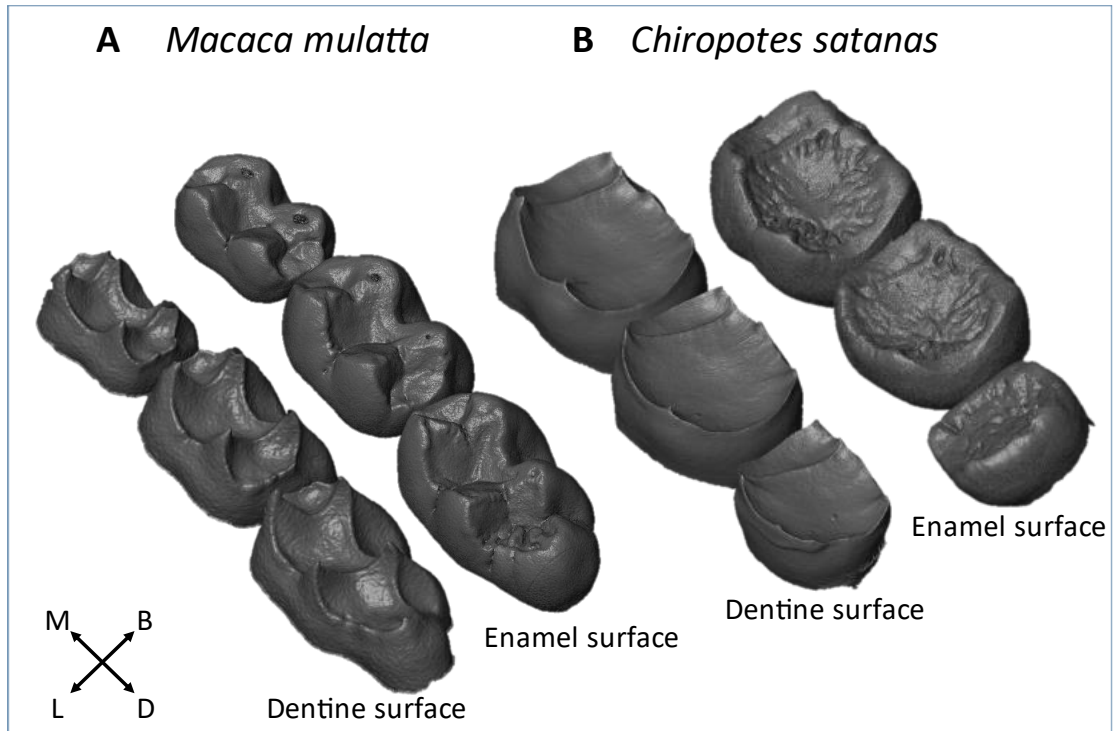


Figure 3. Tooth size gradients in a *Macaca mulatta* specimen ($M1 < M2 < M3$) and *Chiropotes satanas* specimen ($M1 > M2 > M3$). Both absolute and relative tooth size can interact with other components of the framework to influence tooth crown morphology. Images are not to scale.

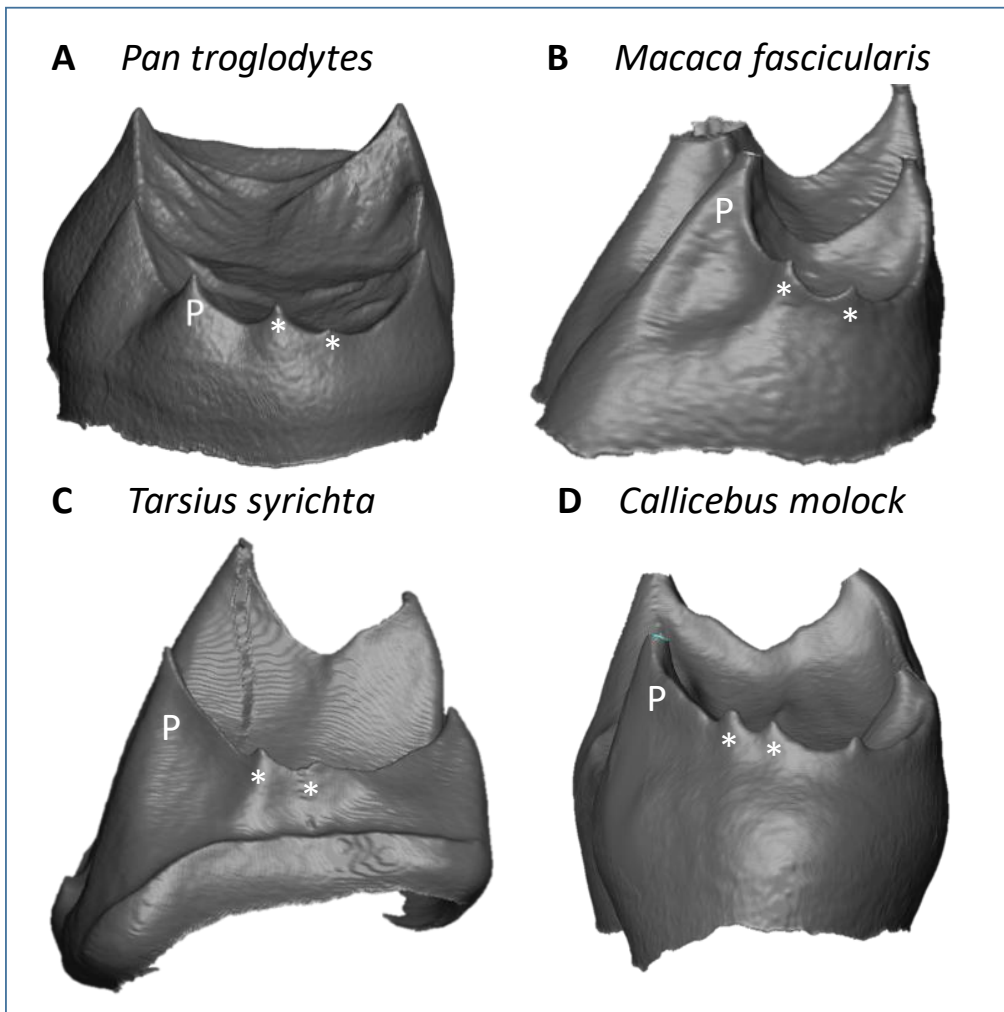


Figure 4. Examples of accessory dentine horns at the enamel-dentine junction from a variety of primate taxa, whose presence and size are consistent with the iterative patterning inherent in the patterning cascade model. Accessory dentine horns (*) form in association with a primary dentine horn (P). All represent lower second molars. Distal view. Images are not to scale.

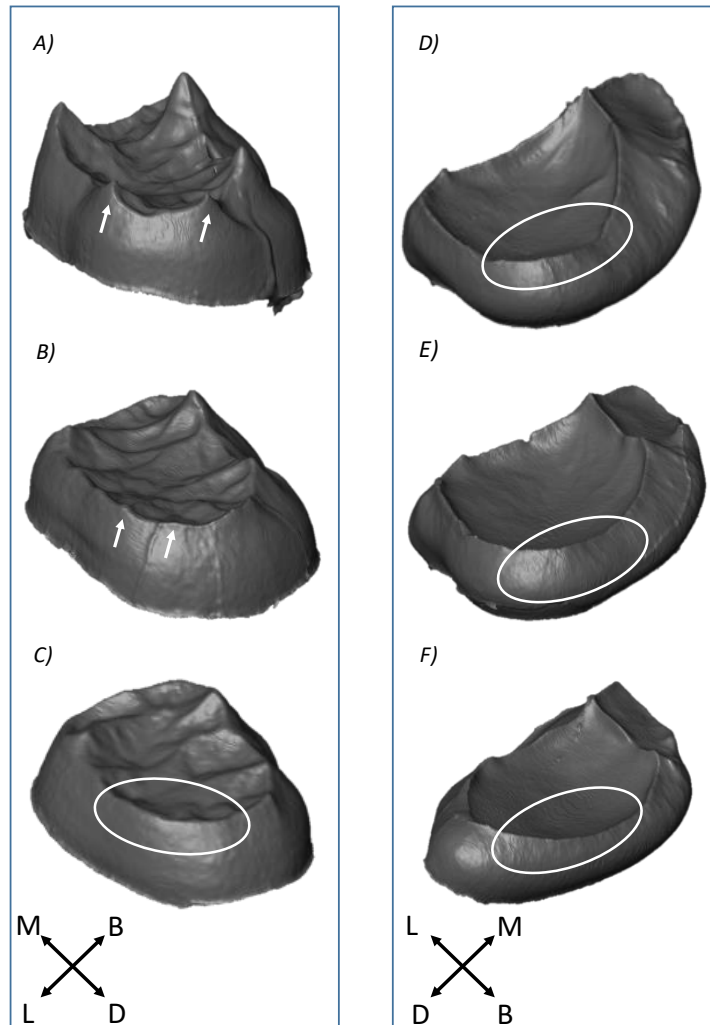


Figure 5. First (top), second (middle) and third (bottom) molars of a fossil *Homo sapiens* individual (left) and a *Cheirogaleus major* individual (right). While some primary dentine horns are present, both specimens exhibit marginal crests (white circles) without a corresponding primary cusp (white arrows). This suggests that the processes of primary crest development may not necessitate the presence of cusps. Images are not to scale.

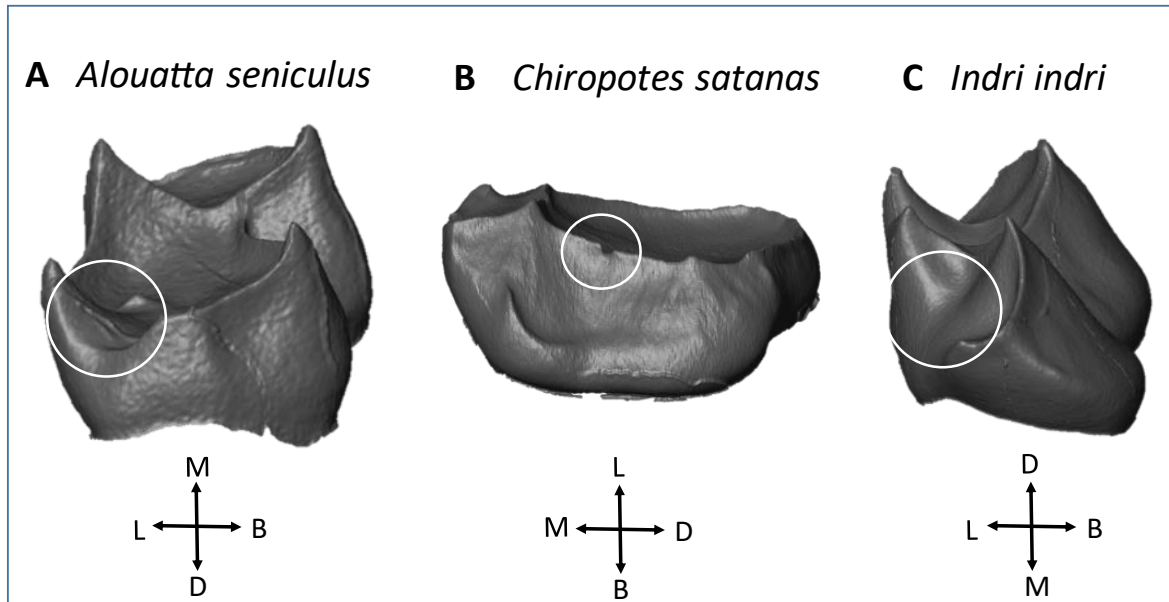


Figure 6. Three examples (white circles) of incomplete crest patterning: (A) *Alouatta seniculus* on the distal marginal ridge, (B) *Chiropotes satanas* on the buccal marginal ridge, and (C) *Indri indri* on the mesial marginal ridge. These images suggest that crests between primary cusps do not simply behave as passive structure produced by cusp-induced tensions of the epithelium. Images are not to scale.

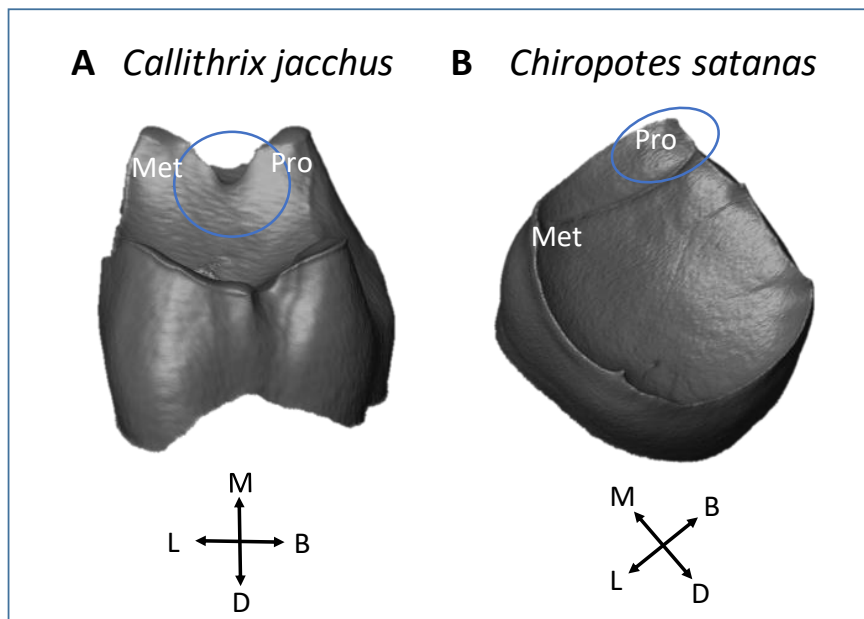


Figure 7. Two examples (blue circles) suggesting that trigonid crest morphology is under a primary crest patterning mechanism that does not necessitate cusp presence. The trigonid crest of the *Callithrix jacchus* specimen (A) displays a discontinuous crest, while the *Chiropotes satanas* specimen (B) demonstrates the presence of a trigonid crest that appears independent of the protoconid (i.e., forming distal to the dentine horn). Abbreviations are: Pro = protoconid, Met = metaconid. Images are not to scale.

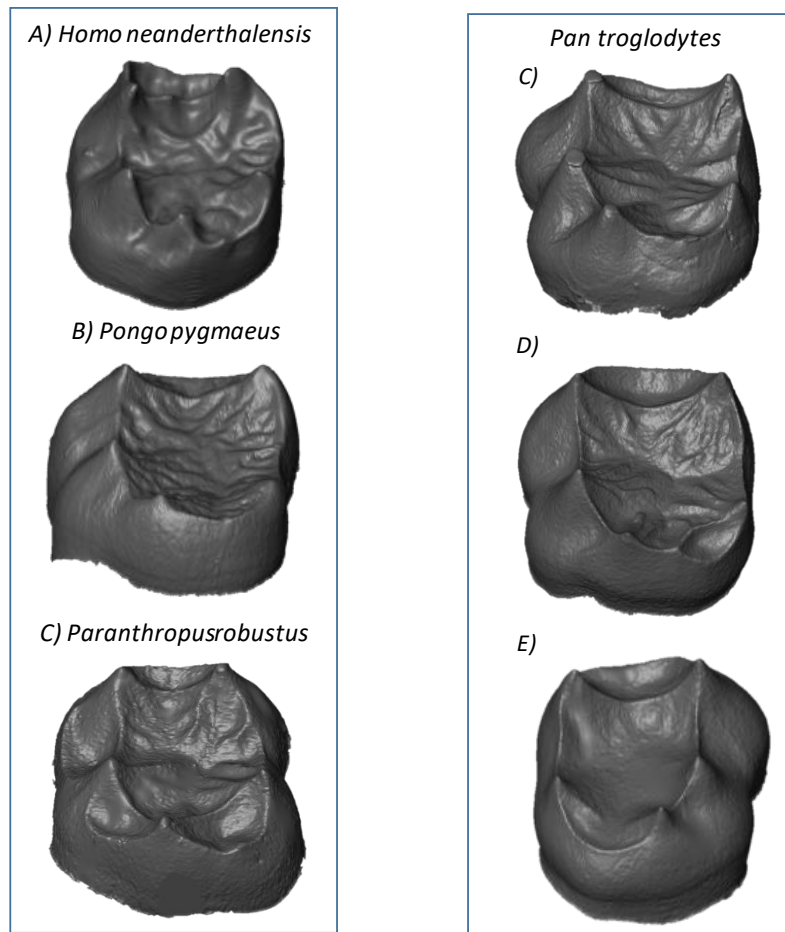


Figure 8. Examples of occlusal basin wrinkling in hominoid molars. (A) *Homo neanderthalensis*, (B) *Pongo pygmaeus*, (C) and *Paranthropus robustus* specimens with complex patterns of occlusal wrinkling that are likely attributed to specific growth processes of the inner enamel epithelium. The *Pan troglodytes* specimens (C, D, E) demonstrate within-species variation present in occlusal wrinkling. Images are not to scale.

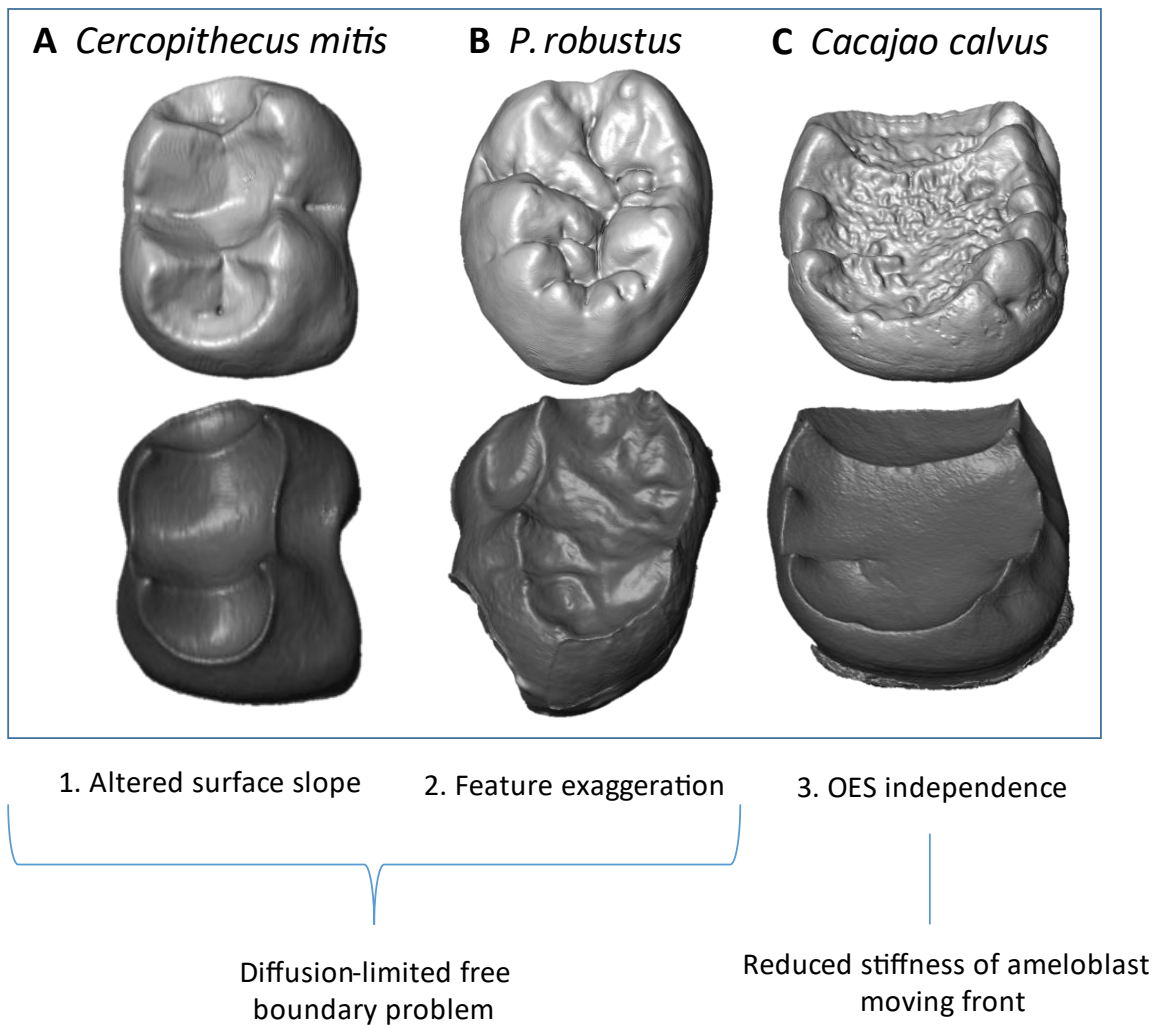


Figure 9. Examples of three patterns of outer enamel surface morphology that differ from the initial shape and patterning of the dentine crown. While variation between the dentine surface and OES in the (A) *Cercopithecus mitis* and (B) *Paranthropus robustus* specimens can be attributed to a diffusion-limited free boundary mechanism, the (C) *Cacajao calvus* deposition pattern may be related to a reduced stiffness of the ameloblast moving front during amelogenesis. Images are not to scale.

CHAPTER 4: Testing the Patterning Cascade Model of Cusp Development in *Macaca fascicularis* mandibular molars

Abstract

Molar crown configuration plays an important role in systematics, functional and comparative morphology, and the reconstruction of the evolutionary history of the primate clade. In particular, the number of cusps on primate molar teeth are often used to identify fossil species and infer their phylogenetic relationships. However, this variability deserves renewed consideration as a growing number of studies are now highlighting important developmental mechanisms that may be responsible for the presence of molar cusps in some mammalian taxa. Experimental studies of rodent molars studies suggest that cusps form under a morphodynamic, patterning cascade model of development (PCM) that involve the iterative formation of enamel knots. This model posits that the size, shape and location of the first-forming cusps determines the presence and positioning of later-forming cusps on the tooth crown. Here I test whether variation in lingual and distal accessory cusp presence in 13 *Macaca fascicularis* mandibular second molars (M2s) is consistent with predictions of the PCM. Using micro-CT, I imaged these M2s and employed geometric morphometrics to examine whether shape variation in the enamel-dentine junction (EDJ) correlates with accessory cusp presence. I find that accessory cusp patterning in macaque M2s is broadly consistent with the PCM. Molars with accessory cusps were larger in size and possessed shorter relative cusp heights compared to molars without accessory cusps. Peripheral cusp formation was also associated with more centrally positioned primary cusps, as predicted by the PCM. While these results demonstrate that a patterning cascade model is broadly appropriate for interpreting cusp variation in *Macaca fascicularis* molars, it does not explain

all manifestations of accessory cusp expression seen in this sample. Further research is needed to understand the potential interactions between multiple accessory cusps on a marginal ridge, and the influence of crest formation on enamel knot initiation and final EDJ shape.

4.1 Introduction

Much of what is known about mammalian tooth morphogenesis and the growth of multicuspid teeth comes from research in experimental genetics, evolutionary morphology, and embryology, and has led to the development of models through which variability in tooth crown morphology can be interpreted. In particular, studies of developing murine teeth (Jernvall, 2000; Jernvall and Thesleff, 2000; Salazar-Ciudad and Jernvall, 2002; Kassai et al., 2005), and computational modelling of mammalian tooth germs (Salazar-Ciudad and Jernvall, 2002, 2010), have shown that the mechanisms responsible for the patterning of multicuspid tooth crowns involve the punctuated and iterative appearance of embryonic signalling centres known as enamel knots. These enamel knots are thought to be equivalent to the signalling centres responsible for the epithelial appendage patterning of scales, feathers, limb buds and hair follicles (Niswander and Martin, 1992; Thesleff and Nieminen, 1996; Vaahtokari et al., 1996). In these examples, pattern formation is regulated and controlled by the spatial distribution of signalling centres that involve the interaction between differentially diffusing activatory and inhibitory morphogens.

Enamel knots have been implicated in the activation of cell proliferation and folding of the inner enamel epithelium, which determines the shape and size of the tooth (Jernvall and Thesleff, 2000; Kassai et al., 2005). They also produce proteins that inhibit the formation of

new enamel knots nearby, creating a spatiotemporal zone of inhibition. As such, new signalling centres can only form outside the zones of inhibition of previously formed enamel knots. The primary enamel knot appears in the tooth germ at the tip of the dentine horn of the first cusp and induces the appearance of secondary enamel knots (SEK) (Jernvall and Thesleff, 2000). These secondary enamel knots appear along the inner enamel epithelium at the sites of the future cusps. They influence the potential expression of further cusps through an interplay between the timing and spacing of enamel knot initiation, the overall size of the tooth germ, and the duration of crown growth before mineralisation. These interactions represent the foundation and principle of the patterning cascade model (PCM), which suggests that cusp formation is not predetermined but based on the interplay between these various processes and interactions (Salazar-Ciudad and Jernvall, 2002). Importantly these developmental parameters can be assessed in fully-formed teeth by studying the overall size of a tooth, the distance between neighbouring cusps, and the height of each cusp (Jernvall, 2000; Kondo and Townsend, 2006; Harris, 2007).

The patterning cascade model has successfully explained variation in cusp number and patterning among Lake Ladoga ringed seals (Jernvall, 2000). Among primates, the vast majority of work has been conducted with Hominidae molars, and findings are generally consistent with predictions made by the PCM. For example, Kondo and Townsend (2006) and Harris (2007) showed that an accessory cusp was more likely to be present on larger molars of humans, which the PCM would suggest was due to a reduced spatial constraint on SEK formation within the tooth germ. Similarly, Skinner and Gunz (2010) report the presence of dentine horns on the distal margin of the enamel-dentine junction (EDJ) of chimpanzee mandibular molars that were consistent with PCM predictions. More recently, Ortiz et al.,

(2018) examined 17 living and fossil hominoid species and reported that while the majority of accessory cusp expression could be explained by the PCM, some accessory cusps presence suggested potential deviations from the developmental model. Extensive research in other primate clades, however, is currently lacking. Monson (2012) and Winchester (2016) noted some discordance between certain aspects of their observed morphology and a PCM-predicted morphology in cercopithecine molars, but this has yet to be formally and extensively studied.

In this study, I examine *Macaca fascicularis* molars to assess whether the processes controlling accessory cusp expression are consistent with the predictions of the PCM. *Macaca fascicularis* molars are ideal candidates for testing the predictions of the PCM because they variably express both distal and lingual accessory cusps, and have a simple primary cusp patterning that can be used to easily divide the teeth into mesial, distal, lingual and buccal sections. By studying *Macaca fascicularis*, I can also provide the first comprehensive assessment of the PCM in Cercopithecine molars, and assess how these mechanisms may contribute to interpretations of cusp patterning in Cercopithecine systematics and taxonomy. I analyse the correlation between EDJ shape (including overall EDJ size, dentine horn height, and dentine horn spacing) and the variable presence of lingual accessory cusps (LAC) and distal accessory cusps (DAC) in macaque mandibular second molars (M2s). While accessory cusps in these positions are often referred to as cusp 7 and cusp 6 respectively, I follow Davies et al., (2021) in using these more generalized terms as they are inherently free of inferences about homology. Based on the predictions of the PCM, **a LAC or DAC is less likely to form when tooth size is comparatively small. A LAC or DAC is also less likely to form when the**

primary dentine horns are large or closely spaced. Conversely, a LAC or DAC cusp is more likely to form with increased tooth size, and relatively small and/or widely spaced cusps.

4.2 Materials and Methods

4.2.1 Study sample

To test the relationship between EDJ shape and accessory cusp presence it is best to limit taxonomic and metamerism variation. The study sample was thus restricted to M2s of *Macaca fascicularis* (n=13) from the Wake Forest University Primate Centre (Winston-Salem, NC). The majority of individuals from this facility were captive, and those with signs of dental or skeletal pathology were excluded. Specimens were chosen to have relatively equal numbers of those with and those without LAC or DAC cusps, while also restricting the sample to those individuals with relatively unworn or undamaged mandibular second molars. As *Macaca fascicularis* molars become worn early in life, acquiring unworn, undamaged molars was a challenge that resulted in a comparatively small sample size.

4.2.2 Scoring Procedure

Accessory cusp scoring was restricted to dichotomous 'Absent' and 'Present' categories to maximise the sample size of each group. As such, the 'Present' category encompasses various manifestations of LAC and DAC expression, including the occurrence of multiple dentine horns along the corresponding ridge (Figure 1). The LAC was scored as present if one or more dentine horns were observed between the metaconid and entoconid cusps. The DAC was scored as present if one or more dentine horns were observed between the entoconid and hypoconid cusps. Importantly, while there is reason to question whether the distal extension and shouldering of the hypoconid in some specimens is a true dentine horn (in that it was

initiated and formed by a secondary enamel knot), it was not present in any of the specimens within the 'Absent' category (see Davies et al., 2021 for further discussion of the relationship between 'shouldering' and accessory cusp presence).

4.2.3 MicroCT, image filtering and tissue segmentation

Dentitions were scanned with one of two micro-CT scanners (Harvard University Centre for Nanoscale Systems X-Tek HMXST 225 CT; Nikon Corporation X-Tek XT H225 CT) with voxel sizes between 17 and 28 cubic microns. Scanning was conducted under standard operating conditions (current, energy, and metallic filters) following established protocols (Kato et al., 2004; Olejniczak et al., 2007; Feeney et al., 2010; Smith et al., 2012). Image stacks for each molar were then filtered to facilitate tissue segmentation using a 3D mean-of-least-variance filter with a kernel size of one. This filtering process sharpens the boundaries between enamel and dentine (Schulze and Pearce, 1994), allowing for a clearer segmentation of tissue types, while having minimal effect on the accurate reconstruction of the EDJ surface (Skinner et al., 2008). Filtering was implemented using MIA open source software (Wollny et al., 2013).

Filtered image stacks were segmented in Avizo 6.3 using a semiautomatic process that separates voxels based on greyscale values. After segmentation, the EDJ was reconstructed as a triangle-based surface model. As a final step before landmark collection, accessory cusps were cropped from EDJ surface models with Geomagic Studio 2014 (3D systems, Rock Hill) in order to quantify the shape of the marginal ridge. This process allowed for the complete placement of landmarks around the marginal ridge of the tooth without the influence of potentially confounding dentine horn-line features.

4.2.4 Landmark collection and derivation of homologous landmark sets

EDJ surface models were used to create three sets of 3D landmarks in Avizo 6.3. The first set (EDJ_MAIN) were placed at the tips of the dentine horn for each primary cusp (Figure 2). The second set (EDJ_RIDGE) were placed along the marginal ridge that connects the four dentine horns, creating a continuous set of landmarks around the basin of the tooth. The third set of landmarks (CEJ_RIDGE) were placed along the cementum-enamel junction. In cases where sections of the CEJ were missing due to cervical enamel fracture, the location of these landmarks were estimated. In two specimens, the CEJ could not be reliably estimated and thus were not including in any analyses incorporating this landmark set.

Geometrically homologous semi-landmarks (Gunz et al., 2005) for the EDJ_RIDGE and CEJ_RIDGE were then derived in R. This process involves the fitting of a smooth curve through the landmarks of the EDJ and CEJ ridge using a cubic-spline function. A fixed number of equally spaced semilandmarks were then placed along the curve; the EDJ_RIDGE had 18 landmarks along the buccal and lingual ridges, and 12 along the mesial and distal ridges. The CEJ_RIDGE had a single set of 30 landmarks that surrounded the CEJ. While the EDJ_MAIN landmarks remain fixed, these landmarks attributed to the EDJ_RIDGE and CEJ_RIDGE are treated as semi-landmarks and allowed to slide along their respective curves to minimise the bending energy of the thin-plate spline interpolation function calculated between each specimen and the Procrustes average for the sample. This sliding process renders these landmarks geometrically homologous, at which point they are converted into shape coordinates using generalised least squares Procrustes superimposition.

4.2.5 Geometric morphometric analysis and visualisation of shape variation

A principle components analysis (PCA) was conducted using the Procrustes coordinates of each specimen in shape space. A PCA is commonly used to reduce the dimensionality of a dataset that has a high number of dimensions per specimen. This is accomplished by projecting data points onto only the first few principal components to obtain lower-dimensional data, while still preserving as much of the variation as possible. This process was conducted on three different sets of EDJ landmarks for both the LAC and DAC: a complete analysis including the EDJ and CEJ landmarks, a marginal ridge analysis that excluded the CEJ and only consisted of EDJ_MAIN and EDJ_RIDGE landmarks, and an isolated ridge analysis that only included the ridge landmarks between the two dentine horns where the accessory cusp is found (isolated distal ridge between the hypoconid and entoconid for the DAC analysis, and isolated lingual ridge between the metaconid and entoconid for the LAC analysis). 2D and 3D PCA plots (whole tooth, marginal ridge, and isolated ridge) were generated to visualize variation in EDJ shape between the 'Present' and 'Absent' groups. Wireframe models were then used to visualise the shape changes along the first two PCs. Shape changes in the wireframes provided have been exaggerated to display the shape of a hypothetical specimen occupying the extreme ends of each PC, and are depicted as two standard deviations from the mean. The size of specimens was analysed with t-tests, using the natural logarithm of centroid size and visualised through boxplots.

4.3 Results

4.3.1 Lingual accessory cusp analysis

Principal component analysis of EDJ and CEJ shape reveals that molars with lingual accessory cusps are distinct from those without an accessory cusp. The 3D PCA plots show clear separation of the 'Present' and 'Absent' categories in all three analyses (Figure 3). A 2D PCA

of the whole tooth shows overlap along PC1 and PC2, but with a tendency towards the presence of a LAC along the negative end of each PC (Figure 4). The corresponding wireframes reveal that the negative end of both PC1 and PC2 are characterized by smaller and more closely spaced mesial and distal cusps, and a deeper marginal ridge gradient. This result supports the predictions of the PCM.

Boxplots of centroid size for the whole tooth analysis show that molars with LACs tend to be slightly larger than those without, although this was a non-significant trend ($p=0.162$). As such, this result provides no support for the prediction of the PCM. A 2D PCA of just the marginal ridge shows clear separation between groups within the first and second principal components (Figure 5), with a tendency towards the presence of a LAC along the negative end of PC1 (slightly smaller and widely-spaced cusps and a wider and deeper lingual fovea) and positive end of PC 2 (slightly shorter and more closely-spaced cusps, and a deeper and more asymmetrical lingual fovea). This result supports the predictions of the model. For the isolated lingual ridge, the groups overlap completely along PC1, but separate well along PC2 (Figure 6). Accessory cusp presence is found along the negative end of PC2, which is associated with a lingual ridge with a slightly taller metaconid, and a shallow and asymmetrical marginal ridge. This provides no support for the PCM. Boxplots of centroid size for the EDJ ridge and isolated ridge show a similar trend of LAC presence among larger molars, but with a greater overlap between the groups and a statistically non-significant trend ($p=0.628$ and $p=0.436$ respectively). As previously mentioned, a non-significant trend in centroid size provides no support for the PCM.

I also examined the mean landmark configurations in each analysis for those specimens with and without a LAC (Figure 7). In the whole tooth landmark set, specimens with a LAC exhibited slightly shorter entoconid and buccal dentine horns, and more closely spaced mesial and distal cusps, providing support for the PCM in the former, but not the latter. For the marginal ridge analysis, specimens with a LAC again exhibited slightly reduced entoconid height, but also a deeper lingual fovea. These findings match the results seen in the exaggerated wireframes, but highlight the subtlety of these differences between the groups. For the lingual ridge landmark set, those with and those without a LAC display a slight difference in metaconid height, with negligible other differences. Mean landmark configurations of the occlusal view of the marginal ridge also reveal negligible differences between the groups from this angle.

4.3.2 Distal accessory cusp analysis

Principal component analysis EDJ shape reveal that molars with distal accessory cusps are morphologically distinct from those without an accessory cusp. The 3D PCA plots show clear separation of the 'Present' and 'Absent' categories in the whole tooth and isolated ridge analysis. For the EDJ ridge analysis, a 3D PCA shows one individual with an accessory cusp within the convex hull of the 'Absent' grouping (Figure 8). A 2D PCA of the whole tooth shows no separation of the groups along PC1 or PC2 (Figure 9). A 2D PCA of just the marginal ridge shows no separation along PC1, but a tendency towards DAC presence along the positive end of PC2 (Figure 10). Wireframes reveal that the positive end of PC2 is exemplified by more closely spaced mesial and distal cusps, and a distally extended marginal ridge that creates a less acute gradient of the rising distal ridge. While the former result does not match the predictions of the model, this may be explained by the positive support for the PCM in the

latter. A 2D PCA of the isolated distal ridge shows no separation of the groups along PC1 or PC2 (Figure 11). Boxplots of centroid size for all analyses show that molars with DAC are slightly larger than those without, but all revealed statistically non-significant results (whole tooth $p=0.471$, EDJ ridge $p=0.549$, distal ridge $p=0.151$). Results of centroid size again lend no support for the PCM.

Examination of the mean landmark configurations in each DAC analysis reveals a consistent trend towards closer spaced mesial and distal dentine horns among those with an accessory cusp. In the whole tooth landmark set, this is combined with a slightly wider distal extension of the CEJ ridge. This may provide support for the PCM, and is discussed further below. In the marginal ridge landmark set, closer spaced mesial and distal primary dentine horns among those with a DAC are also associated with the less acute gradient of the rising distal ridge and extended marginal ridge seen in the exaggerated wireframes. For the distal ridge landmark set, specimens with a DAC exhibited slightly closer spaced and taller distal cusps in a lingual view, however these differences were subtle and provided no support for the model. The occlusal view of the marginal ridge provides an alternative angle with which to observe the extended distal ridge in specimens with a DAC.

4.4 Discussion

Principle component analysis of EDJ and CEJ shape demonstrates that macaque molars with accessory cusps are morphologically distinct from those without accessory cusps. Despite small sample sizes, in five of the six analyses, 3D PCA plots showed complete separation (with only a slight overlap of the convex hulls in the EDJ ridge analysis of the DAC). To understand these shape differences and determine whether they matched the predictions of the

patterning cascade model of cusp development, shape changes along the first two PCs and between the average shape of molars with and without accessory cusps were assessed from wireframes. When examining the shape of the whole tooth, LAC presence was associated with more closely spaced primary cusps. This matches the predictions of the PCM, in that more closely spaced cusps are thought to reduce the available space for cusp initiation and inhibit the formation of additional cusps. Tooth size, however, did not support the predictions of the model. In the EDJ ridge analysis, LAC presence was again associated with shorter primary cusps along both PCs in the exaggerated wireframes. The mean landmark configurations do confirm this tendency toward reduced entoconid height among specimens with LAC, while demonstrating negligible differences in cusp spacing. Although there is no clear trend regarding cusp spacing in these results, LAC presence was consistently associated with shorter primary cusps in these analyses (particularly regarding the height of the entoconid), which is compatible with the predictions of the PCM. All of these are not, however, statistical tests and any results should be considered accordingly.

For the DAC analyses, both the mean landmark configurations and exaggerated wireframes demonstrate an important trend in cusp positioning that may be responsible for differences in distal marginal ridge morphology and subsequent accessory cusp formation. While DAC presence was associated with slightly shorter primary cusps in some analyses, it was consistently associated with significantly more mesially positioned distal dentine horns. The mesial positioning of the distal cusps may be responsible for the increased extension of the distal marginal ridge seen in both the mean models and wireframes, providing more potential space for accessory cusp formation. Ortiz et al. (2018) has previously shown in hominoid molars that small intercusp differences correlate with the presence of cusps on the peripheral

region of the crown. While distal accessory cusps in macaque molars might not meet the criteria of a peripheral cusp, in that they still form on the marginal ridge of the tooth, these results do suggest that the positioning of the primary cusps contribute to the formation of accessory cusps, particularly if more closely-spaced cusps allow for increased peripheral space on the crown surface.

For the isolated ridge analyses, LAC presence was associated with a slightly taller metaconid, but also a more shallow and asymmetrical lingual ridge. Currently, the processes responsible for crest formation in mammalian dentitions are poorly understood. It is unknown whether the development of crests between primary enamel knots could influence or interfere with enamel knot initiation at the location of later forming cusps. Furthermore, it is also unclear whether the formation of an accessory cusp impacts the morphology of the marginal ridge at the EDJ and contribute in some way to the variation between the groups. Finally, it is also worth considering whether later processes of enamel secretion and mineralisation could alter the shape of the EDJ and create morphological complexity that was not present during the active period of the enamel knots.

For the isolated distal ridge, the mean models demonstrate minimal differences in ridge morphology between the groups, but show that DAC presence was associated with slightly taller and closer spaced distal cusps. While this does not match the predictions of the PCM, based on the potential importance of the mesial positioning of the distal cusps relative to the tooth germ, it may be that slightly taller distal cusps have an insignificant effect on potential accessory cusp formation in these peripheral regions of the tooth.

Boxplots of centroid size for all the analyses demonstrate that molars with accessory cusps tend to be larger than those without accessory cusps, although this difference was statistically non-significant. This non-significant trend provides no support for the predictions of the PCM as it relates to tooth size, and may partially reflect the statistical constraints associated with small sample sizes.

While the patterning cascade model appears to be useful in providing some explanation for the variable presence of accessory cusps in primate dentitions, there are several aspects of molar morphology that indicate the existence of other developmental processes or inhibitory mechanisms in the formation of additional cusps. Chapple and Skinner (2023) have recently discussed the typical patterns of cusp expression in primate molars, but also highlighted the numerous locations on the EDJ surface where dentine horns are rarely seen. In the current study I note that, while lingual and distal accessory cusps were commonly observed in the macaque sample, no cusps were observed on the buccal or mesial marginal ridge. As primary cusp size and spacing is relatively symmetrical between buccal and lingual, and mesial and distal sides of the tooth crown, we should expect to see the variable expression of cusps on all marginal ridge locations if the PCM was the only mechanism regulating enamel knot initiation. Furthermore, in no cases was an accessory cusp observed within the occlusal basin of the tooth. This is consistent with a development constraint in cusp patterning in that enamel knots initiation appears to be linked to crests. Whether this relates to the impact these morphologies would have on occlusal dynamics, remains to be tested. Overall, our results indicate that parameters of the PCM are a component of the variation in cusp expression in primate molar morphology, but are not the only source of developmental constraint.

Supporting the predictions of the PCM in this study underscores the importance of recognising the developmental processes (not just phylogenetic value) responsible for tooth crown morphology in primates. Cusp patterning plays an important role in studies of primate systematics and taxonomy, and relies heavily on the assumption that these features are of phylogenetic relevance. This study contributes to an emerging picture that cusp patterning may be determined by subtle changes in the developmental parameters of the PCM, which themselves may be established during the early stages of development of the tooth germ. Instead of attributing the relatively predictable presence of a particular accessory cusp in a certain primate clade or human population to the inheritance or conservation of a specific genetic programme, it may be more appropriate to consider it a reflection of differences in cusp positioning and/or tooth size, which themselves carry some genetic component. While I suspect the PCM to be only one source of constraint in primate cusp formation, the acknowledgement of these developmental mechanisms is crucial for the proper interpretation of tooth crown morphology in primate taxonomy and systematics.

While accessory cusp scoring was restricted only to 'Absent' and 'Present' categories to maximise the sample size of each group, the occurrence of multiple, closely positioned accessory cusps along a single marginal ridge in this sample raises interesting questions regarding the processes and environmental conditions that could lead to such a phenomenon. This phenomenon appears to violate the basic rules of the PCM. In the dental literature, these features have previously been described as 'double' or 'split' cusps (Wood and Abbott, 1983; Aiello and Dean, 1990). Based on observations of accessory cusp patterning at the EDJ surface, Skinner and Gunz (2010) have suggested that these terms may misrepresent the true

developmental processes underlying the formation of these features. To date, Martin et al. (2017) has provided the most convincing observations of what might be considered true twinned or split dentine horns in fossil hominins. Importantly, these features appear morphologically distinct from the more commonly observed manifestations of multiple dentine horns present in this sample (Figure 1) and among many other primate taxa.

In rare cases, the expression of multiple dentine horns between primary cusps appears to directly reflect the iterative process one would expect from a patterning cascade model, with progressively smaller cusps forming along a ridge as development progresses towards the CEJ (see Skinner and Gunz, 2010, Fig.3 D). In the majority of cases however, multiple accessory cusps instead appear as closely spaced and equally sized dentine horns. Currently, it is difficult to conceptualize how these features could occur under the PCM when the enamel knot of one dentine horn should inhibit the development of the other. Therefore, while the PCM seems to be useful for interpreting variation in single-cusp expression, additional research is required to understand the phenomenon of closely spaced cusp patterns on the same region of the marginal ridge in primates.

In this study, I have shown that accessory cusp patterning in macaque M2s is broadly consistent with a patterning cascade model of cusp development but that, as currently formulated, it cannot explain all manifestations of accessory cusps. Furthermore, it finds no clear support that tooth size is associated with accessory cusp expression, as the PCM predicts. Overall, these findings partially consistent with previous studies of other living and extinct primate taxa (Skinner & Gunz, 2010; Ortiz et al. 2018), as well as several non-primate mammalian species (Polly, 1998; Jernvall, 2000), suggesting that this mechanism of cusp

patterning is highly conserved within mammals. These findings highlight the importance of understanding the developmental mechanisms responsible for tooth crown morphology, and how these considerations contribute to interpretations of cusp patterning in primate systematics and taxonomy.

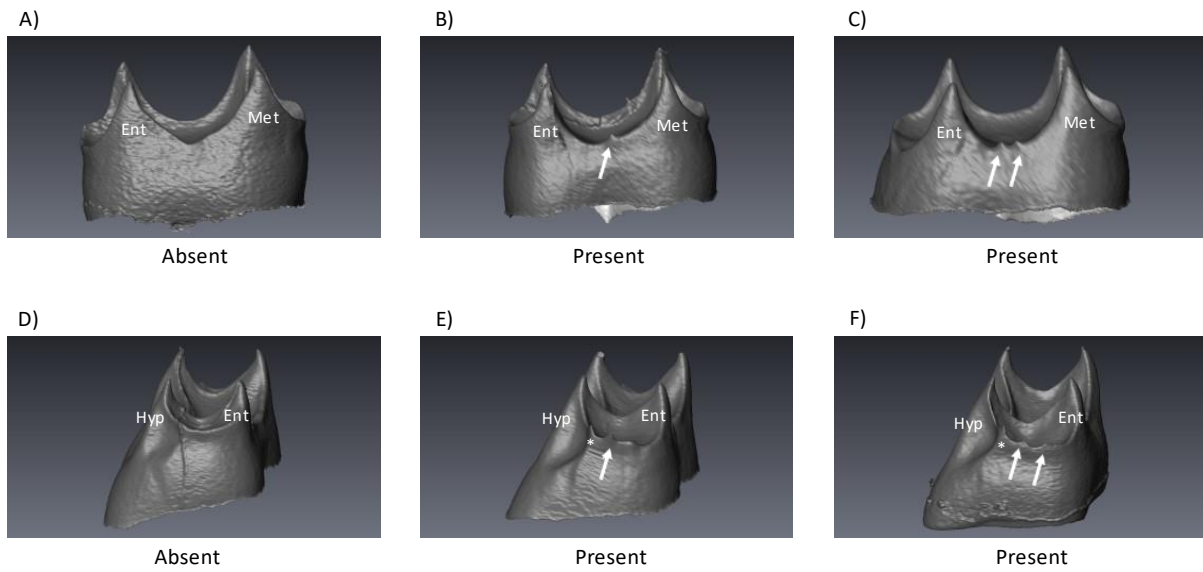


Figure 1. Accessory Cusp Scoring as 'Absent' or 'Present'. Above - Lingual accessory cusp (LAC). Lingual view. (A) No evidence of a dentine horn; (B) Presence of one accessory cusp on the lingual ridge; (C) Presence of two distinct accessory cusps on the lingual ridge. Below - Distal accessory cusp (DAC). Distal view. (D) No evidence of a dentine horn; (E) Presence of one accessory cusp on the distal ridge; (F) Presence of two distinct accessory cusps on the distal ridge. Ent = Entoconid, Met = Metaconid, Hyp = Hypoconid. *denotes the presence of a distal hypoconid shoulder that is not included in the scoring procedure.

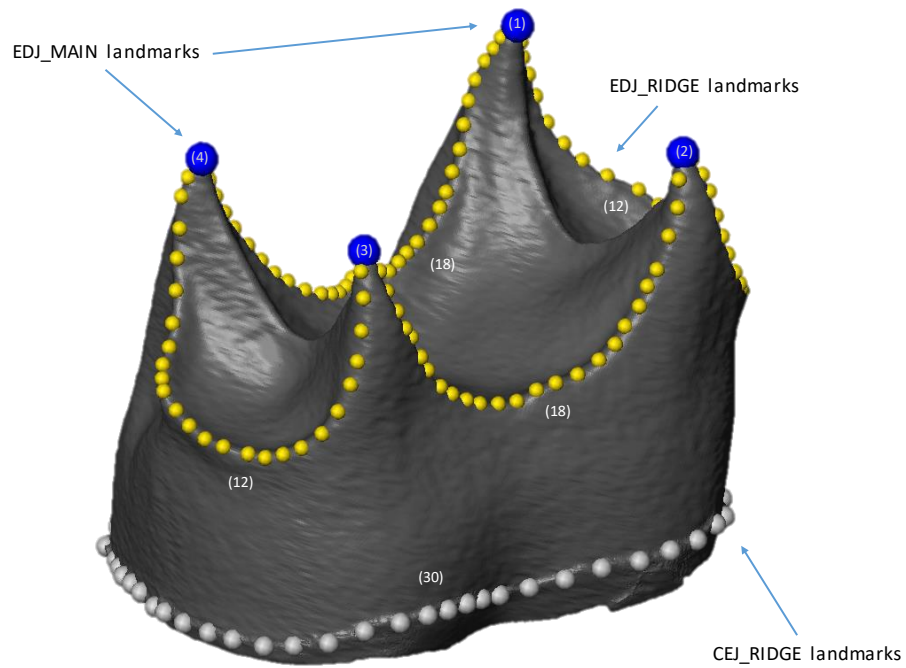


Figure 2. Disto-lingual view of a digital model of a macaque lower second molar crown with the enamel cap removed to reveal the surface of the EDJ. Landmarks used to capture the size and positioning of the primary cusps and tooth outline are shown as spheres. Blue spheres are EDJ_MAIN landmarks, yellow spheres are EDJ_RIDGE curve landmarks, and the grey spheres are the CEJ_RIDGE curve landmarks.

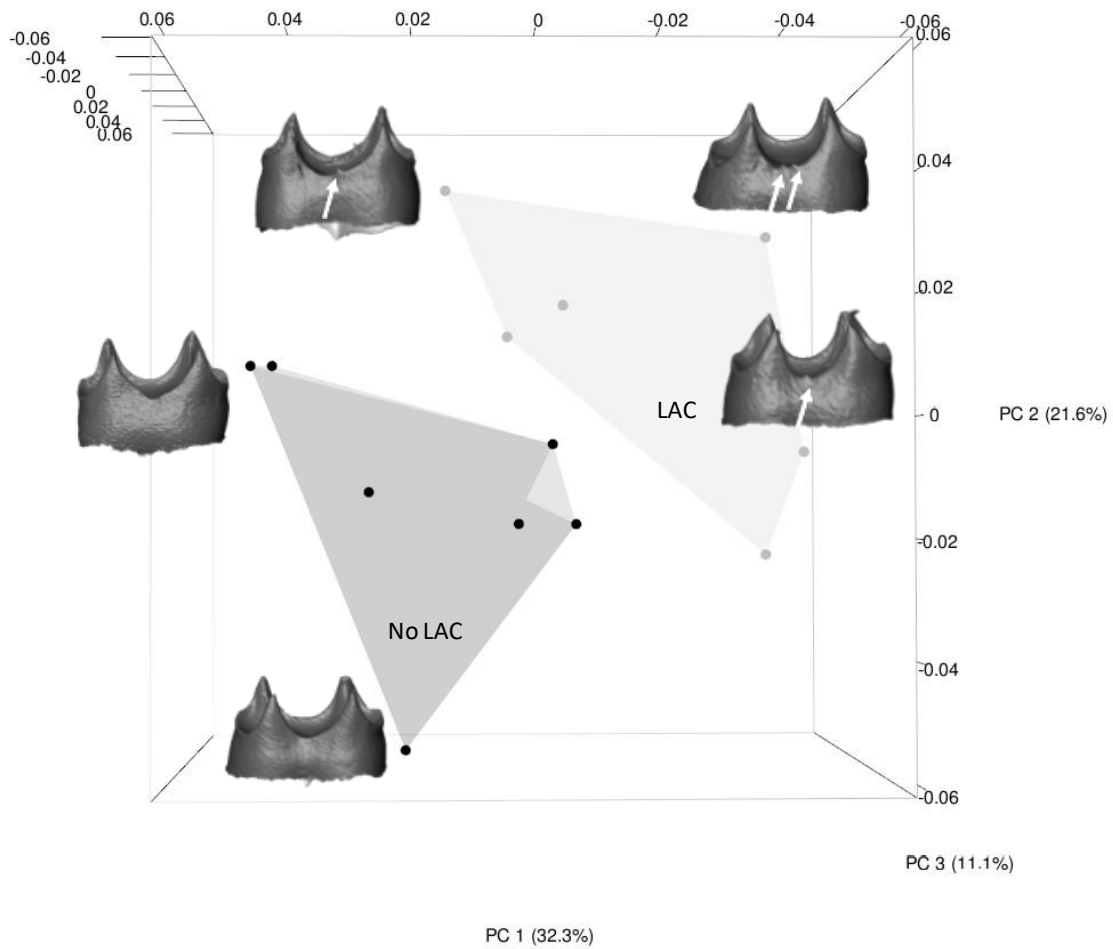


Figure 3. 3D plot of the first three principle components of an analysis of EDJ ridge shape variation between specimens with variable expression of a LAC. Accessory cusp absence corresponds to the lighter grey convex hull and grey spheres. Accessory cusp presence corresponds to the darker grey convex hull and black spheres (n=13).

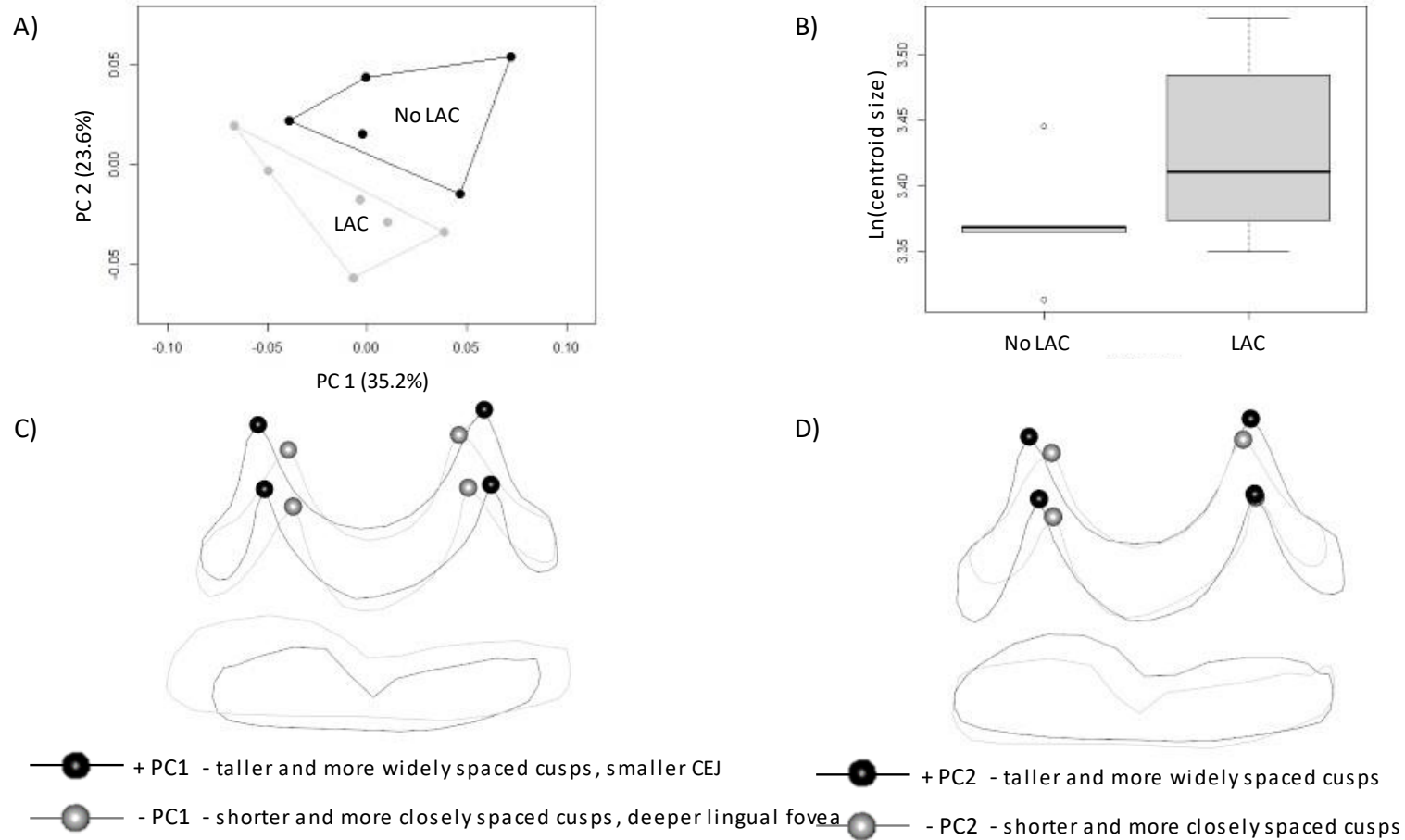


Figure 4. (A) Plot of the first and second principal components of an analysis of whole tooth shape variation between molars with variable expression of a LAC. (B) Centroid size of macaque lower second molars with and without a LAC. (C) Exaggerated wireframe model of the shape change along PC1 (exaggerations defined as two standard deviations from the mean). Lingual view. (D) Exaggerated wireframe model of the shape change along PC2. Lingual view. (n=11).

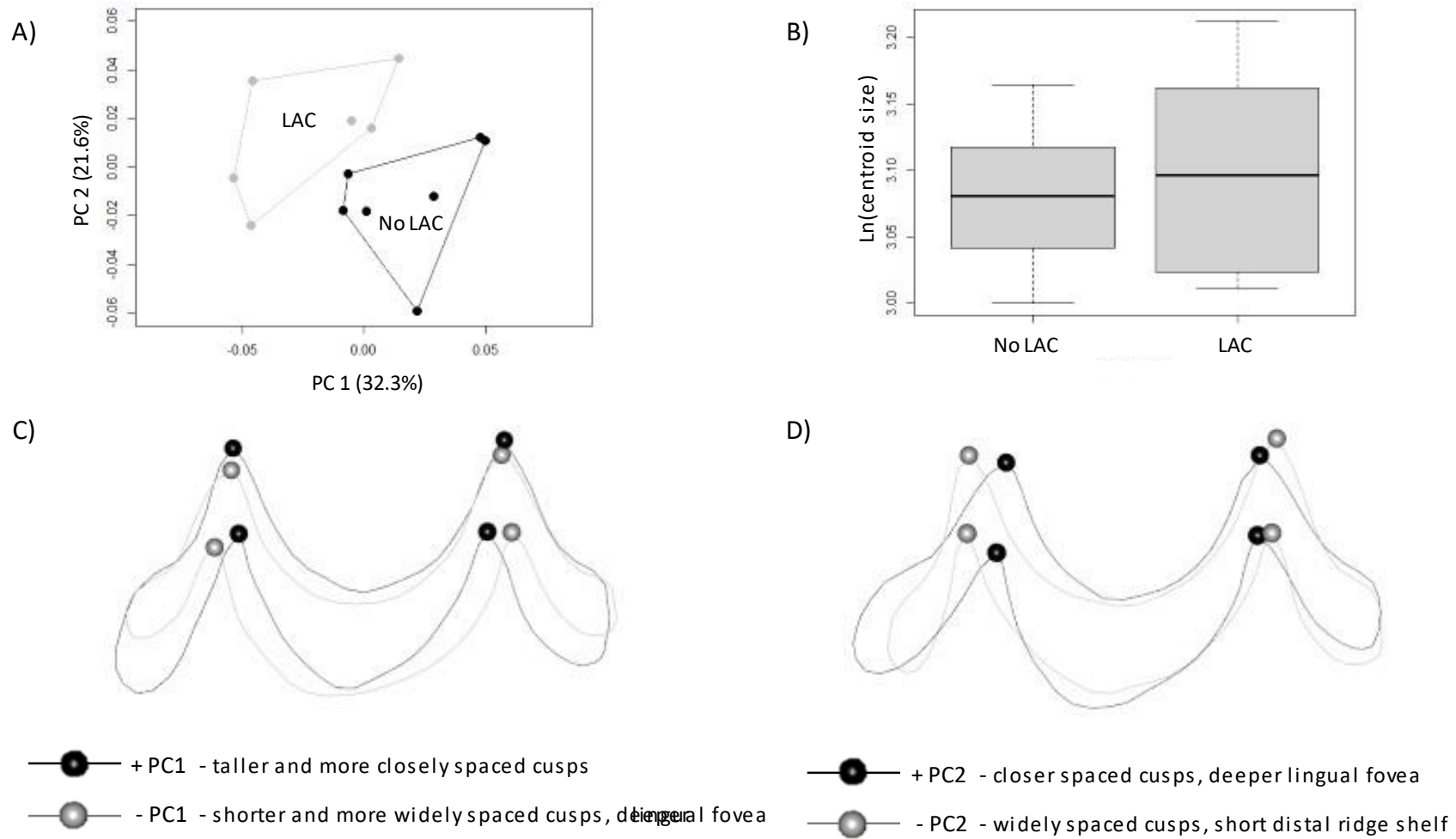


Figure 5. Plot of the first and second principal components of an analysis of EDJ ridge shape variation between molars with variable expression of a LAC. (B) Centroid size of macaque lower second molars with and without a LAC. (C) Exaggerated wireframe model of the shape change along PC1 (exaggerations defined as two standard deviations from the mean.) Lingual view. (D) Exaggerated wireframe model of the shape change along PC2. Lingual view. (n=13).

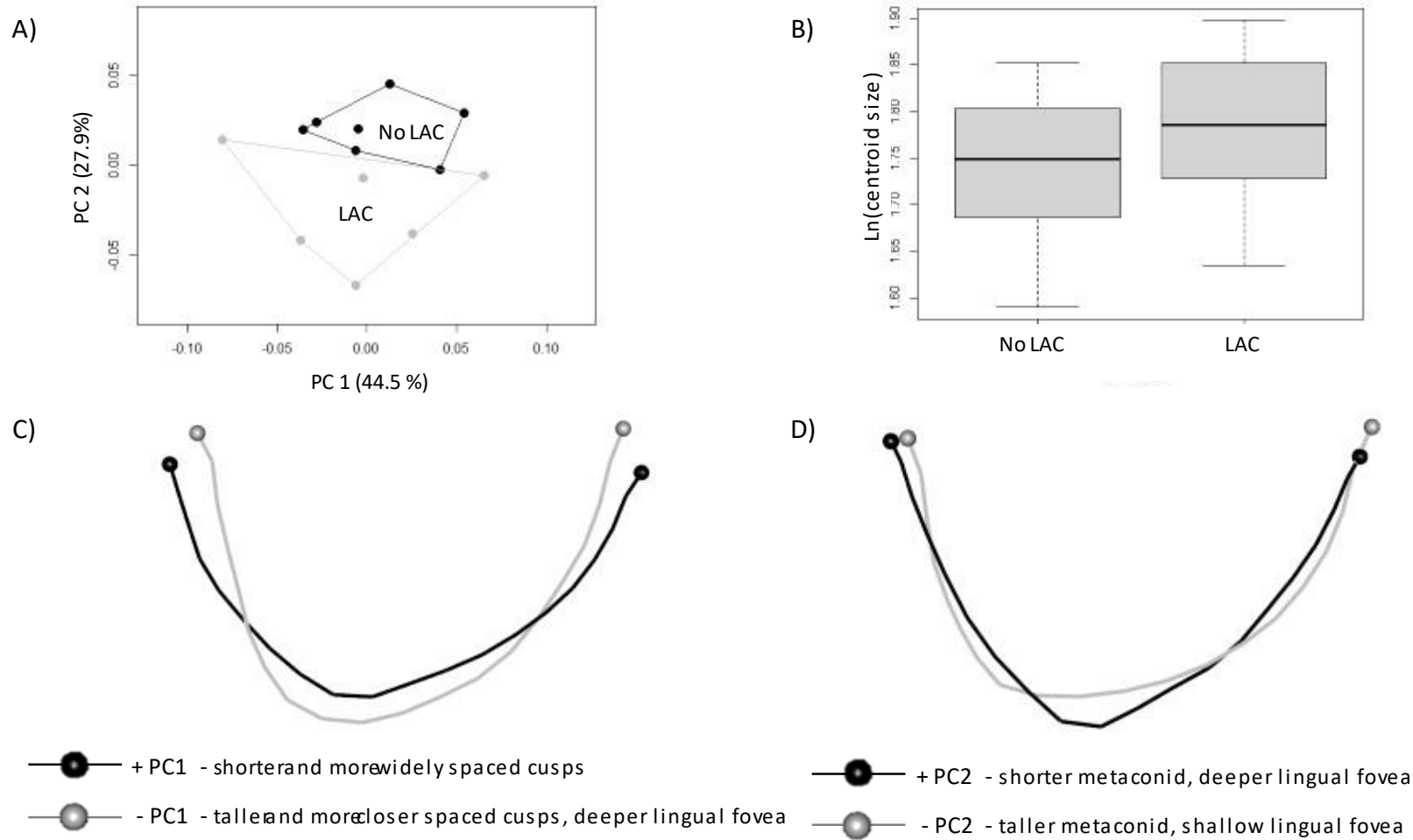


Figure 6. Plot of the first and second principal components of an analysis of the isolated lingual ridge shape variation between molars with variable expression of a LAC. (B) Centroid size of macaque lower second molars with and without a LAC. (C) Exaggerated wireframe model of the shape change along PC1 (exaggerations defined as two standard deviations from the mean.) Lingual view. (D) Exaggerated wireframe model of the shape change along PC2. Lingual view. (n=13).

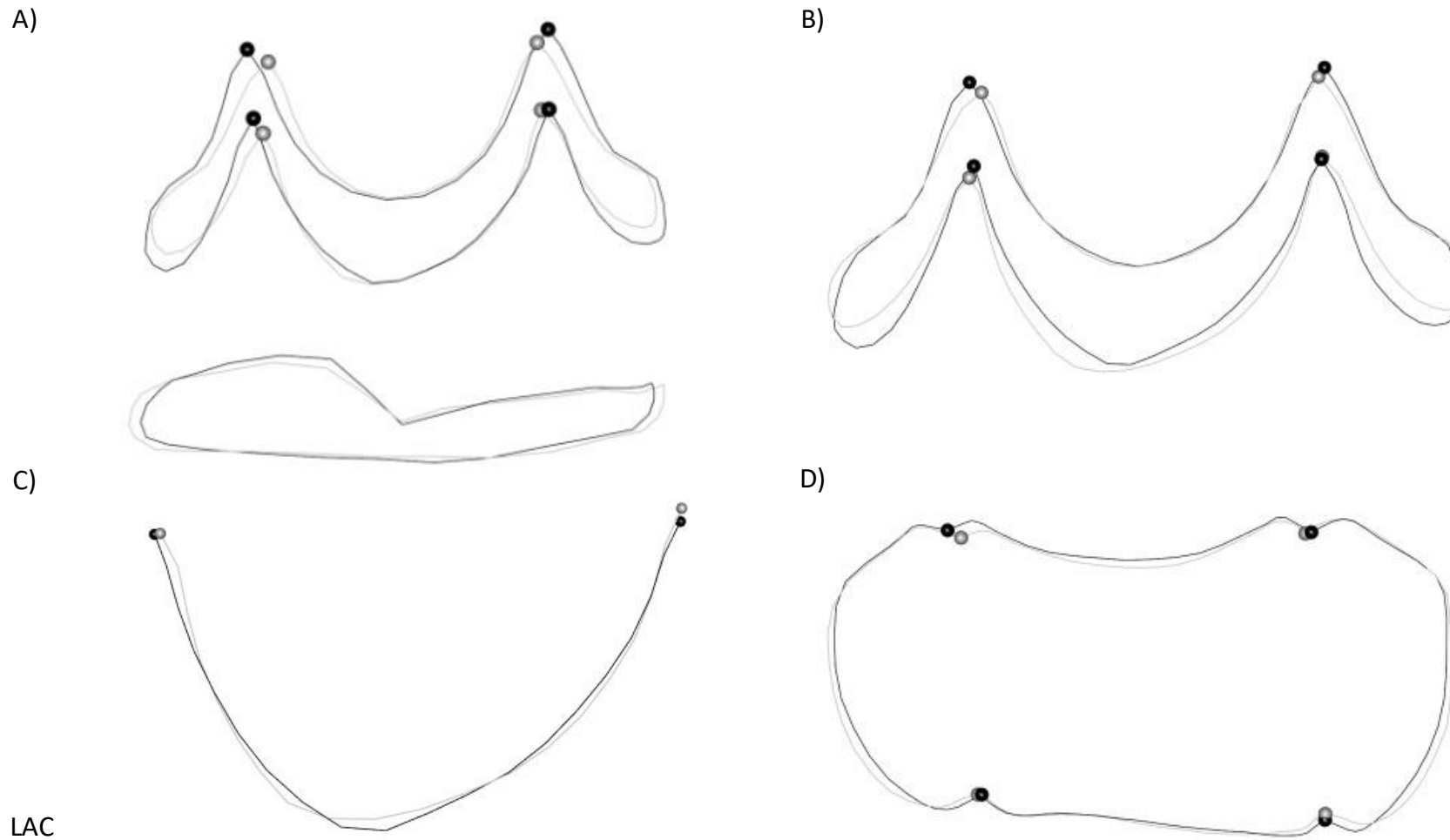


Figure 7. Mean landmark configurations for specimens with and without a LAC. Black = LAC absent. Grey = LAC present. (A) Whole tooth mean model. Lingual view; (B) EDJ ridge mean model. Lingual view; (C) Isolated lingual ridge mean model. Lingual view; (D) EDJ ridge mean model. Occlusal view.

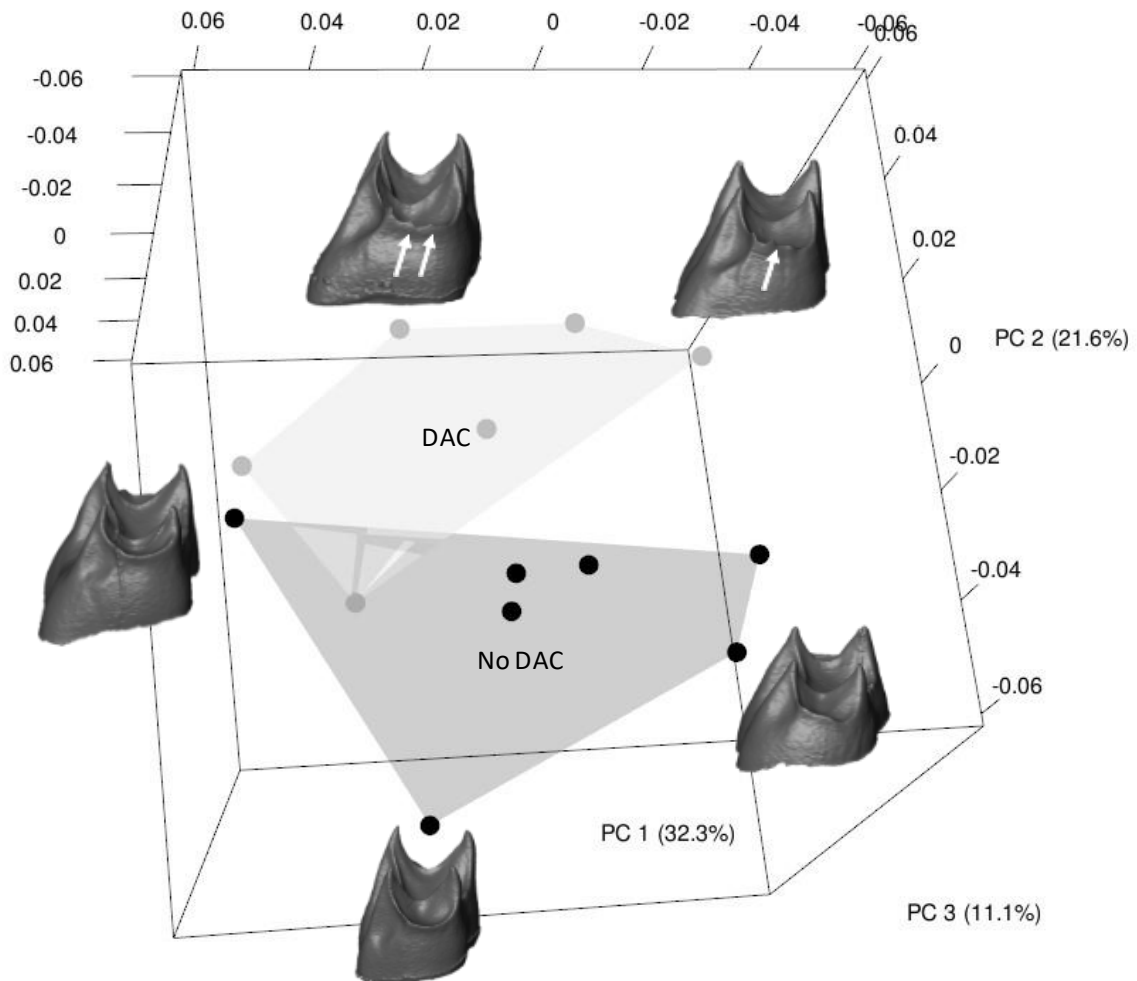


Figure 8. 3D plot of the first three principle components of an analysis of EDJ ridge shape variation between specimens with variable expression of a DAC. Accessory cusp absence corresponds to the lighter grey convex hull and grey spheres. Accessory cusp presence corresponds to the darker grey convex hull and black spheres (n=13).

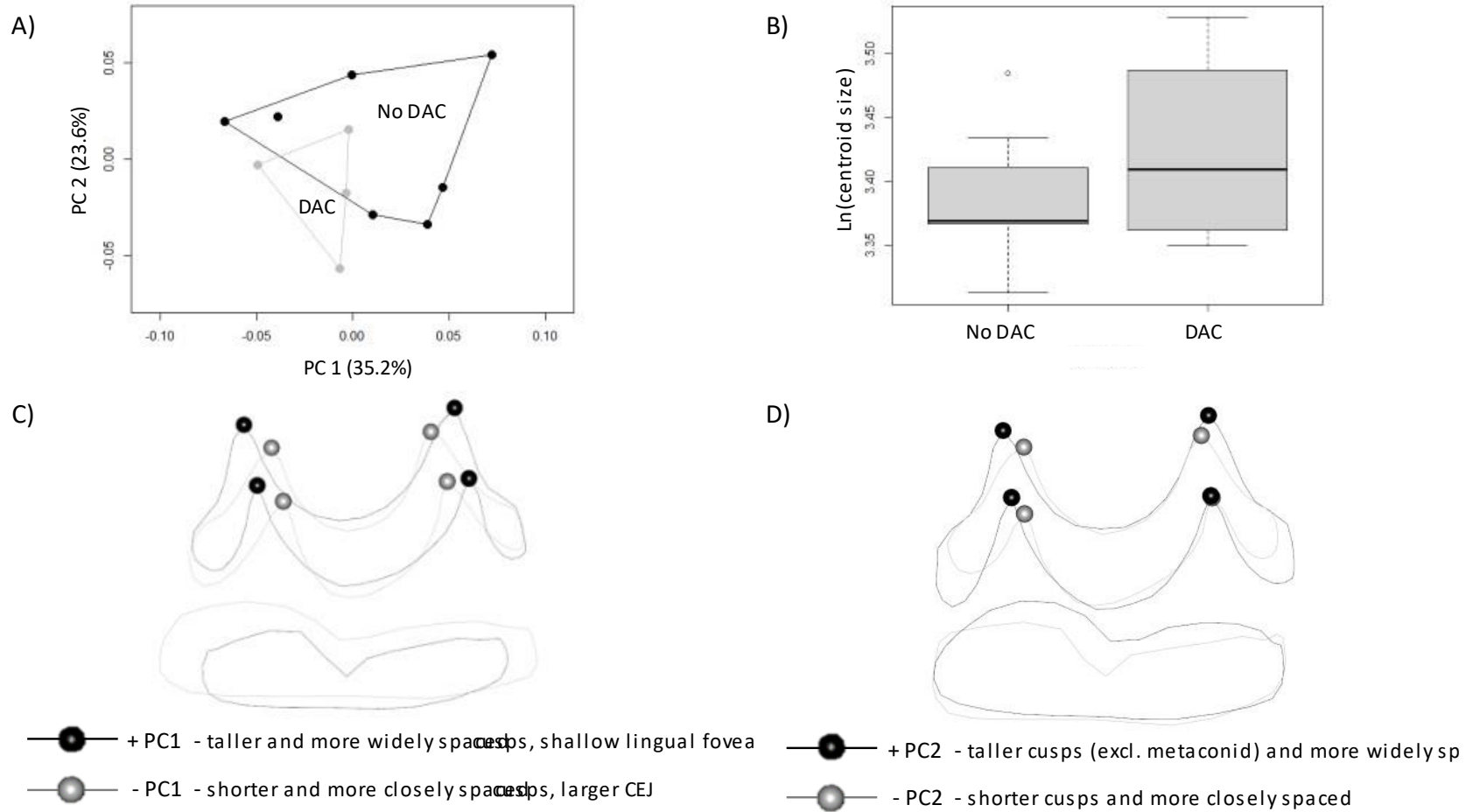
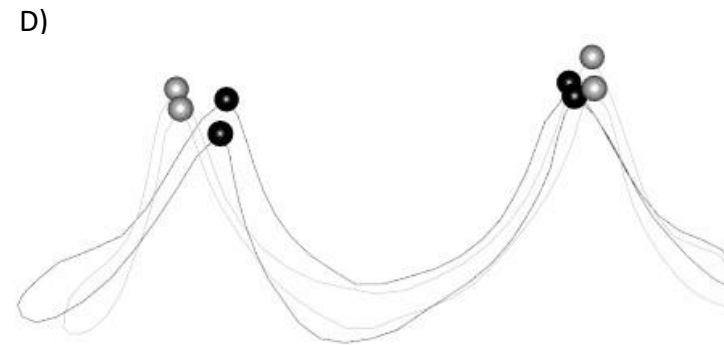
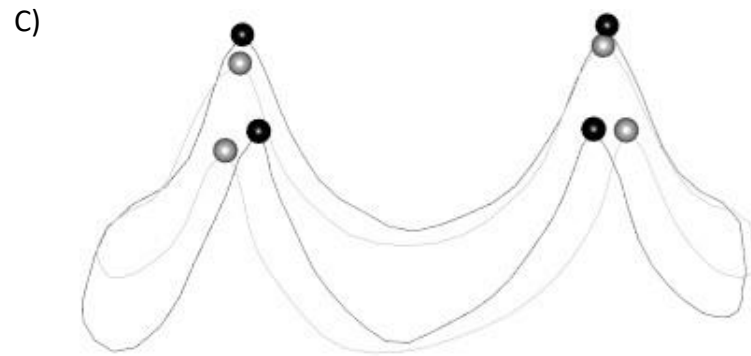
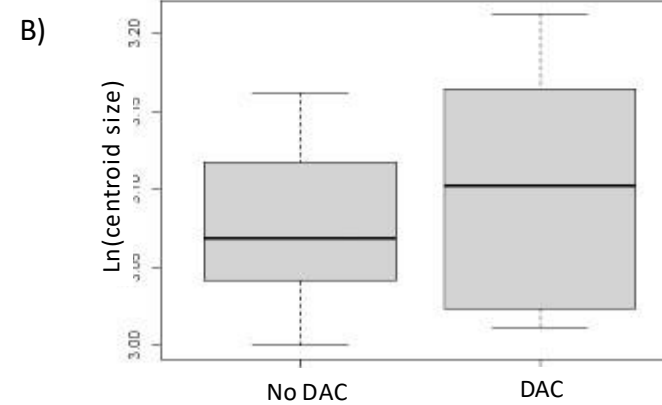
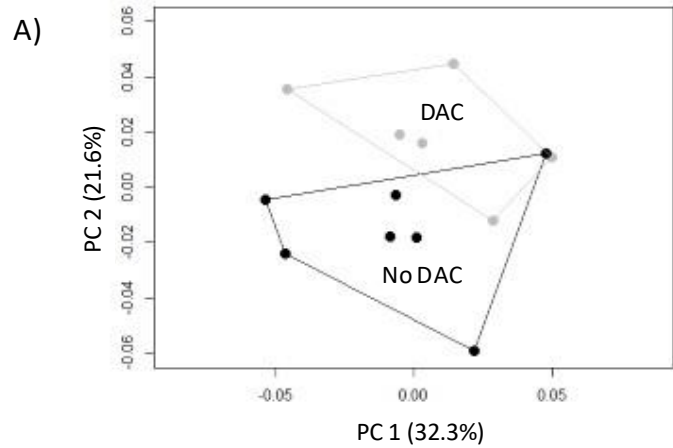


Figure 9. (A) Plot of the first and second principal components of an analysis of whole tooth shape variation between molars with variable expression of a DAC. (B) Centroid size of macaque lower second molars with and without a DAC. (C) Exaggerated wireframe model of the shape change along PC1 (exaggerations defined as two standard deviations from the mean). Lingual view. (D) Exaggerated wireframe model of the shape change along PC2. Lingual view. (n=11).



- + PC1 - taller and more closely spaced cusps, low mesial and distal ridge
- - PC1 - shorter and closer spaced cusps, deeper buccal and lingual fovea
- + PC2 - closer spaced cusps, mesial lean to distal dentin
- - PC2 - wider spaced cusps, short distal marginal ridge

Figure 10. Plot of the first and second principal components of an analysis of EDJ ridge shape variation between molars with variable expression of a DAC. (B) Centroid size of macaque lower second molars with and without a DAC. (C) Exaggerated wireframe model of the shape change along PC1 (exaggerations defined as two standard deviations from the mean.) Lingual view. (D) Exaggerated wireframe model of the shape change along PC2. Lingual view. (n=13).

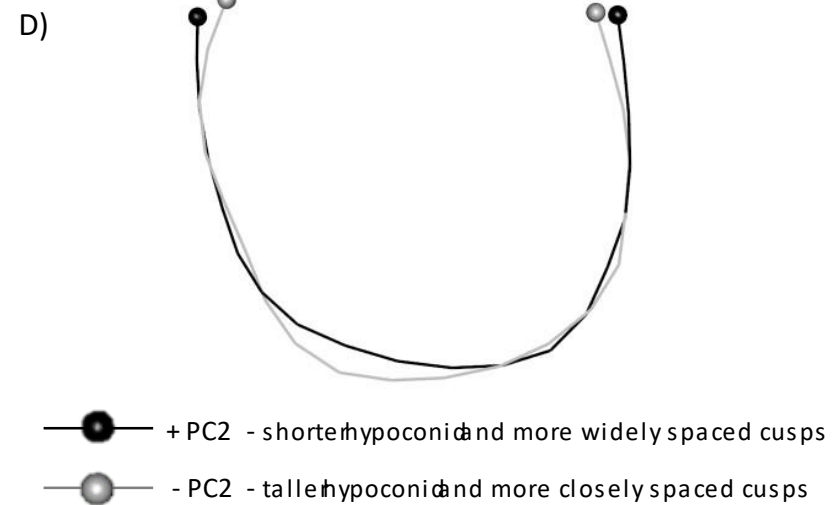
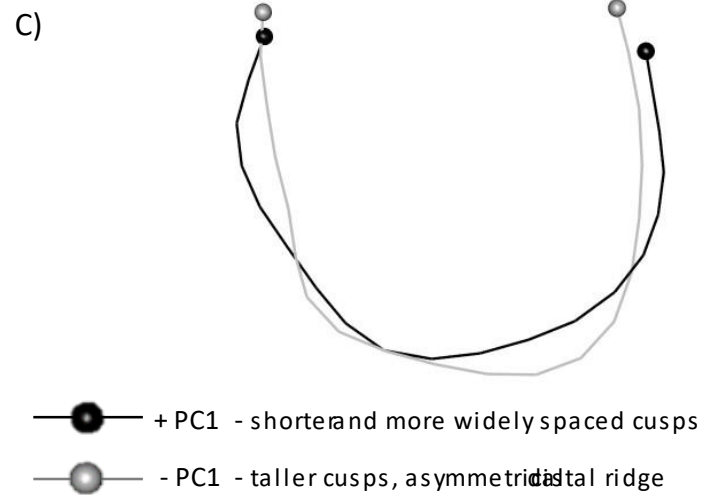
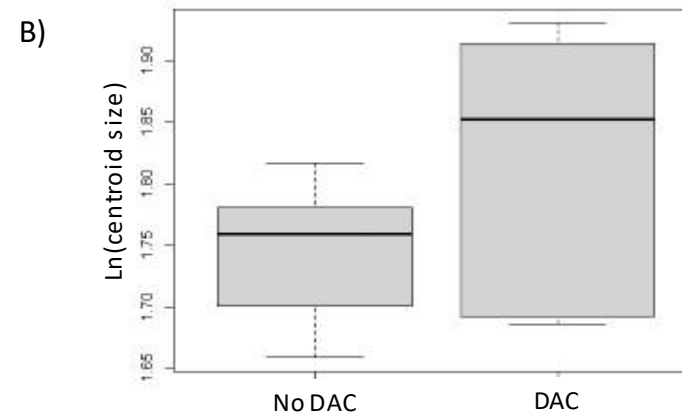
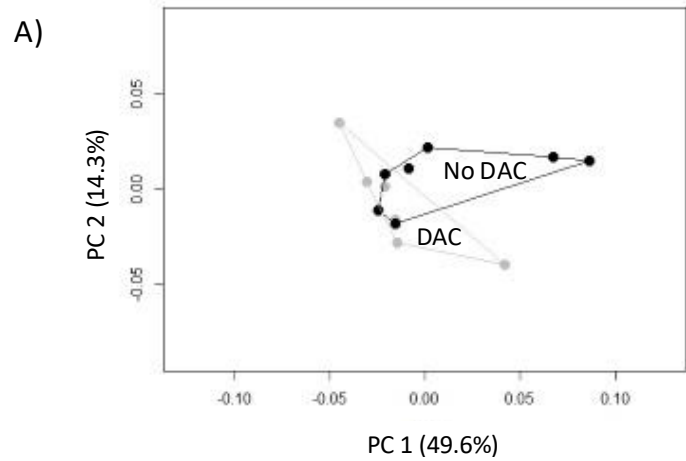


Figure 11. Plot of the first and second principal components of an analysis of the isolated distal ridge shape variation between molars with variable expression of a DAC. (B) Centroid size of macaque lower second molars with and without a DAC. (C) Exaggerated wireframe model of the shape change along PC1 (exaggerations defined as two standard deviations from the mean.) Distal view. (D) Exaggerated wireframe model of the shape change along PC2. Distal view. (n=13).

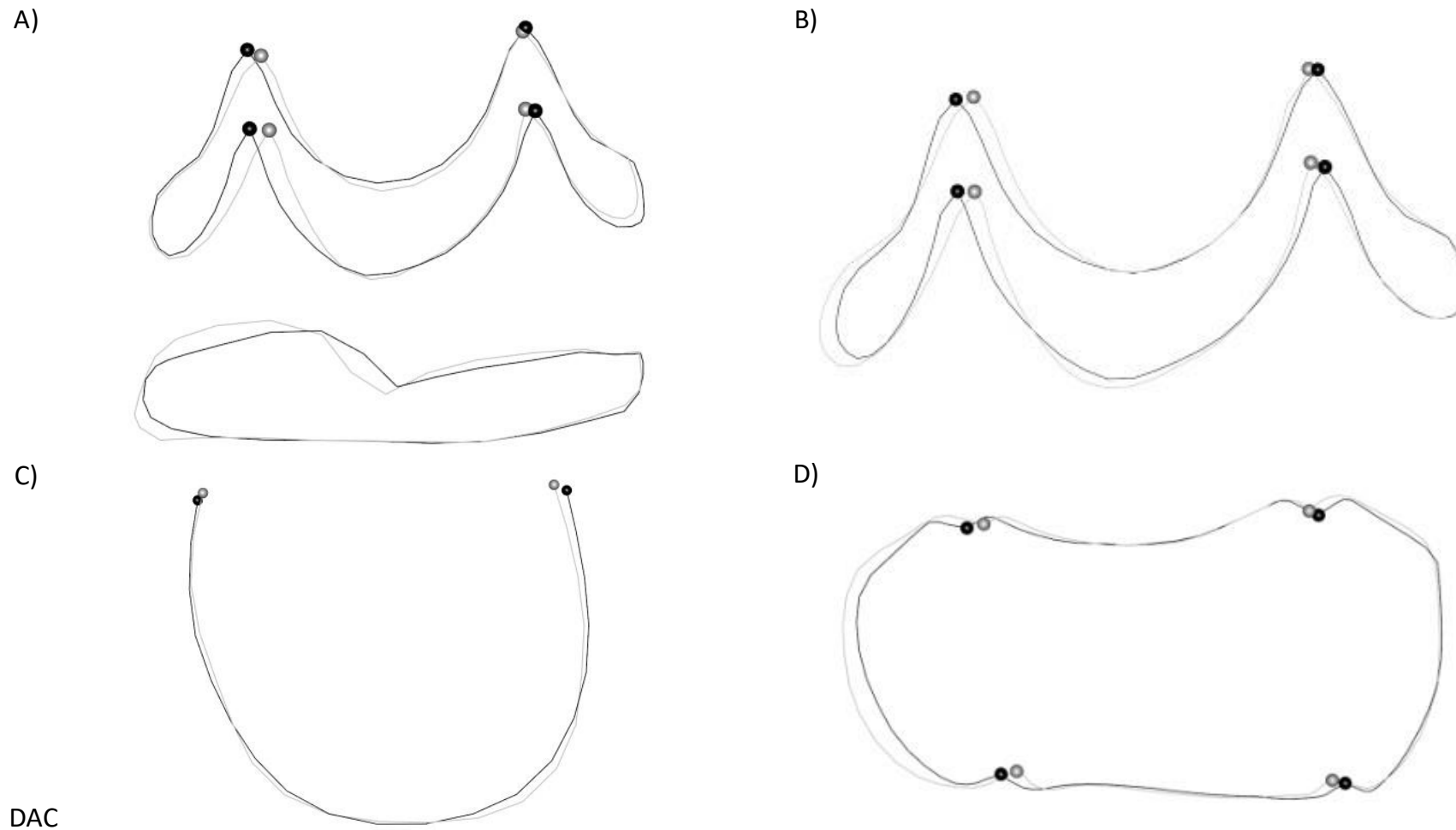


Figure 12. Mean landmark configurations for specimens with and without a DAC. Black = DAC absent. Grey = DAC present. (A) Whole tooth mean model. Lingual view.; (B) EDJ ridge mean model. Lingual view; (C) Isolated distal ridge mean model. Distal view; (D) EDJ ridge mean model. Occlusal view.

CHAPTER 5: Primate Tooth Crown Nomenclature Revisited

Abstract

Cusp patterning on living and extinct primate molar teeth plays a crucial role in species diagnoses, phylogenetic inference, and the reconstruction of the evolutionary history of the primate clade. These studies rely on a system of nomenclature that can accurately identify and distinguish between the various structures of the crown surface. However, studies at the enamel-dentine junction (EDJ) of some primate taxa have demonstrated a greater degree of cusp variation and expression at the crown surface than current systems of nomenclature allow. In this study, I review the current nomenclature and its applicability across all the major primate clades based on investigations of mandibular crown morphology at the enamel-dentine junction revealed through microtomography. From these observations, I reveal numerous new patterns of lower molar accessory cusp expression in primates. I highlight numerous discrepancies between the expected patterns of variation inferred from the current academic literature, and the new patterns of expected variation seen in this study. Based on the current issues associated with the crown nomenclature, and an incomplete understanding of the precise developmental processes associated with each individual crown feature, I introduce these structures within a conservative, non-homologous naming scheme that focuses on simple location-based categorisations. Until there is a better insight into the developmental and phylogenetic origin of these crown features, these categorisations are the most practical way of addressing these structures. Until then, I also suggest the cautious use of accessory cusps for studies of taxonomy and phylogeny.

5.1 Introduction

Primate dental morphology plays a critical role in reconstructing the phylogenetic relationships (Wood and Abbott, 1983; Bailey, 2000; Pilbrow, 2003; Skinner et al., 2009; Singleton et al., 2011), diet (Kay, 1977; Bunn et al., 2011; Cooke, 2011), and ethology of mammalian taxa (Ungar, 2004; Seiffert et al., 2005). The occlusal surface of tooth crowns in particular often exhibits a complex and variable suite of morphological features that are extensively used in systematics, functional and comparative morphology, and the reconstruction of the evolutionary history of the primate clade. For over a century the study of the occlusal surface of tooth crowns has required a system of nomenclature that identifies various structures such as cusps and crests. However, over this time the current system of nomenclature has become beset by a number of problems regarding definitions of named structures, multiple names for the same structure, and a growing conflict between current models of tooth crown development (influenced in particular by advances in developmental genetics), and the fundamental paradigm upon which the nomenclature is based. Our primary research question is therefore whether current systems of nomenclature are sufficient to accurately describe crown morphology across all Primate groups. In this study, I review the current nomenclature and its applicability across all the major primate clades, based in particular on our novel investigation of the detailed aspects of mandibular crown morphology at the enamel-dentine junction revealed through microtomography.

The most widely used and established system of nomenclature was initially developed from Edward Drinker Cope's work on the evolution of mammalian tooth form, and Henry Fairfield Osborn's elaboration of these ideas into a nomenclature (Cope, 1883; Osborn, 1888). Cope's work described a model for the evolution and development of tribosphenic, multicuspid molars from the primitive cone-shaped teeth of mammalian ancestors. According to the

model, the ancestral condition was haplodonty; a single, cone-shaped structure that Osborn (1888) called the protocone for the upper dentition, and protoconid for the lower dentition (See Figure 2. in section 1.6). Two additional cusps then developed from this cone, initially in mesial and distal orientation to the protocone(id), and were named the paracone(-id) and metacone(-id), respectively. From this triconodont configuration, Cope believed the paracone and metacone of the upper teeth migrated in a buccal direction, while the protocone moved lingually, creating a V-shaped symmetrodont configuration. In the lower molars, a similar migration of cusps was thought to have occurred. However, in this case the paraconid and metaconid rotated lingually relative to the protoconid, creating a reversed triangle configuration between upper and lower dentitions. In the quadritubercular upper molar, a fourth cusp distal to the protocone later formed on a low shelf and was named the hypocone. In the lower molars, a low shelf also formed distal to the symmetrodont triangle, from which developed the entoconid on the lingual margin, the hypoconid on the buccal margin, and the hypoconulid on the distal margin. In addition to the primary cusps of the mammalian molar, secondary features of upper and lower molars were named using the prefixes associated with their neighbouring primary cusps, along with an appropriate suffix to denote the type of feature in question (conules or conulids for cusps, and crista or cristid for crests). For crests, these names are further preceded with a pre- or post- connotation to indicate the location or 'direction' of the crest relative to the anterior-posterior orientation of the tooth and associated cusp.

Unfortunately, as researchers began to identify and study new fossil species, it became clear that some stages of evolution described by Cope and Osborn's model did not form a strict phylogenetic sequence as they had assumed. Additionally, it is now known that multicuspid

configurations developed independently in several therapsid groups, and that the cheek teeth of the earliest known mammals were not haplodont (Patterson, 1956; Butler, 1978). Ultimately, Cope and Osborn had misinterpreted cusp homologies and got the order of cusp appearance wrong. As a consequence, Osborn's nomenclature, which was originally intended to denote evolutionary processes and historical homology, was found to be flawed. Palaeontological evidence now indicates that the primitive cusp of early upper and lower molars is the mesio-buccal cone, or the paracone and protoconid of Osborn's nomenclature (Butler, 1978). Furthermore, the mesial cusp of the triconodont configuration is not the paracone seen in extant taxa, but is now recognised as the stylocone (Butler, 1978). While the metacone is still homologous with the metaconid, the other upper and lower primary cusps of the same prefix are no longer considered homologous. Such fundamental flaws in nomenclature resulted in what Hershkovitz (1971, p.95) described as the "corruption of dental evolutionary thought through use of similar terms for non-homologous upper and lower dental elements, and dissimilar terms for the homologous element(s)".

Since the introduction of Osborn's nomenclature, numerous alternative systems and names have been devised and adopted, either to address some of the known issues of homology that had been recognised in Osborn's terminology, due to a perceived better representation and corresponding description of the feature in question, or in an attempt to communicate a structure in a way that is free of developmental implication. In some cases, this involved a substantial revision and a proposal of a new system (Vandebroek, 1961), while in other cases it simply involved the introduction of new terms as they were recognised and studied (Dahlberg, 1950). In 1961, Vandebroek proposed a new system of nomenclature for tribosphenic molars that attempted to address some of the issues in Osborn's terminology

(e.g., suggesting the term 'eocone' for the 'paracone', and 'epicone' for the 'protocone'). However, despite some support and use of this system in the academic literature, it was not widely accepted. A decade later, Hershkovitz (1971) proposed his revision of the nomenclature that suggested to serve as a "master plan of coronal pattern of upper and lower eutheromorphic molars" (p. 135). This system maintained some of Osborn's terms, adopted the eocone and epicone of Vandebroek (1961), and introduced several new terms and previously unstudied dental elements. This resulted in a nomenclature that acknowledged 92 different features on the upper and lower molar crown. While several aspects of this amalgamated nomenclature were adopted, many previously proposed terms were preferred and maintained, resulting in a mosaic, interchangeable, and highly inconsistent nomenclature that varies in its use of the many positional, Osbornian, numerical, Latin, and clinical terms that currently exist (Figure 1).

Due to the convoluted history of the current nomenclature, the above noted proliferation, mixing, and multiplication of terms, and the influence that individual researchers working on particular mammalian groups has had on the current nomenclature, a number of issues should be acknowledged and addressed. First, early systems only described the basic morphologies, did so with simple descriptions or diagrams, and the original description is often difficult to reconcile with more recent systems. Second, many nomenclatures attempt to apply their systems to taxonomically broad groups (e.g., all primates/mammals). However, while these, in principal, can allow for discourse on the evolution and homology of dental crown features across wide groups, in reality they become burdened by inconsistencies or inapplicability to the variation that is present in the groups they are applied to. For example, terminologies initially created based on observations of crown morphology of a specific clade

of mammal (e.g., Gregory, 1916), may be unsuitable for all primates. Third, many of the current systems do not provide enough topographical information (both directional and positional) to ensure their accurate use (e.g., the interconulid and the varied use of this term for different morphological structures). Similarly, some systems are very complex and require the identification of a single and specific term from a diagram with many closely-positioned but distinct features (e.g., Hershkovitz's many ectostylid forms). Additionally, some terms reflect assumptions about the developmental origin of the feature and/or their association with adjacent features, when we lack direct evidence of an actual developmental link. Fourth, some systems still maintain names for features that are associated with an extinct nomenclature, such as the inappropriate use of the term eoconulid if one is not using the term eoconid for the mesio-buccal primary cusp (e.g., Vandebroek, 1961). Finally, as new terms were often introduced as direct equivalents to previously named features, authors have attempted to provide lists of current terms and synonyms that are considered equivalent. However, due to many of the factors discussed above, these synonyms are not always accurate and therefore introduce further error into the system (Swindler, 2002 and the many synonymic errors in Table 1.2).

Of particular relevance to the modern application of tooth crown nomenclatures is our growing understanding on the developmental processes that control cusp patterning on tooth crowns. In particular, advances in our understanding of multicupid tooth development suggest that accessory cusp presence and expression may not be predetermined, and may instead be based on a number of upstream factors such as the size, shape and location of the surrounding primary cusps and tooth germ (Jernvall, 2000; Jernvall and Thesleff, 2000). This process has been called the patterning cascade model of cusp development (Polly, 1998), and

suggests that accessory cusp initiation and patterning may be an iterative process that is particularly sensitive to small variations in the shape and positionings of earlier-forming, neighbouring cusps. This iterative nature of cusp patterning is important when evaluating the appropriateness of detailed aspects of a nomenclature. For example, most systems of nomenclature allow for the presence of between four and seven cusps on hominoid lower molars. However, Skinner et al. (2008) showed that up to nine cusps can be present, with many of these displaying variable degrees of expression and positioning along the occlusal surface. Traditionally, practitioners have used terms such as 'double' to denote the presence of two cusps in a particular region, however, these terms do not appear to accurately reflect their developmental origin (Skinner et al., 2008).

A major advance in our ability to visualize and interpret tooth crown morphology for the purpose of revisiting primate crown nomenclature has come from high resolution imaging of the enamel-dentine junction (EDJ). The EDJ preserves the morphology of the basement membrane of the developing tooth germ prior to mineralization (Nager, 1960; Krause & Jordan, 1965), and therefore represents the first stage of crown development in which cusps and crests appear. Imaging the EDJ has been shown to not only to record the presence and size of dental crown features with increased accuracy, but also allows greater insights into the developmental origin and individual morphology of dental traits (Skinner et al., 2008, 2010). For example, Martinez de Pinillo et al. (2014) and Martin et al. (2017) addressed the potential taxonomic and phylogenetic utility of dental non-metric traits at the EDJ in Late Pleistocene hominins and modern humans, while others have addressed concerns regarding the homology and identity of certain crown features previously described at the outer enamel surface in fossil hominins (Anemone et al., 2012; Ortiz et al., 2018; Davies et al., 2021).

The aim of this study is to critically evaluate the current nomenclature scheme used for primate molar crowns, using micro-computed tomography (micro-CT) to image the EDJ in a taxonomically broad sample of primate mandibular first and second molars. Currently, this study is isolated to mandibular molars due to the extensive time and financial costs associated with CT scanning. The study has three objectives. The first is to document variation in cusp patterning within major clades of the order Primates. Having done so, I can investigate my primary research question regarding the suitability and applicability of current nomenclature schemes to each Primate clade. This will also allow us to propose clade-specific nomenclatures when/if appropriate. Finally, I present an updated approach to the use of nomenclature schemes for the purpose of primate systematics.

5.2 Materials

The study sample is shown in Table 1. The sample consists of mandibular first and second molars from 420 specimens, representing 71 primate species (a complete list of specimens is provided in the Supporting Information). The study sample was selected to include species from all major clades. Sex was not considered as there is no evidence that it impacts the presence of cusps. Sample sizes for some species are low due to difficulties in identifying and microCT scanning specimens with unworn mandibular molars (this is particularly challenging as most primate species are relatively thin-enamelled). Specimens with low to moderate attrition were included as it did not impact our ability to identify particular crown features with confidence. Due to these small sample sizes, the frequency of traits is not assessed and no statistical analyses are conducted.

5.3 Methods

Specimens were scanned on a number of different microCT systems including beamline ID 19 at the European Synchrotron Radiation Facility (ESRF, Grenoble, France), or a BIR ACTIS 225/300 or SkyScan 1172 microtomographic scanner at the Department of Human Evolution, Max Planck Institute for Evolutionary Anthropology. Scanning was conducted under standard operating conditions following established protocols (Olejniczak et al., 2007). Scan resolution varied between 10-60 microns. This resolution is sufficient to identify small crown features, although it is acknowledged that very tiny dentine horns may be poorly resolved making their assessment difficult. Individual molars were initially cropped in Avizo 9.0 (www.thermofisher.com). To facilitate tissue segmentation, image stacks of each molar were then filtered using a 3D mean-of-least-variance filter with a kernel size of one. This process sharpens the boundaries between enamel and dentine (Schulze and Pearce, 1994), allowing for a clearer segmentation of tissue types. Filtering was implemented using MIA open-source software (Wollny et al., 2013). Enamel and dentine were segmented in Avizo 6.3 using a seed growing watershed algorithm employed via a custom Avizo plugin, before being manually checked. After segmentation, triangle-based surface models of the EDJ were produced using the generate surface module in Avizo, and then saved in polygon file format (.ply).

For the purpose of evaluating current nomenclatures and creating new nomenclatures species are grouped at the highest taxonomic level possible where similarities in mandibular crown morphology allow. In the results section for each group, I first create a 'current variation' schematic based on a review of the published literature that acknowledges crown features that have previously been observed and discussed. In many cases, this has never

been assessed at the taxonomic levels that I identify here as relevant and necessary. I then report on crown feature variation at the EDJ present in the study sample and propose a ‘new’ expected variation schematic for each group. Davies et al. (2021) recently proposed the adoption of conservative terms for accessory cusps on hominin lower molars due to difficulties in defining variations in dentine horn presence on the lingual and distal marginal ridge of the EDJ. Specifically, they adopted the terms distal accessory cusp(s) and lingual accessory cusp(s) instead of cusp 6 and cusp 7, respectively. Our observations of accessory cusp presence on lower molars in this study sample reinforce the utility of the use of such generic terms and here I expand this to both the mesial and buccal marginal ridges of the EDJ, as well as, the cingulum (Figure 2). As a result, I propose the following terms to classify accessory cusps (AC) on the marginal ridge of the EDJ that runs between the four primary cusps (protoconid, metaconid, entoconid, hypoconid): DM – distal margin; LM – lingual margin; MM – mesial margin; BM – buccal margin. Additionally, I propose the following terms to classify accessory cusps on the cingulum: BC – buccal cingulum; LC – lingual cingulum. By introducing each feature within a scheme that focuses on simple location-based categorisations, there is no inference of homology. Until there is a better insight into the developmental processes and phylogenetic history associated with each individual crown feature, these categorisations appear to represent the most practical and safest way of addressing these structures in studies of dental morphology.

5.4 Results

5.4.1 Strepsirrhini

In the family Lemuridae, the two mesial primary cusps are compressed bucco-lingually, are set close together, and are connected by a transverse crest. A distinct crest also traverses down the mesial slope of the protoconid, where it eventually turns and proceeds disto-lingually as a broad ledge to the base of the metaconid. The hypoconid and entoconid are not connected by a crest, and the talonid basin is shallow and circumscribed by the marginal ridge. The entoconid is absent in *Varecia variegata* (Schwartz and Tattersall, 1985). While a paraconid was present in fossil notharctids of the early Eocene (Gregory, 1920), it is absent in extant Lemuridae. Cuzzo and Yamashita state that lemurids “have lost the paraconid and lack a hypoconulid” (2006, p.76), however Swindler (2002, p.69) describes the presence of a “distal heel-like process” in some members of this clade and considers it to be a true hypoconulid. Swindler (2002) also reports the presence of a *tuberculum intermedium* in all six *Haplemur griseus* lower first molars, and in five of the six second molars. Similarly, Schwartz and Tattersall (1985) describe a thickening of the postmetacristid in *Lemur catta* molars that results in the expression of what they term a ‘metastylid’. Some form of buccal cingulid expression is noted in all Lemuridae molars. Thus, the current variation scheme can be summarized with four primary cusps, a hypoconulid on the distal ridge, and a *tuberculum intermedium* on the lingual ridge (Figure 3A). Our observations support descriptions of a cusp on the distal marginal ridge of some specimens (Figure 3D), which I identify and label as a DMAC in the new schematic for lemurid (Figure 3B). Additionally, I also corroborate the reports of accessory cusp presence on the lingual marginal ridge, with LMACs observed in the *Prolemur simus* and *Eulemur fulvus* specimens in our sample (Figure 3E and 3F respectively). The image of the *Varecia variegata* specimen (Figure 3G) demonstrates the absence of an entoconid in this taxon, but the expression of several LMACs along the marginal ridge.

The family Lepilemuridae consists of only one extant genus, *Lepilemur*. The molars have four primary cusps, with a diagonal transverse crest connecting a mesially-placed protoconid to a comparatively more distally-placed metaconid. Swindler (2002) reports that the crest travelling down the mesial slope of the protoconid may connect with the mesio-buccal elevation of the cingulid, forming a mesiostylid where two crests join. Descriptions also note a distinct and complete buccal cingulid, and a strong cristid obliqua that terminates on the lingual side of the protoconid (Schwartz and Tattersall, 1985). While there has been limited commentary regarding accessory cusps expression in this clade, the potential presence and identification of a fifth cusp has been extensively discussed (James 1960; Seligsohn and Szalay 1978; Schwartz and Tattersall 1985). Unfortunately, these discussions remain focused on hypoconulid expression in lower third molars, and there is little mention of similar manifestations in first or second molars. A further topic of debate is the identification of the cusp positioned distal to the metaconid. Based on comparisons with other strepsirhines like indriids and *Copelemur*, Schwartz and Tattersall (1985) suggest that the entoconid is absent in *Lepilemur* and that the cusp distal to the metaconid is a metastylid. Swindler (2002, p.72) argues that “an obvious developmental groove” that separates the two cusps at the outer enamel surface would suggest that Schwartz and Tattersall’s (1985) metastylid is the entoconid. The current variation schematic for this clade therefore includes a hypoconulid, and a potential entoconid or metastylid (Figure 4A). Our two *Lepilemur* specimens do not demonstrate the presence of a mesiostylid or hypoconulid (Figure 4C-H). Nevertheless, due to sample size limitations, I cannot rule out their existence in other individuals and therefore include MMAC and DMAC features in the new schematic for Lepilemuridae (Figure 4B). Figure 4D and 4G reveal lingual crown morphology at the EDJ surface, and in particular, the positioning and appearance of the cusp distal to the metaconid.

Unlike LMAC expression in our Lemuridae sample, which are positioned on the distal slope of the metaconid, the disto-lingual cusp in *Lepilemur* sits further back on the crown and appears developmentally distinct from the metaconid. As such, I label it the entoconid in our new schematic (Figure 4B). No other features of relevance were identified.

In the family Cheirogaleidae, the protoconid and metaconid are closely positioned, and are connected by a transverse crest that separates a small trigonid from a spacious talonid basin. In *Cheirogaleus major*, Schwartz and Tattersall (1985, p.38) remark that the molar cusps “lack virtually all detail and delineation of individual features”, and that structures can therefore only be discussed in a vague sense. Descriptions of hypoconulid expression in cheirogalids are restricted to *Microcebus* lower third molars (James, 1960; Schwartz and Tattersall, 1985; Cuzzo et al., 2013), while Swindler (2002) reports the presence of a buccal cingulid in all lower molars. Thus, the current variation scheme can be summarized as a relatively simple tooth crown with only four primary cusps (Figure 5A). Our assessment of *Cheirogaleus* molars is in agreement with the comments regarding a lack of discernible features by Schwartz and Tattersall (1985). Even from the detail provided by high resolution images of the EDJ, *Cheirogaleus* molars lack any clearly defined cusps (Figure 5C and 5D). As such, commentary regarding potential accessory cusp expression in this taxon is avoided. Contrastingly, in our *Phaner furcifer* specimen, a prominent buccal cingulid accompanies four well-defined primary cusps. Figure 5E demonstrates the presence of a large BCAC on the buccal cingulid, which represents the only addition to the new expected variation schematic for Cheirogaleidae molars (Figure 5B).

The molars of Indriidae have four well-formed primary cusps. In the lower first molars, the protoconid is mesial to the metaconid, and the mesial marginal ridge is incomplete mesio-lingually. At the terminus of this incomplete ridge, Swindler (2002) mentions the presence of a parastylid. In the lower second molars, the protoconid and metaconid are positioned at similar mesio-distal positions on the crown, the mesial marginal ridge is complete, and the cusps are also connected by a faint transverse crest. Hypoconulid presence is only referenced in relation to lower third molars (Swindler, 2002). Bennejeant (1936) mentions the frequent appearance of a *tuberculum intermedium* on the distal surface of the metaconid in *Avahi*, while Schwartz and Tattersall (1985) also report the presence of an equivalent feature at the terminus of a thick postmetacristid. The current variation scheme provided therefore incorporates both parastylids and *tuberculum intermediums*, in addition to four primary cusps (Figure 6A). It should be noted that both in the relative positioning of the cusps, and the arrangement of the marginal ridge, these schematic diagrams remain relatively accurate for lower first molars but do not reflect the general shape and patterning of some Indriidae lower second molars. Our observations of indriid molar morphology at the EDJ found no evidence for hypoconulid (or DMAC) expression in our sample. Figure 6C demonstrates the incomplete mesial marginal ridge in an *Indri indri* first molar, while Figure 6D shows the presence of a small MMAC on the complete marginal ridge of a second molar. No LMACs were observed in this sample, however Figure 6E demonstrates the thick lingually deflected postmetacristid in *Avahi* described by Schwartz and Tattersall (1985). Despite not observing a lingual accessory cusp in this sample, the new schematic for Indriidae includes the presence of an LMAC (Figure 6B), along with the MMAC observed in the *Indri* lower left second molar.

In the family Galagidae, the first and second molars have four primary cusps, and a well-developed cristid obliqua (Swindler 2002). As is common within many strepsirrhini clades, a compressed crest descends down the mesial face of the protoconid before angling back toward the metaconid as a broad, horizontal ledge. Discussion regarding hypoconulid presence is limited to lower third molars, and mention of a centrally emplaced heel in *Galago senegalensis*, and more lingually displaced heel in *Galago alleni* (Schwartz and Tattersall, 1985). Schwartz and Tattersall (1985) also describe the presence of a protostylid in *Euoticus elegantulus*, as well as a low conulid on the cristid obliqua at the base of the protoconid in *Galago crassicaudatus*. The current variation schematic therefore depicts four primary cusps, a protostylid, and an unnamed conulid on the buccal margin (Figure 7A). From our observations, I demonstrate the presence of multiple DMACs in a *Galago senegalensis* first molar (Figure 7C). In the same specimen I also identify an MMAC positioned where the mesial marginal ridge sharply bends towards the metaconid (Figure 7D). I find no evidence of a protostylid in any galagid specimen, however the lingual positioning of the cristid obliqua and buccal flaring of the protoconid would appear to be consistent with morphological conditions commonly associated with protostylid presence. As such, a BCAC is included in the new schematic (Figure 7B). In relation to the conulid observed by Schwartz and Tattersall (1985) on the cristid obliqua of *Galago crassicaudatus*, I demonstrate the similar presence of a dentine horn distal to the protoconid in *Euoticus elegantulus* that I more appropriately label as a BMAC (Figure 7E).

The family Lorisidae are stated to have four well-developed cusps, a hypoconulid that is restricted to third molars, a prominent cristid obliqua, and a transverse crest that separates

the trigonid basin from a spacious talonid basin (Swindler 2002). In *Arctocebus calabarensis*, Swindler (2002) reports a paracristid that extends down the protoconid and ends as a mesiostylid (Figure 8A). While the presence of a cusp at the terminus or turning point of the paracristid is common in strepsirrhini, I find no evidence of a dentine horn in our current Lorisidae sample. Based on previous observations however, I include the presence of a mesio-buccally positioned MMAC in the new schematic (Figure 8B). Of particular note and relevance in this clade are the observations of distal and disto-lingual accessory cusp expression. *Loris tardigradus*, *Arctocebus calabarensis*, *Nycticebus coucong* and *Perodicticus potto* specimens all demonstrate single and/or multiple DMAC expression on the distal border of the crown (Figure 8C-G). In one of the *Perodicticus potto* specimens (Figure 8F), it may be unclear which of the two disto-lingual cusps is the entoconid, and therefore it is unclear whether this molar has a double DMAC configuration, or a single DMAC and LMAC pattern. However, as the entoconid is situated in a strongly lingual position in our other specimens, our new schematic includes a double DMAC pattern in Lorisidae (Figure 8B).

5.4.2 Tarsiidae

In the family Tarsiidae, the lower molars are tribosphenic, with well-formed paraconid, protoconid, and metaconid cusps, and a broad lower talonid basin with entoconid and hypoconid cusps (Schwartz, 1984). Swindler (2002) describes the presence of a hypoconulid on lower third molars, but no mention of a distal cusp in M1-M2. A cristid obliqua is present, as well as a distinct buccal cingulid in all molars (Swindler, 2002). Thus, the current variation scheme can be summarized as a tooth crown with five primary cusps and no other cusp features (Figure 9A). In addition to a prominent buccal cingulid that continues along the distal

margin of the tooth in some of our sample, I report the presence of multiple accessory dentine horns in Tarsiidae molars. Figure 9A reveals the presence of an LMAC and BMAC in one *Tarsius spectrum* specimen. Figure 9D similarly demonstrates the presence of a BMAC in *Tarsius*, but also a BCAC close to the base of the protoconid. Figure 9E and 9F reveal patterns of multiple DMAC expression in a *Tarsius spectrum* lower first molar, and *Tarsius syrichta* lower second molar. Based on these observations, the new schematic for Tarsiidae has the addition of several accessory cusp features (Figure 9B).

5.4.3 Ceboidea

In the subfamily Callitrichinae, the lower molars have four cusps, with the mesial primary cusps connected by a crest that separates a small trigonid from a much larger talonid basin. The only notable mention of additional features in this clade is the presence of buccal cingulids on the first and second molars in most taxa except *Callimico* (Kinzey, 1973; Swindler, 2002). Thus, the current variation schematic can be summarized as four cusped tooth (Figure 10A). While our observations match previous comments regarding the common presence of buccal cingulids in Callitrichinae, I extend this description by demonstrating that in some cases, these buccal features may express themselves as small dentine horns along the buccal cingulum. Where present, I identify these structures as BCACs (Figure 10C). In addition to the buccal features presented, I also reveal the presence of multiple LMACs on the lingual marginal ridge of a *Leontopithecus rosalia* lower second molar (Figure 10D). *Saguinas* and *Callithrix* specimens in the sample had no discernible crown features of interest (Figures 10E and 10F). Based on these observations, the new schematic has the addition of LMACs and BCACs (Figure 10B).

Cebinae lower molars have four cusps, with a prominent crest that separates the taller trigonid from the lower positioned talonid basin. Swindler (2002) states that the hypoconulid is absent in this clade, as is any form of lingual cingulid. Buccal cingulids are however reported as being variably expressed in all molars (Kinzey, 1973; Orlosky, 1973). The current variation schematic is depicted as a simple tooth crown with the four primary cusps (Figure 11A). Contrary to Swindler's comment's however, I identify the presence of what Swindler (2002) would consider a hypoconulid (or more accurately, a DMAC) in a *Sapajus apella* lower first molar (Figure 11C). Although there was no discernible lingual cingulid in our sample, the same *Sapajus apella* specimen also exhibited a small dentine horn on the outer slope of the metaconid. While this could be identified as a LCAC, lingual cingulid cusps were not observed in other specimens and therefore I tentatively attribute this to developmental abnormality (Figure 11D). Regarding buccal cingulid expression, I corroborate the comments regarding buccal cingulid expression in this group and again identify the presence of a dentine horn (or BCAC) along the buccal cingulum in a *Saimiri sp.* specimen (Figure 11E). Figure 11B illustrates the new schematic that I consider more appropriate and applicable to the cusp configuration of Cebinae lower molars.

In the subfamily Pitheciinae, all molars are commonly stated as possessing four cusps, with a crest connecting the protoconid and metaconid that creates a comparatively narrow trigonid and spacious taloned basin (Swindler, 2002). Very little is mentioned of any additional cusp-like structures in this clade, which may reflect the difficulties presented in identifying dental crown feature at the outer enamel surface in taxa with short cusps and crenulated enamel.

As such, the current variation schematic is depicted as a tooth with only the four primary cusps (Figure 12A). Our observations at the EDJ however identify the frequent presence of accessory cusps on the marginal ridges of Pitheciinae first and second molars. Figure 12C and 12D demonstrates the presence of DMAC and LMAC features in one *Cacajao calvus* specimen, while Figure 12E provides evidence of multiple BMAC cusps on the buccal marginal ridge of a *Chiropotes satanas* lower first molar. In all pitheciinae specimens, I identify the presence of an accessory cusp directly mesial to the protoconid (Figure 12F). Unlike the diminutive nature of most accessory features, this cusp is often comparable in size to the neighbouring protoconid and may be mistaken for the primary cusp in some cases. While I classify this feature as an MMAC in the schematic as it is positioned on the marginal ridge between the protoconid and metaconid, further mention and consideration of this cusp will be made in the discussion. Figure 12B represents a new schematic that I consider more appropriate and applicable to the cusp configuration of Pitheciinae lower molars.

The Callicebinae subfamily in this study is represented by a small number of *Callicebus moloch* specimens, but nevertheless demonstrates the presence of numerous accessory cusp features at the EDJ surface. First and second molars are reported to have four cusps, a small trigonid basin, a larger talonid basin, and a well-defined cristid obliqua (Swindler, 2002). In a sample of 40 *Callicebus torquatus* specimens, a 'distostylid' was identified with a frequency of 56% in lower M1 and 83% in lower M2 (Kinzey, 1973), while Swindler (2002) also remarks on the presence of this cusp in a sample of four *Callicebus moloch*. Distostylids are therefore included in the current variation schematic for Callicebinae (Figure 13A). Our observations at the EDJ point to the presence of several DMACs on the distal marginal ridge (Figure 13E and

13G). Additionally, I identify the presence of several MMACs on the mesial ridge (Figure 13C), and a LMAC on the lingual ridge of a lower second molar (Figure 13F). Finally, I demonstrate the presence of a prominent BCAC on the same second molar (Figure 13D). Figure 13B presents the new schematic of Callicebinae lower molars that I consider to represent crown patterning in this clade.

In the subfamily Atelinae, lower first and second molars have four cusps, with a prominent crest that separates the trigonid basin from a wide talonid basin. In *Ateles*, Orlosky (1973) identifies the presence of hypoconulids in all lower molars. In *Alouatta* third molars, Swindler (2002) reports the regular appearance of hypoconulid and *tuberculum intermedium* cusps, however there is no mention of these features in first and second molars. Clark (1971) also described the presence of paraconid cusps on the lower molars of *Alouatta*. Incorporating these observations, the current variation scheme can be summarized as a tooth crown with four primary cusps, a hypoconulid, and a potential paraconid (Figure 14A). Our observations at the EDJ confirm the variable presence of DMACs on the distal ridge of *Ateles* and *Alouatta* (Figure 14C and 14F, respectively). No MMAC or LMAC were observed in Atelinae first or second molars. Figure 14D demonstrates the lack of discernible features on the lingual ridge of an *Alouatta* specimen. In relation to Clark's (1971) description of a paraconid in *Alouatta*, I find no examples of paraconid expression in our limited sample. Figure 14E does however demonstrate notable lipping and elevation of the mesial marginal ridge in an *Alouatta* individual. As this type of ridge morphology may resemble cusp-like structures at the outer enamel surface in some specimens, I tentatively attribute the descriptions of potential

paraconid expression to this phenomenon and exclude them from the new schematic for Atelinae until they have been confidently detected (Figure 14B).

5.4.4 Cercopithecidae

The two subfamilies of Cercopithecidae are presented separately, and the Cercopithecinae subfamily is further separated into their Cercopithecini and Papionini tribes, due to notable differences in molar morphology and accessory cusp expression between the groups.

In the Tribe Cercopithecini, the molars are bilophodont and have high, well-defined cusps. There are a limited number of studies on variation in crown morphology from this group but from a large sample of guenons, Swindler (2002) reported the lack of hypoconulid presence on all lower molars, but the common expression of a protostylid on the lower molars of *Chlorocebus aethiops* (85% of specimens) and *Miopithecus talapoin* (100% of specimens). Thus, the current variation scheme can be summarized as a relatively simple tooth crown with the four primary cusps and a protostylid located on the mesiobuccal corner of the crown (Figure 15A). Our observations at the EDJ of guenon first and second molars correspond with Swindler's (2002) observations regarding the lack of hypoconulid (or DMAC) presence (Figures 15C, 15D, 15E and 15F). Whether this relates to developmental constraints associated with a notably small distal fovea in this clade, remains to be determined. Unlike Swindler's (2002) observations in relation to protostylid expression however, I find no evidence of a protostylid (or BCAC) in any specimen. This is consistently true, even when alternative definitions of protostylids are adopted (see Hlusko, 2004, and Skinner et al., 2008 for discussion of protostylid definitions). Due to the limited sample size available for this study, I cannot rule out the presence of a BCAC in some individuals and thus it is included in our new

Cercopithecini schematic (Figure 15B). Unlike the other Cercopithecidae groups, no other cusp features beyond the four main cusps were observed.

In the Tribe Papionini, molars are bilophodont and display a pronounced buccal flare. Swindler (2002) reports that accessory cusps are variably expressed in several members of this tribe, although are more commonly observed in *Macaca* and *Papio* molars. In *Macaca fuscata* lower second molars, *tuberculum intermedium* presence on the lingual aspect of the crown was reported in 38% of specimens, and in 56.8% of *Papio* first lower molars (Swindler, 2002). These features are therefore incorporated into the current variation scheme for Papionini (Figure 16A). While our observations match Swindler's comments regarding the common presence of a *tuberculum intermedium* cusp (or LMAC) in Papionini molars, I extend this description by demonstrating the presence of multiple lingual accessory cusps on the marginal ridge between the metaconid and entoconid in some taxa (Figure 16C). In these specimens, LMACs are often positioned either deep within the lingual fovea, or on the distal shoulder of the metaconid. Currently, no more than two LMACs have been observed on any Papionini lower M1 or M2, however the new nomenclature allows for the addition of extra cusps if observed. Regarding distal accessory cusp expression, Swindler (2002) comments that it is well known that a shelf or cusp extends from the distal surface of Papionini molars, and that in the lower M3, it is considered the hypoconulid. Szalay and Delson (2013) describe in *Theropithecus* molars the presence of a "large distal accessory cuspule, which projects backward towards the succeeding tooth" (p.375). There is no indication of a name from Szalay and Delson (2013) regarding this structure and how they would define it, however Swindler (1983) has suggested that the distal cusps on the lower M1-2 are serially homologous with

the hypoconulid of the M3. It should be noted however, that this is based on topographical and functional associations, not phylogenetic. Our studies at the EDJ support the comments regarding the common observation of distal accessory cusps in Papionini molars. Developing on these descriptions, I report a variable and complex pattern of cusp expression in this clade, including the large single cuspules described by Szalay and Delson (2013), as well as the common occurrence of multiple dentine horn presence along the distal ridge (Figure 16D, 16E, and 16F). Importantly, from the images of multiple distal accessory cusp expression in this clade, I would argue that even if one wishes to label these features within the current system of nomenclature, the identification and differentiation of a 'hypoconulid' from the other cusps present could not be made with confidence. As such, I consider this to support the adoption of the term 'DMAC' for all distal accessory cusps in this clade.

In relation to cusp features beyond the cusps commonly situated on the buccal and distal aspects of the crown, Hlusko (2002) studied variation in 'interconulid' expression among a large sample of *Papio hamadryas*, and identified some form of expression in almost the entire collection (95%). In this case, Hlusko (2002) used Swindler's (1976) definition of an 'interconulid' as a stylid between the protoconid and hypoconid of mandibular molars. As previously mentioned however, photographs provided of interconulid expression types in this study appear to show features on the buccal cingulum and perhaps better reflect what has previously been termed an 'ectostylid' (Kinzey, 1973). Nevertheless, similar buccal features have also been observed at the EDJ in our sample. These include cusp-like structures on the buccal marginal ridge, and on the buccal cingulum (Figure 16H). Based on the potential confusion regarding the term interconulid, and the acknowledgement of cusp-like features

on the buccal marginal ridge (which do not appear to have a suitable or commonly referenced name), I incorporate BMAC (buccal marginal accessory cusp) and BCAC (buccal cingulum accessory cusp) terms into the new nomenclature to facilitate the identification and differentiation of these features (Figure 16B). Additionally, I also demonstrate the presence of MMACs (mesial marginal accessory cusps) on the mesial marginal ridge of Papionini molars. Similar to DMAC presence in Papionini M1-M2, patterns of MMAC expression vary from absent to multiple dentine horn expression along the marginal ridge (Figure 16G).

In the other subfamily of Cercopithecidae, the Colobinae, there is limited discussion in the literature of any particular morphological feature on the molar crowns that may be of interest to this study. The Colobinae are described as having four cusps on the first and second molars, with a variably expressed hypoconulid on the M3. Swindler (2002) notes the variable presence of a *tuberculum intermedium* in *Rhinopithecus* on the lower M1 (7%) and M2 (62%), and on the M1 (9%) of *Pygathrix*. The current nomenclature for this clade can therefore be summarized as a simple tooth crown with four primary cusps, and a potential C7 (aka LMAC) on the lingual marginal ridge (Figure 17A). While *Rhinopithecus* is not included in our sample, I see no examples of what I would consider a LMAC in any of our Colobinae specimens. Nevertheless, due to low sample sizes among some groups, and incomplete representation of the whole subfamily of Colobinae, I cannot rule out the presence of lingual accessory cusps in some individuals, and would recommend the LMAC designation for these features in future studies. Figure 17C shows the presence of a DMAC in a *Colobus guereza* lower right second molar, and a DMAC in two *Presbytis melaophos* molars (Figure 17D and 17E). Specimens F-H in Figure 17 demonstrate the simple M1/M2 molar morphology in this clade, and lack of

discernible accessory features within these specimens. Based on these findings, the new schematic has the inclusion of both LMAC and DMAC (Figure 17B).

5.4.5 Hominoidea

In the family Hominidae, molars generally have five main cusps, arranged in a Y-5 pattern. Importantly, because the fifth cusp (or hypoconulid) is consistently expressed in M1-M2 in this clade, it is not considered to be an accessory feature and is included as a 'hypoconulid' in the following schematics. Further dialogue regarding the inclusion of the term hypoconulid in this clade follows in the discussion. In addition to these five cusps, the variable presence of a *tuberculum sextum* and *tuberculum intermedium* are commonly reported in certain members of this clade. Swindler (2002) reports that *Gorilla* have the highest frequency of C6, while *Pongo* have the least. Previous studies of dental trait expression at the EDJ have provided a more detailed analysis of C6 and C7 expression in hominoids, noting variation in the placement of the accessory dentine horns on their respective marginal ridges, as well as observations of double C6 in some Homininae specimens (Skinner et al. 2008). The current variation schematic can therefore be summarized as a tooth crown with four primary cusps, a variable C7 cusp, and multiple potential C6 cusps (Figure 18A). Our observations corroborate the presence of multiple DMACs on the distal ridge between the hypoconulid and entoconid of some Homininae molars (Figure 18C and 18D). Assuming that the larger of the two distal cusps is the hypoconulid, Figure 18D demonstrates the rare presence of a DMAC between the hypoconulid and hypoconid. While variation in the patterning and placement of these cusps may reflect developmental differences in their formation and expression, I still consider the use of the term DMAC for all distal accessory cusps appropriate as it does not intend to imply

homology. In addition to DMAC expression, I also note the presence of LMACs in several of our Hominidae sample. Figure 18E and 18F demonstrate the presence of single LMACs in a *Homo sapiens* and *Gorilla gorilla* specimen respectively. No other accessory features were observed. As such, the new schematic of Hominidae lower molars does not include any new features but does replace C6 and C7 terms with the more appropriate DMAC and LMAC designations (Figure 18B).

In the family Hylobatidae, the lower molars possess five cusps, a narrow trigonid, and a more spacious talonid basin. Reports of a Y-5 pattern follow frequencies of roughly 100% in LM1, and 97% in LM2 (Frisch, 1965; Swindler, 2002). Swindler (2002) reports *tuberculum intermedium* expression of 0.07% in LM1 and 18% in LM2 in a sample of *Hylobates* molars. Tuberculum sextum presence, or any other form of accessory trait expression, was not discussed. The current variation schematic can be summarized as a crown with four primary cusps, a prominent hypoconulid, and a potential *tuberculum intermedium* (Figure 19A). From our observations, I identify the presence of a small DMAC between the hypoconulid and entoconid in a *Hylobates muelleri* M2 (Figure 19C), and a single example of a very mesially-positioned LMAC in *Hylobates muelleri* M1 (Figure 19D). No dentine horns beyond the five primary cusps were observed in our *Symphalangus* sample (Figure 19E and 19F). Figure 19B represents the new schematic of Hylobatidae lower molars that I consider to represent a better reflection of crown patterning in this clade.

5.5 Discussion

Our primary research question was whether current systems of nomenclature are sufficient to accurately describe crown morphology across all Primate groups. This broad study of primate EDJ morphology demonstrates the presence of numerous dental crown features that either have not been previously observed, have not been previously identified in their respective taxa or clade, or display a greater level of variation and complexity than has previously been assumed. I therefore conclude that the current systems of nomenclature are unable to accurately describe crown morphology across all Primate groups. As many of the observed features present further complications and uncertainties to an already challenging and sometimes misleading system of nomenclature, from these results I introduce and discuss each accessory cusp within a proposed system that focuses on a simple location-based categorisation (e.g., BCAC, LMAC, etc.). Until there is a better understanding of the developmental origin, evolutionary history, and forms of variation and expression of these features in each clade, I consider this system to be the most practical way of discussing these structures. Previously, dental morphologists have conceded to naming accessory features within one of the current entrenched systems of nomenclature, despite an awareness of its potential unsuitability. While intentionally void of homological, evolutionary, and developmental information, the system proposed here allows for the clear identification and positioning of crown features, without using a term that is historically or developmentally loaded. As micro-CT scanning and observations of EDJ morphology in primates continue, it is hoped that a better understanding of the various forms of trait expression in each clade can be understood.

In addition to the acknowledgement of novel cusp patterning in numerous primate groups, this study also emphasises the importance of why a single nomenclature or diagram for all

primate molars is impractical. While there is an obvious appeal to the establishment and utilisation of a single nomenclature, the extent of the variation in cusp presence and expression shown in this study demonstrates how this is not possible or justifiable. Based on our limited understanding of the development and phylogenetic history of many of these features at this time, the creation of a single diagram or schematic for all primate molars requires either 1) the inclusion and separation of all crown features seen across all primate groups, creating a densely inhabited collection of individual features that would commonly repeat equivalent structures, 2) or attempt to reduce all observable variation down to a small number of crown features that are topographically similar, which would grossly overlook the subtle but unique crown patterning seen in certain clades. As such, I consider clade-specific diagrams to be the most logical solution. Clade-specific diagrams provided in this study group taxa of similar cusp patterning by the highest taxonomic rank possible, including clades at the family, subfamily, and tribe rank. As molars from additional members of these groups are observed and a deeper understanding of trait expression in each clade is gained, these diagrams may need to adjust their taxonomic rank to accurately reflect and distinguish between new patterns of expression among closely-related taxa.

While the proposed terms and clade-specific diagrams provided here suggest a complete departure from all previous systems of nomenclature for accessory cusps, and thereby a departure from any system that attempts to infer homology or phylogenetic relation, this is not the recommendation for all future work. Currently, based on the variation demonstrated here, I advise the use of the location-based categorisation introduced here as an alternative to the variously flawed current terms. However, when a better understanding of the

development and history of a particular crown feature is known, I encourage the reintroduction or establishment of new, more appropriate terms. Furthermore, a current limitation of this system is its ability to distinguish between two features on the same section of marginal ridge. Reintroducing or establishing new, more appropriate terms should only be attempted, however, if the individual cusp can be consistently and clearly identified to the exclusion of other nearby cusps, is consistently expressed in most/all members of a specific group, and can be identified and tracked through early representative of the clade. Importantly, these new terms should be exclusive to their respective group, and not used to describe similar features in phylogenetically distant taxa. From observations of a large sample of Hominoidea lower molars, I consider the large cusp of the distal marginal ridge to match these criteria and have thus attributed it to the term 'hypoconulid'. Similar (re)introductions may also be appropriate for the accessory cusp directly mesial to the protoconid in Pitheciinae molars, however small sample sizes restrict us from making more definitive assertions.

Based on a need for simplicity and an insufficient understanding of the precise developmental processes responsible for accessory cusp formation, it is sensible at this time to attribute all cusps to the simple location-based categorisations I have provided. However, the expression type and positioning of many cusp features hint at potential variations in the developmental processes or contributory factors responsible for certain cusp patterns that may warrant the introduction of individual and more suitable terms as this variation is understood. For example, while all cusps on the lingual marginal ridge are labelled as LMACs and are often positioned deep within the fovea between the metaconid and entoconid, they also commonly occur on the distal slope of the metaconid (see *Hylobates muelleri* specimen AMNH 103726

in Figure 19D). Skinner et al. (2008) and Davies et al. (2021) have previously identified different forms of C6 and C7 expression and positioning along the lingual and distal margins of hominoid molars, and differentiated them accordingly in their schematics and discussion. Potential complications regarding cusp expression types and positioning are further exaggerated with the acknowledgement and inclusion of cusp shouldering features. The current schematics recognise only clearly identifiable cusps, with an elevated dentine horn relative to all corresponding sides of the horn tip. However, there are several examples of cusp shouldering in primate molars, in which the shoulder is present only as a convexity of the marginal ridge close to a larger cusp (see *Galago senegalensis* ZMB 64278 in Figure 15C).

Currently, it is unclear whether cusp shouldering is developmentally homologous to a dentine horn and should be considered equivalent to the minor expression of an accessory cusp. Similar issues regarding the potential distinction between cusps and crest-like features are also present at the cingulum. For example, while some recognise a protostylid as a cusp found on the buccal surface of the protoconid (Turner et al., 1991; Hlusko, 2004), others have suggested that an elevation or ridge on the anterior part of the buccal surface may be the product of the same developmental process and thus should also be considered within protostylid expression (Skinner et al., 2008, 2009). As there is limited understanding of the developmental processes responsible for crest patterning, and the focus of this study was regarding cusp patterns specifically, non-cusp related cingulid features were not included in the schematics. While the observations in this study recognise several different forms of cusp expression in primates that may relate to important differences in the development and growth of these features, attempts to distinguish between these cusp patterns in the

schematics was avoided. While it may be useful to separate these expression types in some cases, the overwhelming degree of variation that exists in individual cusp positioning in primates would introduce numerous inconsistencies regarding the confident categorisation of expression types. Furthermore, the introduction of separate terms that in any way imply that these features are developmentally distinct would not be appropriate at this time.

While this study focuses on the crown morphology of primate mandibular first and second molars, novel patterns of cusp expression are also present in other tooth positions. Due to the significant cost and effort associated with micro-CT scanning and image processing, this study focused only on mandibular first and second molars, preferring a broad sample of taxa than of tooth position. It is highly likely however, that similar patterns of cusp expression will be present on upper molars. Additionally, the intentional exclusion of third molars from this study partially reflects the high degree of variability and expression at the crown surface, that is often notably exaggerated or restrained relative to the other molars. For many taxa, third molars will require their own schematic diagrams, and involve difficult decisions regarding the confident identification of features. For example, certain members of Papionini and Colobinae clades exhibit multiple large cusps along the distal marginal ridge of lower third molars that would currently be extremely difficult to accurately identify and differentiate. While it will be important to decide whether morphologically similar anatomical structures on third molars are homologous with those on first and second molars, serial homology and the application of equivalent terms will also be relevant to studies of premolar morphology. Finally, I expect that similar challenges presented here also exist for the analysis of upper dentitions, and will likely require the introduction of similar schematics and categorisations.

5.6 Conclusions

In this study, I reveal new patterns of lower molar accessory cusp expression in primates. In particular, I highlight the numerous discrepancies between the expected patterns of variation inferred from the current academic literature, and the new patterns of expected variation seen in this study. This new variation includes the presence of dental crown features that have not been previously observed or reported in any primate taxa. In other cases, I extend previous observations of crown structures in certain primate groups to new primate clades or taxa. Importantly in the majority of cases, I do not consider these latter observations to be homologous with their original reporting. As such, rather than attempting to label these features within one of the previously used and established systems of nomenclature, I introduce each feature within a conservative, non-homologous scheme that focuses on simple location-based categorisations. Until there is a better insight into the developmental processes and phylogenetic history associated with each individual feature in each clade, these categorisations are the most practical way of addressing these structures. As an understanding of the development and evolutionary history of crown features improves, I encourage the establishment of more appropriate, informative, clade-specific terms.

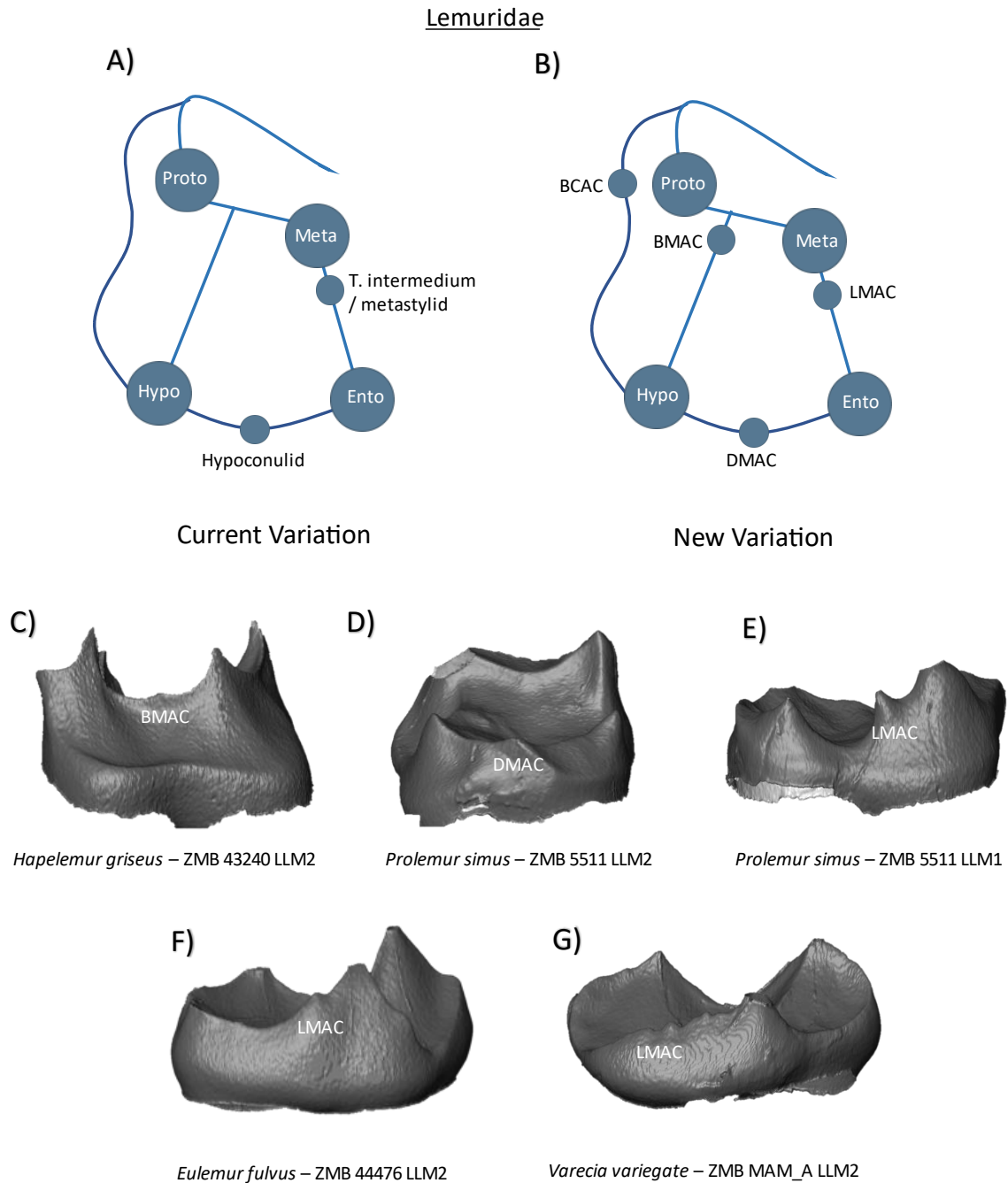


Figure 3. **Crown patterning in Lemuridae.** (A) Current variation schematic for Lemuridae, based on a review of the published literature. (B) New variation schematic for Lemuridae, based on observations at the enamel-dentine junction. (C) *Haplemur griseus* lower second molar with BMAC expression. (D) *Prolemur simus* lower second molar with DMAC expression. (E) *Prolemur simus* lower first molar with LMAC expression. (F) *Eulemur fulvus* lower second molar with LMAC expression. (G) *Varecia variegata* lower second molar with no discernible entoconid, but several LMAC cusps.

Lepilemuridae

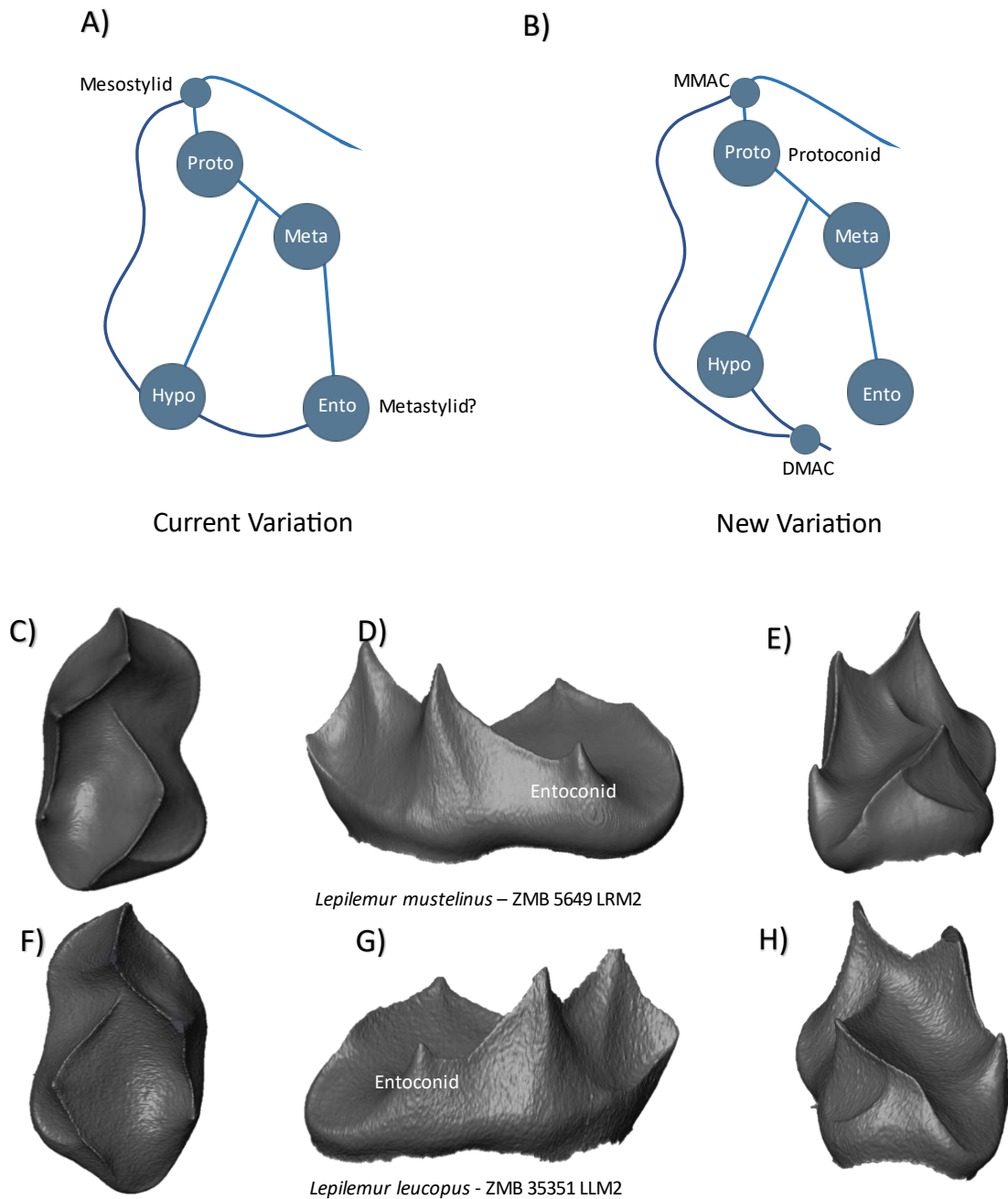


Figure 4. **Crown patterning in Lepilemuridae.** (A) Current variation schematic for Lepilemuridae, based on a review of the published literature. (B) New variation schematic for Lepilemuridae, based on observations at the enamel-dentine junction. (C) *Lepilemur mustelinus* lower second molar with no discernible features of interest. (D) *Lepilemur mustelinus* lower second molar with a short entoconid cusp. (E) *Lepilemur mustelinus* lower second molar with no discernible features of interest. (F) *Lepilemur leucopus* lower second molar with no discernible features of interest. (G) *Lepilemur leucopus* lower second molar with a short entoconid cusp. (H) *Lepilemur leucopus* lower second molar with no discernible features of interest.

Cheirogaleidae

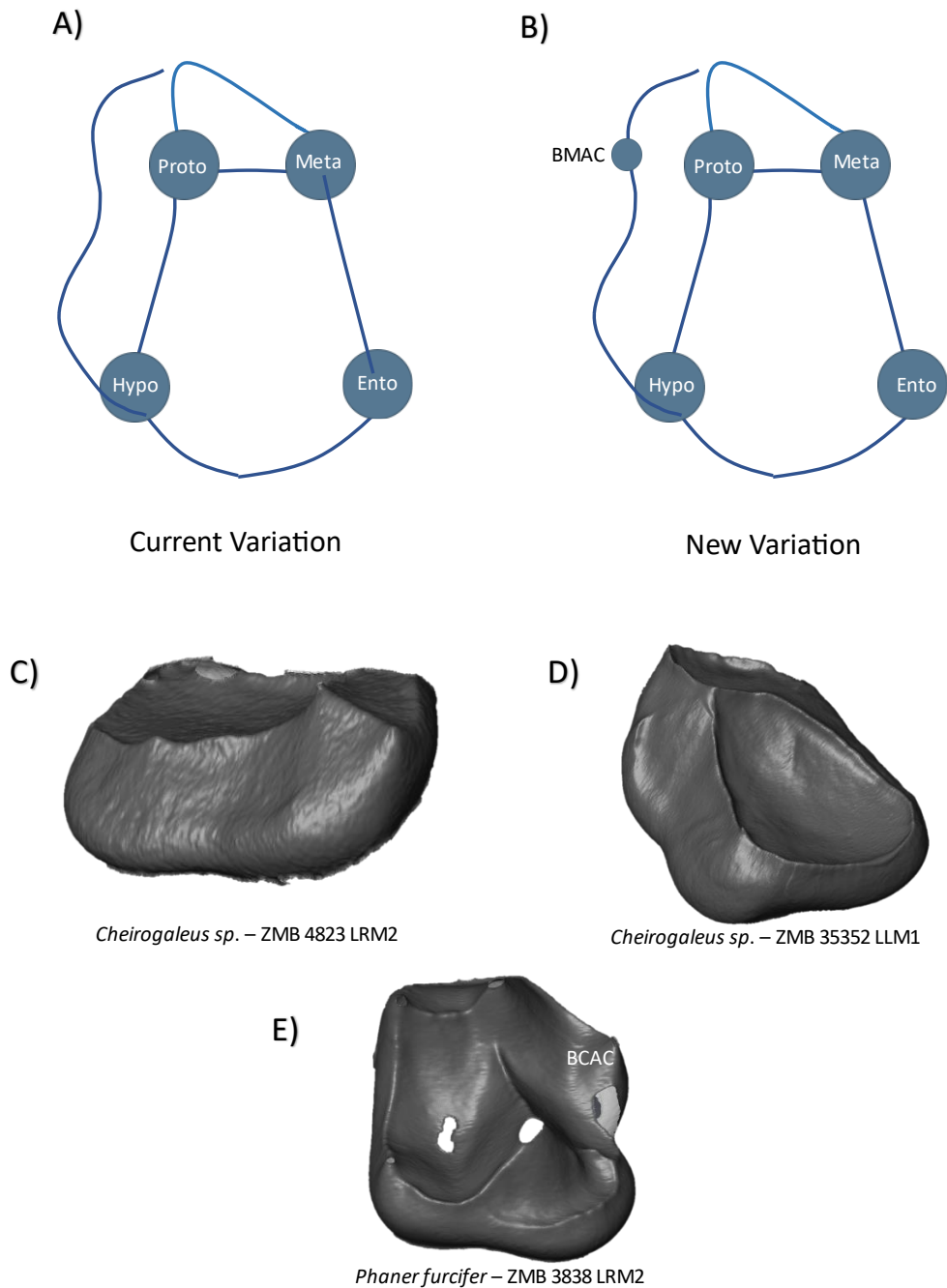


Figure 5. **Crown patterning in Cheirogaleidae.** (A) Current variation schematic for Cheirogaleidae, based on a review of the published literature. (B) New variation schematic for Cheirogaleidae, based on observations at the enamel-dentine junction. (C) *Cheirogaleus sp.* lower second molar with no discernible features of interest. (D) *Cheirogaleus sp.* lower first molar with no discernible features of interest. (E) *Phanerfurfifer* lower second molar with BCAC expression.

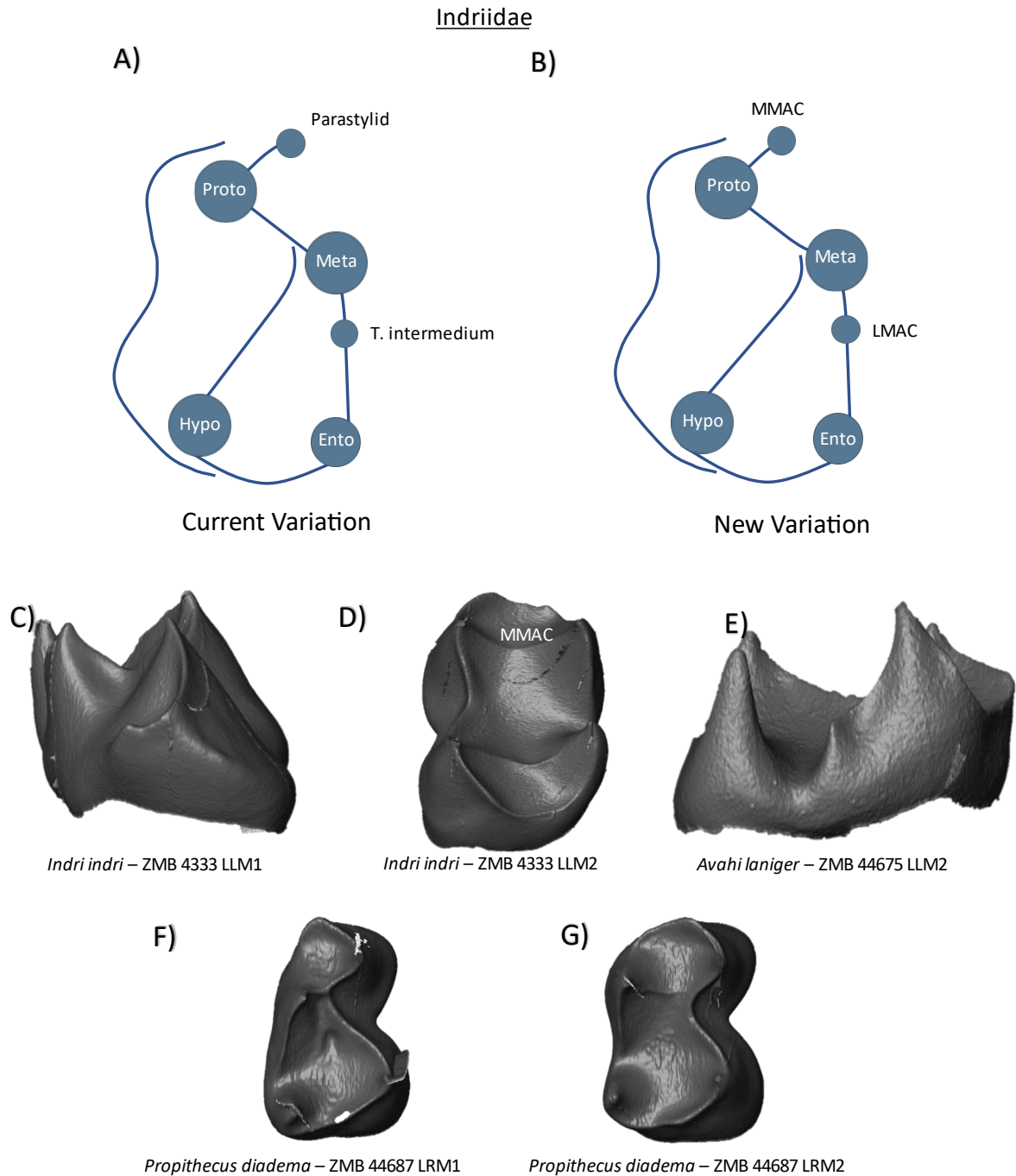


Figure 6. **Crown patterning in Indriidae.** (A) Current variation schematic for Indriidae, based on a review of the published literature. (B) New variation schematic for Indriidae, based on observations at the enamel-dentine junction. (C) *Indri indri* lower first molar with no discernible features of interest. (D) *Indri indri* lower second molar with MMAC expression. (E) *Avahi laniger* lower second molar with no discernible features of interest. (F) *Propithecus diadema* lower first molar with no discernible features of interest. (G) *Propithecus diadema* lower second molar with no discernible features of interest.

Galagidae

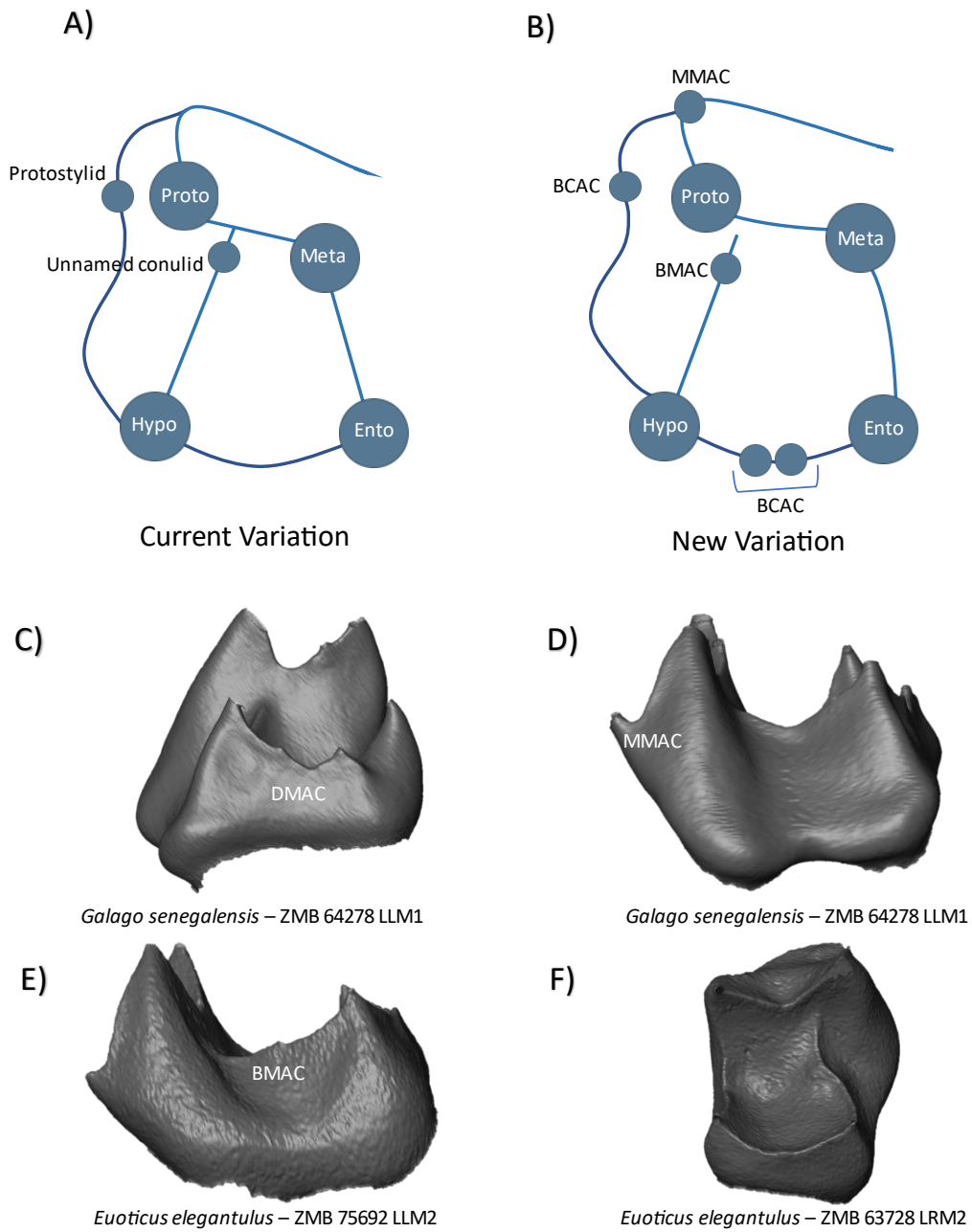


Figure 7. **Crown patterning in Galagidae.** (A) Current variation schematic for Galagidae, based on a review of the published literature. (B) New variation schematic for Galagidae, based on observations at the enamel-dentine junction. (C) *Galago senegalensis* lower first molar with DMAC expression. (D) *Galago senegalensis* lower first molar with MMAC expression. (E) *Euoticus elegantulus* lower second molar with BMAC expression. (F) *Euoticus elegantulus* lower second molar with no discernible features of interest.

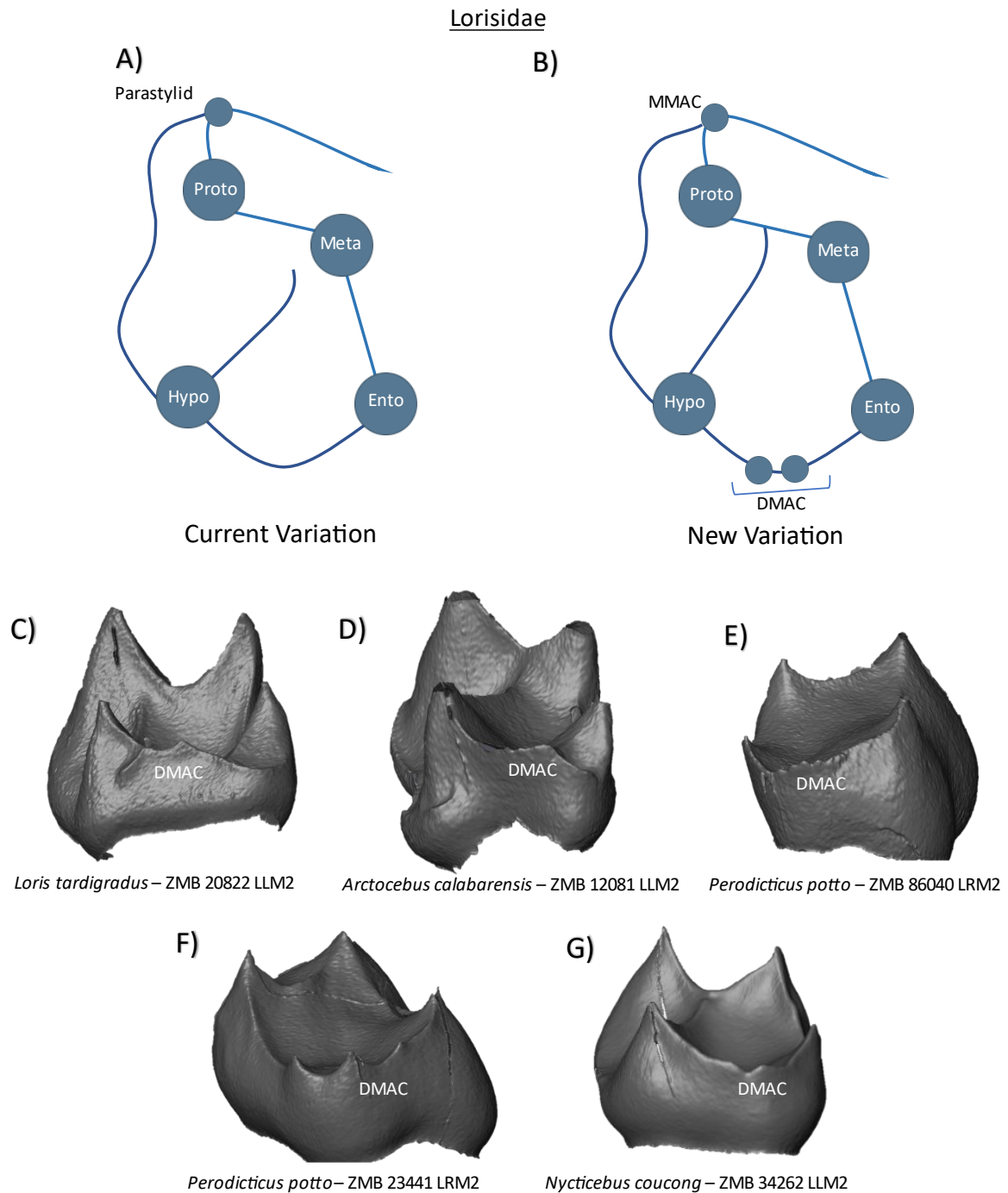


Figure 8. **Crown patterning in Lorisidae.** (A) Current variation schematic for Lorisidae, based on a review of the published literature. (B) New variation schematic for Lorisidae, based on observations at the enamel-dentine junction. (C) *Loris tardigradus* lower second molar with DMAC expression. (D) *Arctocebus calabarensis* lower second molar with DMAC expression. (E) *Perodicticus potto* lower second molar with multiple DMAC expression. (F) *Perodicticus potto* lower second molar with multiple DMAC expression. (G) *Nycticebus coucong* lower second molar with DMAC expression.

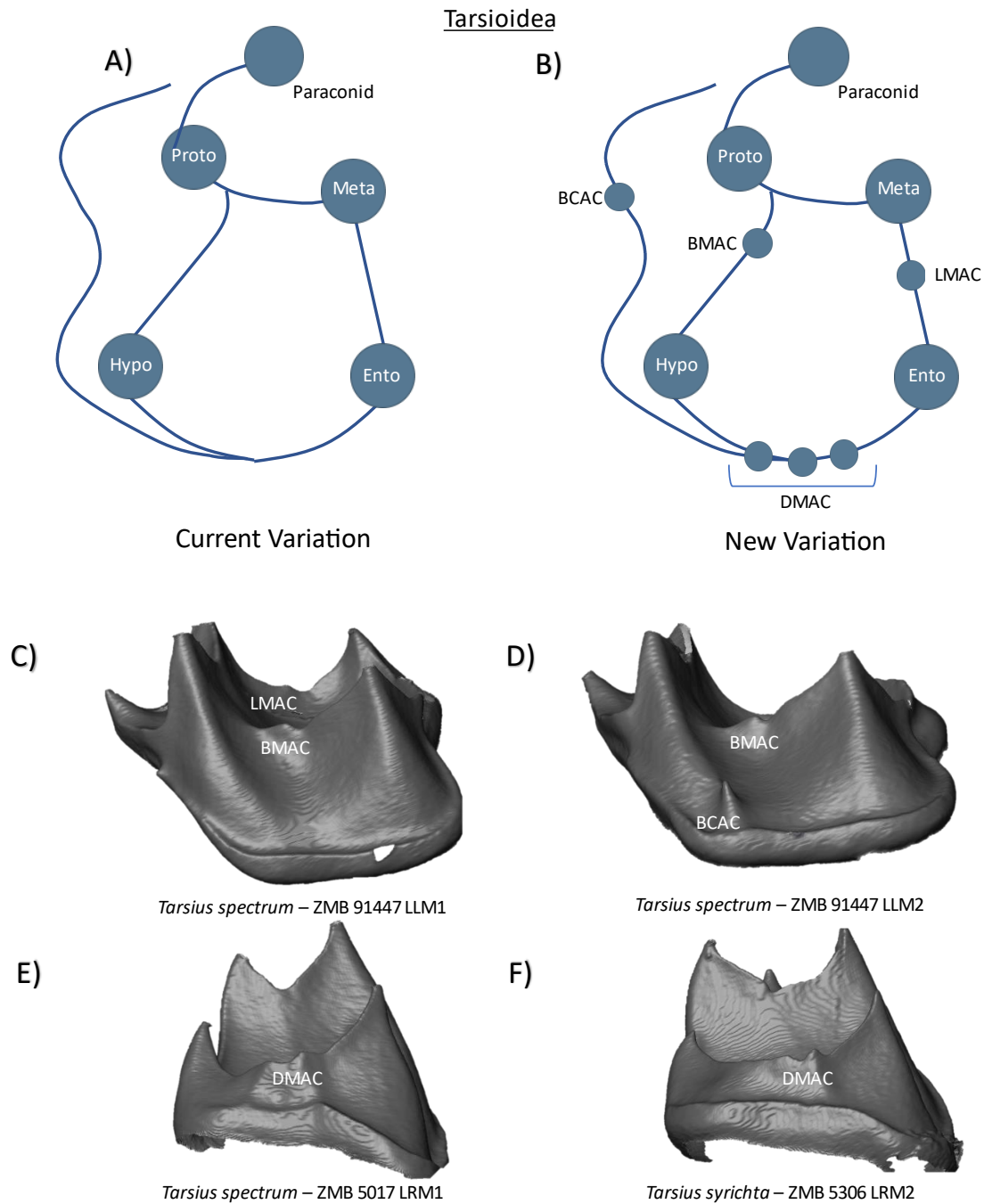


Figure 9. **Crown patterning in Tarsioidea.** (A) Current variation schematic for Tarsioidea, based on a review of the published literature. (B) New variation schematic for Tarsioidea, based on observations at the enamel-dentine junction. (C) *Tarsius spectrum* lower first molar with LMAC and BMAC expression. (D) *Tarsius spectrum* lower second molar with BMAC and BCAC expression. (E) *Tarsius spectrum* lower first molar with DMAC expression. (F) *Tarsius syrigha* lower second molar with DMAC expression.

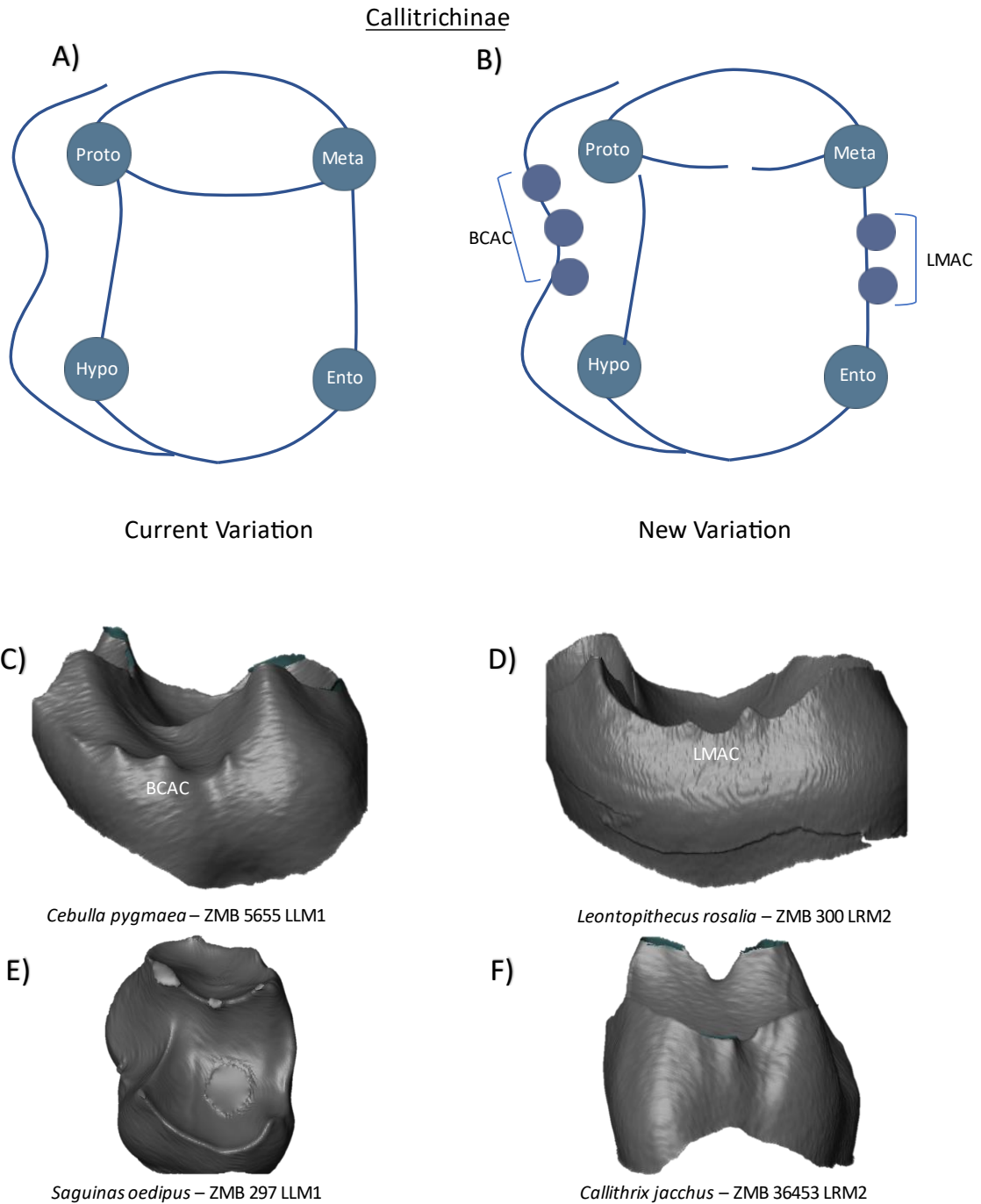


Figure 10. **Crown patterning in Callitrichinae.** (A) Current variation schematic for Callitrichinae, based on a review of the published literature. (B) New variation schematic for Callitrichinae, based on observations at the enamel-dentine junction. (C) *Cebulla pygmaea* lower first molar with BCAC expression. (D) *Leontopithecus rosalia* lower second molar with double LMAC expression. (E) *Saguinas oedipus* lower first molar with no discernible features of interest. (F) *Callithrix jacchus* lower second molar with no discernible features of interest.

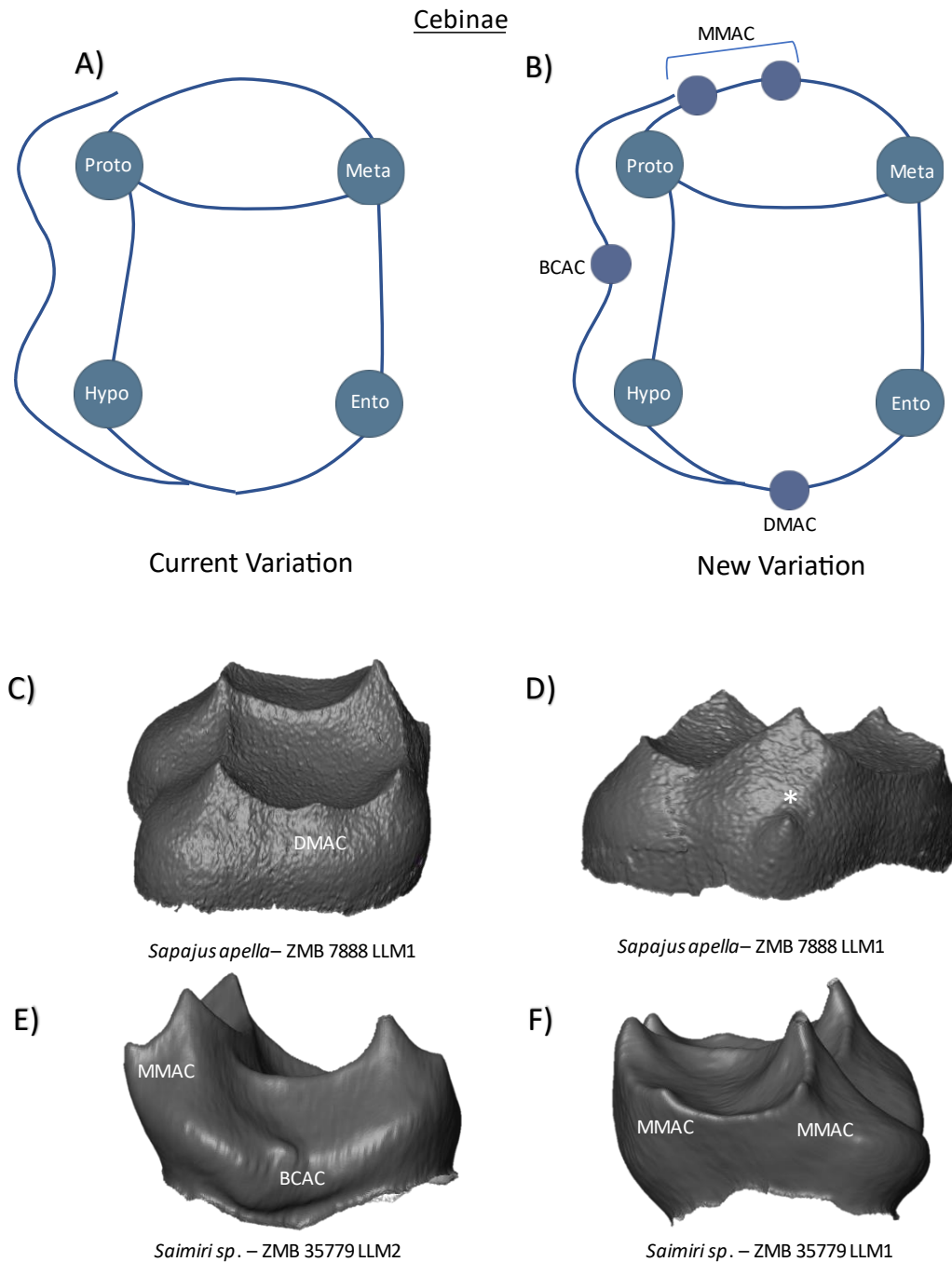


Figure 11. **Crown patterning in Cebinae.** (A) Current variation schematic for Cebinae, based on a review of the published literature. (B) New variation schematic for Cebinae, based on observations at the enamel-dentine junction. (C) *Sapajus apella* lower first molar with DMAC expression. (D) *Sapajus apella* lower first molar with developmental abnormality resembling a possible LCAC. (E) *Saimiri sp.* lower second molar with MMAC and BCAC expression (F) *Saimiri sp.* lower first molar with double MMAC expression.

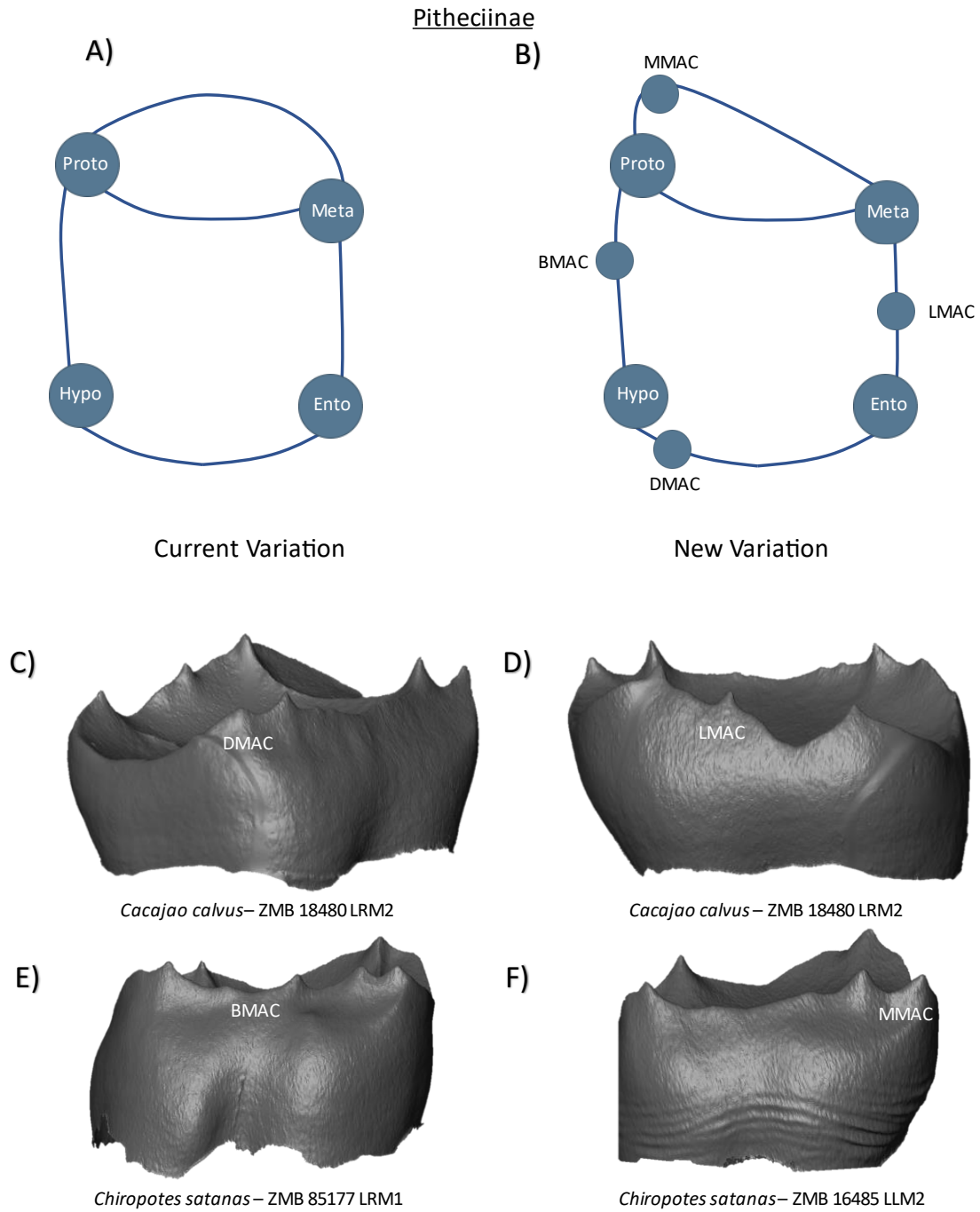


Figure 12. **Crown patterning in Pitheciinae.** (A) Current variation schematic for Pitheciinae, based on a review of the published literature. (B) New variation schematic for Pitheciinae, based on observations at the enamel-dentine junction. (C) *Cacajao calvus* lower second molar with DMAC expression. (D) *Cacajao calvus* lower second molar with LMAC expression. (E) *Chiropotes satanas* lower first molar with double BMAC expression (F) *Chiropotes satanas* lower second molar with MMAC expression.

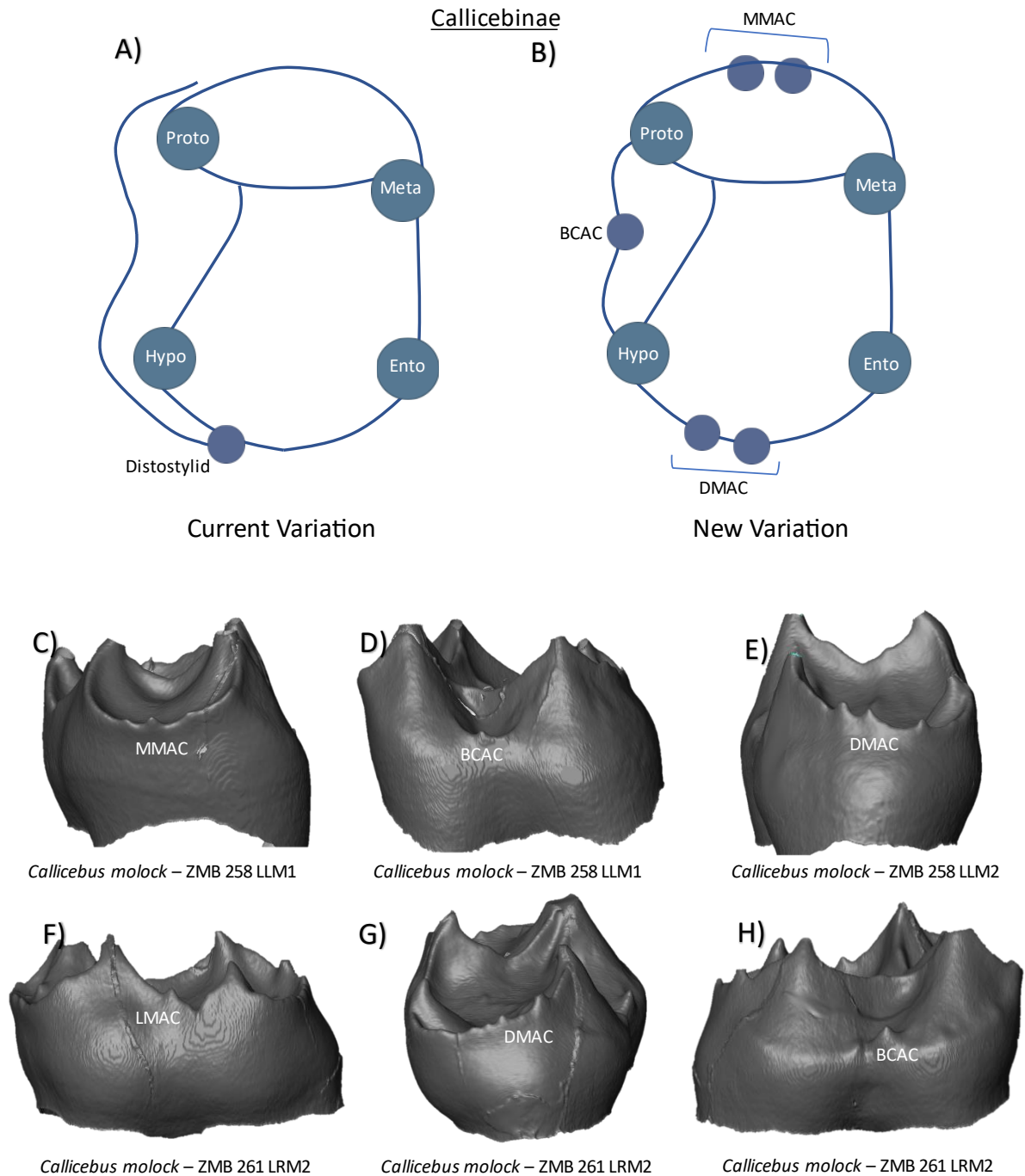


Figure 13. **Crown patterning in Callicebinae.** (A) Current variation schematic for Callicebinae, based on a review of the published literature. (B) New variation schematic for Callicebinae, based on observations at the enamel-dentine junction. (C) *Callicebus molock* lower first molar with MMAC expression. (D) *Callicebus molock* lower first molar with BCAC expression. (E) *Callicebus molock* lower second molar with multiple DMAC cusps (F) *Callicebus molock* lower second molar with LMAC expression. (G) *Callicebus molock* lower second molar with multiple DMAC cusps. (H) *Callicebus molock* lower second molar with BCAC expression.

Atelinae

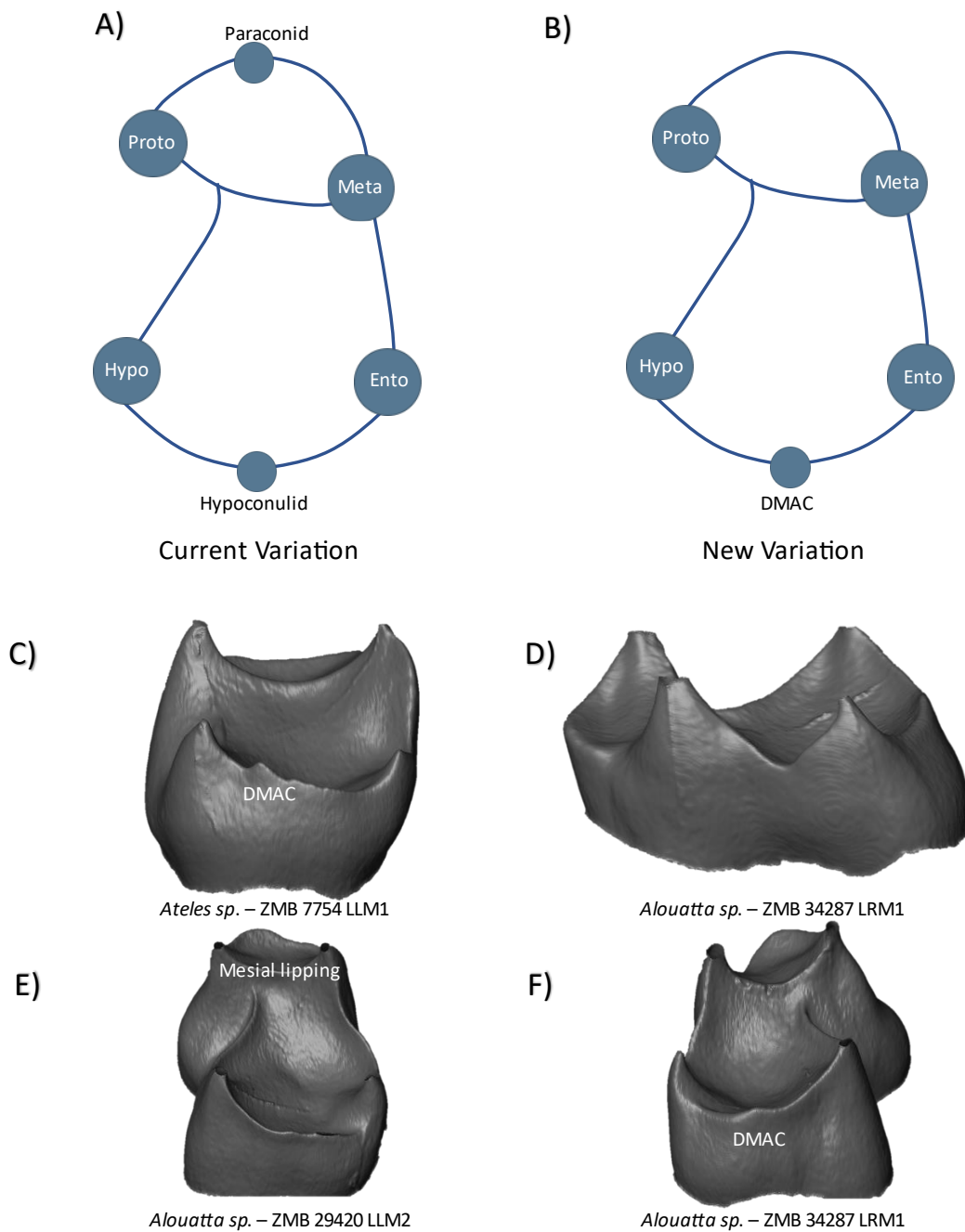


Figure 14. **Crown patterning in Atelinae.** (A) Current variation schematic for Atelinae, based on a review of the published literature. (B) New variation schematic for Atelinae, based on observations at the enamel-dentine junction. (C) *Ateles sp.* lower first molar with DMAC expression. (D) *Alouatta sp.* lower first molar with no discernible features of interest. (E) *Alouatta sp.* lower second molar with mesial marginal lipping, but no discernible accessory cusp (F) *Alouatta sp.* lower first molar with DMAC expression.

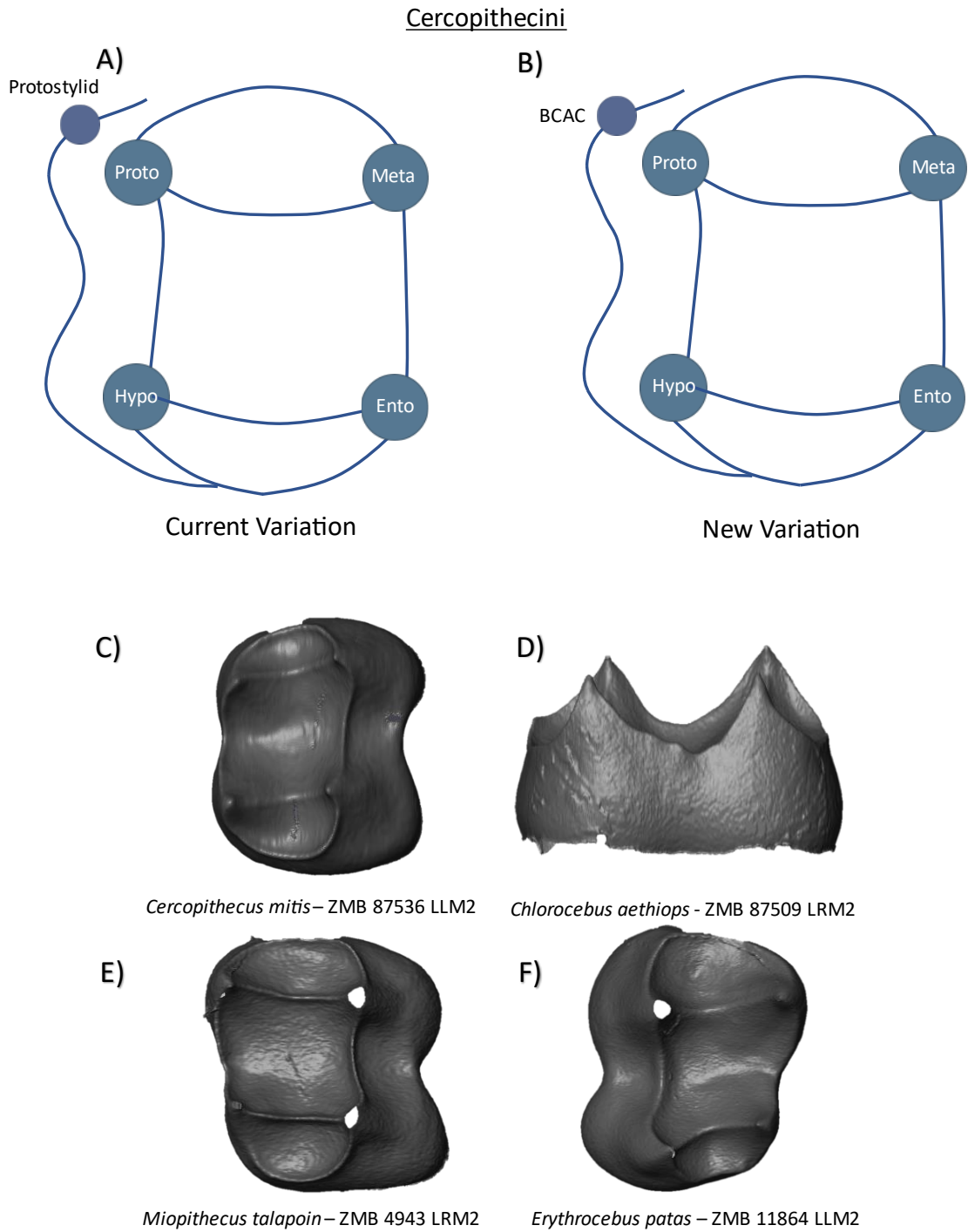


Figure 15. **Crown patterning in Cercopithecini.** (A) Current variation schematic for Cercopithecini, based on a review of the published literature. (B) New variation schematic for Cercopithecini, based on observations at the enamel-dentine junction. (C) *Cercopithecus mitis* lower second molar with no discernible features of interest. (D) *Chlorocebus aethiops* lower second molar with no discernible features of interest. (E) *Miopithecus talapoin* lower second molar with no discernible features of interest. (F) *Erythrocebus patas* lower second molar with no discernible features of interest.

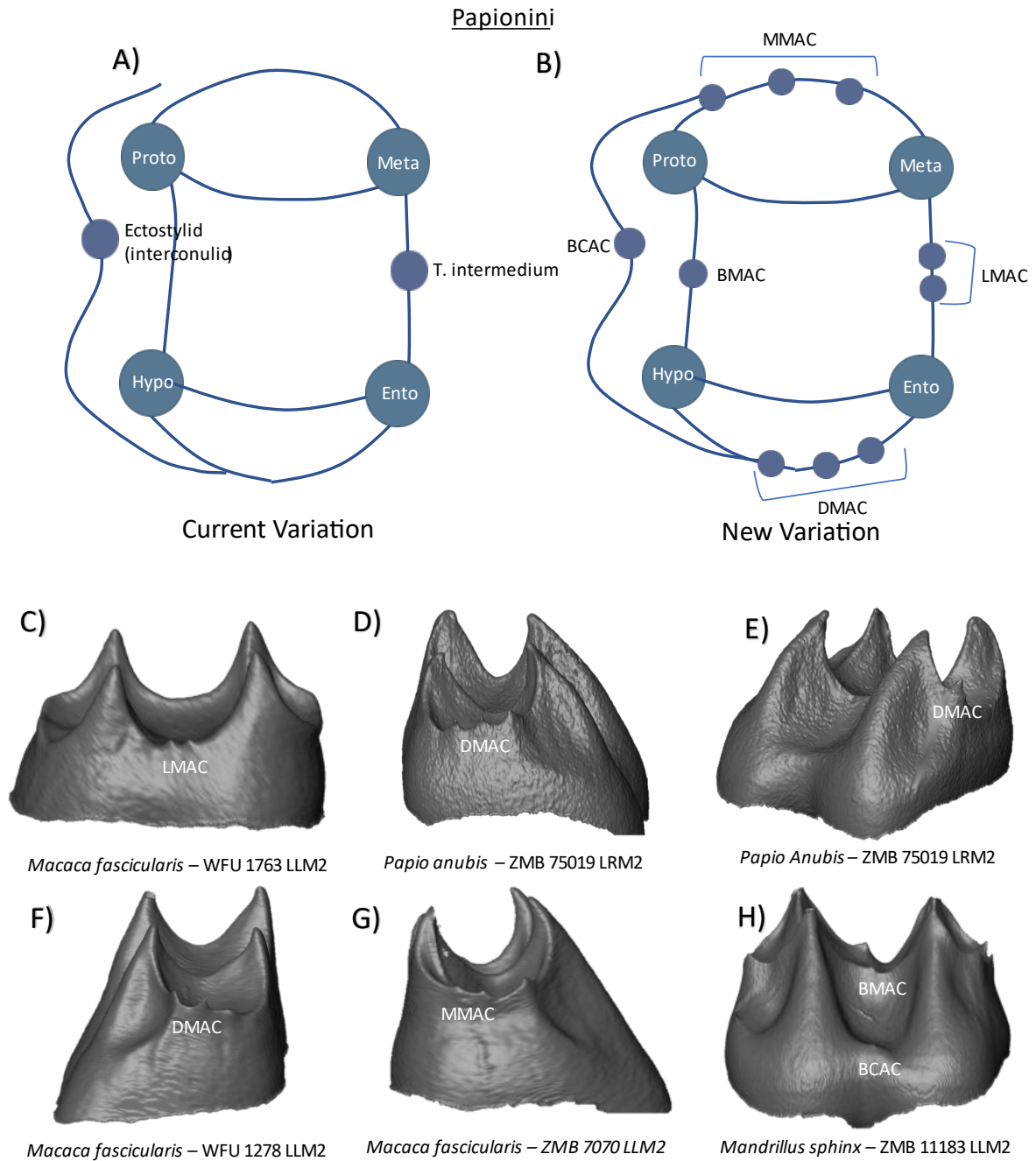


Figure 16. **Crown patterning in Papionini.** (A) Current variation schematic for Papionini, based on a review of the published literature. (B) New variation schematic for Papionini, based on observations at the enamel-dentine junction. (C) *Macaca fascicularis* lower second molar with double LMAC expression. (D) *Papio anubis* lower second molar with double DMAC expression. (E) *Papio anubis* lower second molar with DMAC expression. (F) *Macaca fascicularis* lower second molar with DMAC expression. (G) *Macaca fascicularis* lower first molar with double MMAC expression. (H) *Mandrillus sphinx* lower second molar with BMAC and BCAC expression.

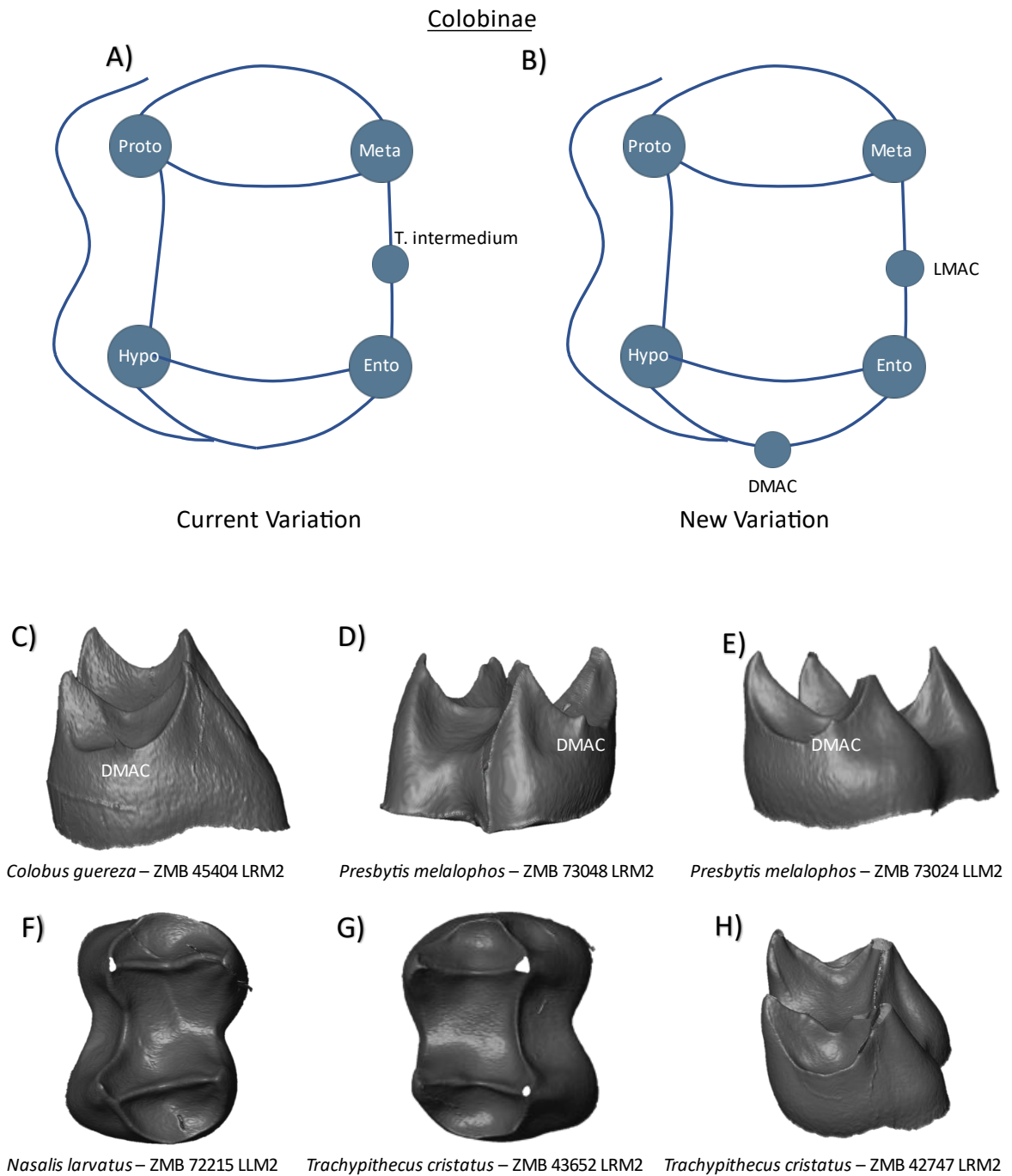


Figure 17. **Crown patterning in Colobinae.** (A) Current variation schematic for Colobinae, based on a review of the published literature. (B) New variation schematic for Colobinae, based on observations at the enamel-dentine junction. (C) *Colobus guereza* lower second molar with DMAC expression. (D) *Presbytis melalophos* lower second molar with DMAC expression. (E) *Presbytis melalophos* lower second molar with DMAC expression (F) *Nasalis larvatus* lower second molar with no discernible features of interest. (G) *Trachypithecus cristatus* second first molar with no discernible features of interest. (H) *Trachypithecus cristatus* lower second molar with no discernible features of interest.

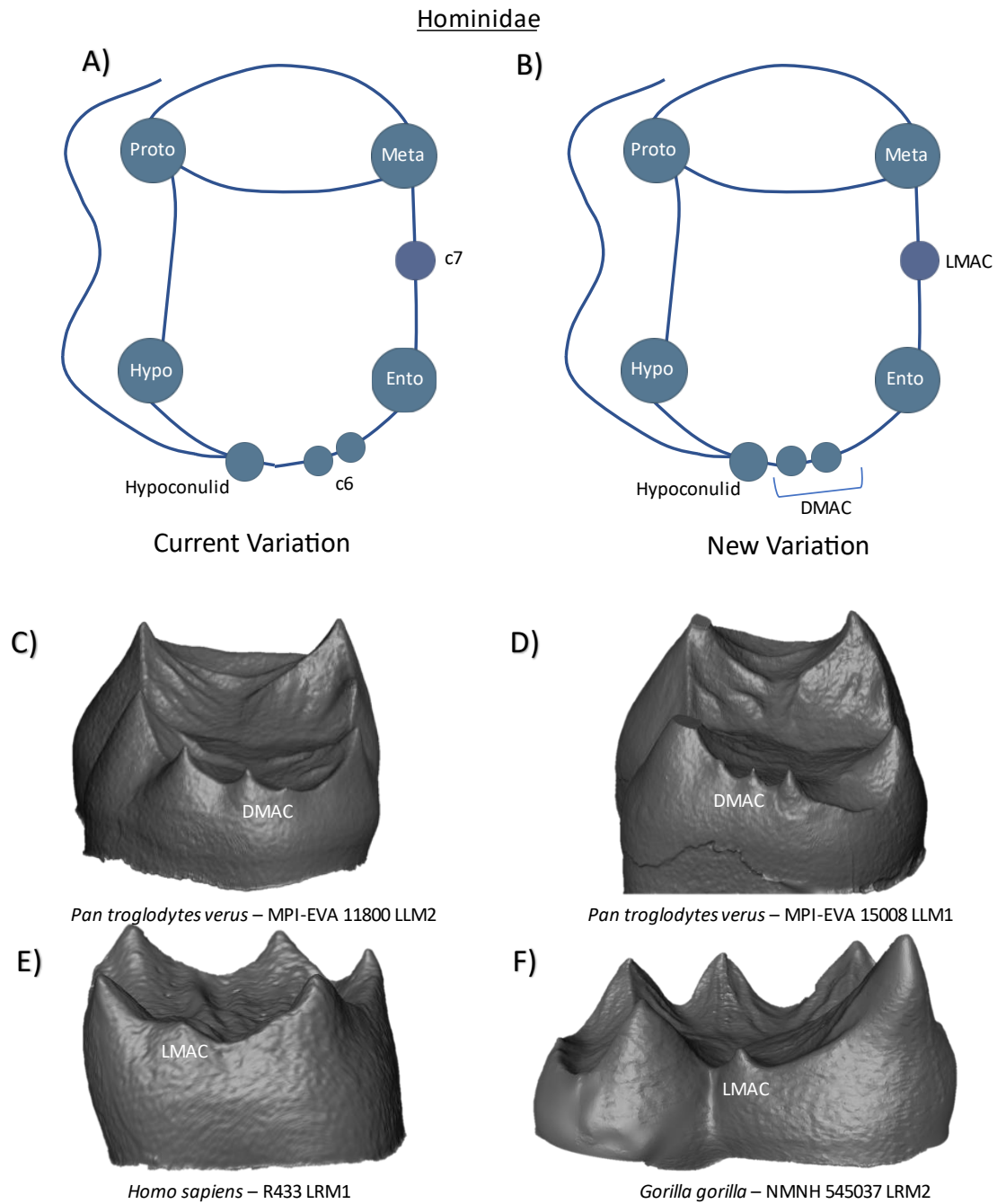


Figure 18. **Crown patterning in Hominidae.** (A) Current variation schematic for Hominidae, based on a review of the published literature. (B) New variation schematic for Hominidae, based on observations at the enamel-dentine junction. (C) *Pan troglodytes verus* lower second molar with double DMAC expression. (D) *Pan troglodytes verus* lower first molar with double DMAC expression. (E) *Homo sapiens* lower first molar with LMAC expression. (F) *Gorilla gorilla* lower second molar with LMAC expression.

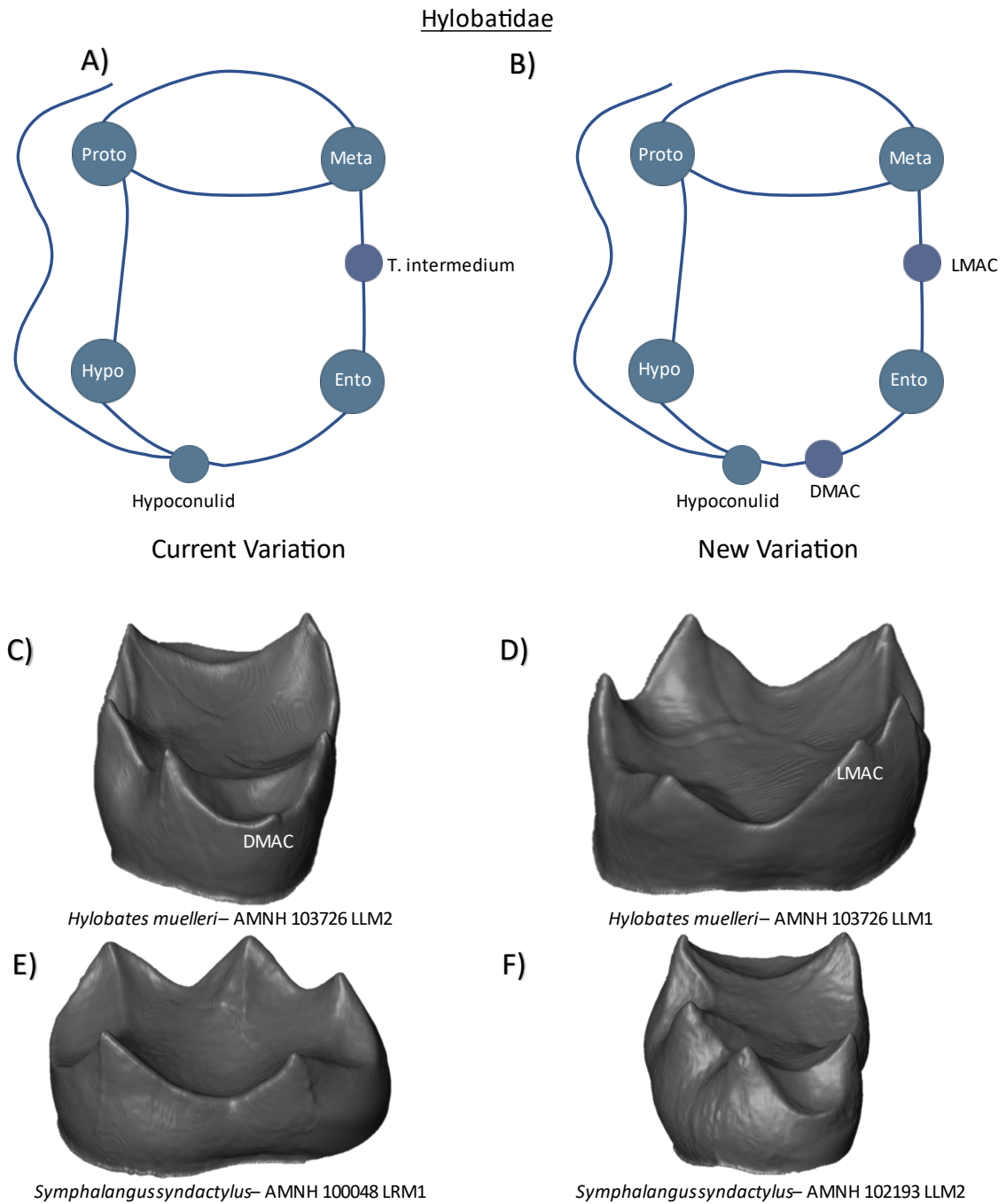


Figure 19. **Crown patterning in Hylobatidae.** (A) Current variation schematic for Hylobatidae, based on a review of the published literature. (B) New variation schematic for Hylobatidae, based on observations at the enamel-dentine junction. (C) *Hylobates muelleri* lower second molar with DMAC expression. (D) *Hylobates muelleri* lower first molar with LMAC expression. (E) *Symphalangus syndactylus* lower first molar with no discernible features of interest. (F) *Symphalangus syndactylus* lower second molar with no discernible features of interest.

CHAPTER 6: Discussion and Conclusions

6.1 Thesis summary

As a growing number of studies have recently implicated important developmental models and mechanisms in the cusp patterning and overall crown morphology of certain mammal taxa, it was essential to assess the relevance of these processes to the primate dentition, and their potential implications to studies of primate crown morphology. In doing so, this also allowed for the assessment of current primate crown nomenclature schemes, which growing evidence has suggested may be critically flawed. This thesis focused on an examination of the enamel-dentine junction (EDJ) of lower molars in a taxonomically broad sample of primate taxa to address these two concerns. This work represents the first attempt to gain a broad perspective of crown patterning across all primates at the EDJ surface, and from this, present a more appropriate and unified assessment of cusp patterning and nomenclature that acknowledges the important developmental processes responsible for cusp expression. While taxonomically broad in its approach to many of these questions, this project also provides the most detailed and controlled assessment of the patterning cascade model of cusp development to date. As discussed further below, the accurate understanding and appreciation of this developmental model is particularly crucial to the use and interpretation of primate crown morphology.

Chapter 3 assessed the multiple phylogenetic and developmental components that appear to be responsible for crown patterning in mammals, and considered their application and consequence to the study of primate crown morphology. From this, the Tooth Crown Morphology Framework (TCMF) was introduced. This involved a detailed review and

assessment of the relevant literature, and several qualitative contributions that have increased the understanding and appreciation for how these developmental mechanisms manifest themselves in the primate dentition. Additionally, important examples of previously unrecognized aspects of growth were introduced and considered within the context of these developmental models.

While all components of the proposed framework in Chapter 3 have their relevance for studies of primate crown morphology, cusp patterning often plays a particularly key role in these studies. As such, Chapter 4 tested a specific model outlined in the framework that is associated with variation in cusp expression in some mammalian taxa. Controlling for species, population, and tooth position, Chapter 4 employed geometric morphometrics to examine whether shape variation in the enamel-dentine junction (EDJ) correlated with cusp presence in a population of macaque lower second molars. While the results demonstrated that the patterning cascade model of cusp development was broadly appropriate for interpreting cusp variation in *Macaca fascicularis* molars, it did not explain all manifestations of accessory cusp expression. These conclusions are in agreement with the findings in Chapter 3 that other additional factors may be responsible for cusp patterning in primates.

Finally, through observations of mandibular first and second molars from the taxonomically broad sample used in this project, Chapter 5 documented variation in cusp patterning within the major primate clades and from this assessed the applicability of the current nomenclature schemes to each clade. Results reveal numerous new patterns of lower molar

accessory cusp expression in primates, and highlight the frequent discrepancies between the expected patterns of variation inferred from the current literature and the new patterns of expected variation seen in this study. Based on the issues associated with the current systems of nomenclature discussed in Chapter 1, the developmental influences on cusp expression emphasised in Chapter 3, and the qualitative observations described in Chapter 5, crown features have been introduced and discussed within a proposed system that focuses on simple location-based categorisations. Until there is a greater understanding of the developmental origin and evolutionary history of these features, this system is the most practical way of discussing these structures in the discipline.

6.2 Discussion

As discussed in the introduction of this thesis, Chapters 3-5 are written in the form of individual manuscripts. As such, the discussion sections of each chapter adopt a more conservative and reserved approach to the interpretation and discussion of certain results. The following section focuses on some of the unresolved questions and topics of particular interest that were not discussed in sufficient detail in these sections.

The first topic that deserves further discussion are the findings associated with crest patterning. Based on an examination across a broad sample of primate taxa, Chapter 3 demonstrated that primary crest patterning may not necessitate the presence of cusps, while also providing the first meaningful developmental distinction between primary crests (those that form the marginal ridge of the crown) and secondary crest patterning (those found within the occlusal basin or beyond the marginal ridge). What the discipline appears

to be less clear and definitive on is the precise distinction between cusps and crests. Based on an understanding of developmental genetics, the viewpoint adopted by this thesis is that a cusp *must* be associated with an enamel knot and subsequent dentine horn. However, the protostylid has previously been viewed and discussed as both an accessory cusp *and* crest on the buccal surface of the protoconid (Dahlberg, 1950). Furthermore, categories of expression type for several crown traits like the protostylid are often discussed on a spectrum that transitions from grooves and crests, through to the presence of large cuspules (Turner et al., 1991; Ortiz et al., 2012). How these could represent categories of the same developmental feature, when one is formed by enamel knot signalling, and the other by some other unknown mechanism, remains to be determined. An alternative perspective is that the temporal-spatial parameters associated with enamel knot initiation are similar to the conditions also necessary for crest formation. Skinner et al. (2008) have already suggested that the presence and expression of protostylid crests in hominoids may be influenced by the size, shape, and spacing of the primary dentine horns. This may also explain the tight anatomical association between accessory cusps and crests on the crown surface. As limited research on crest patterning is conducted in the field of developmental genetics, it may fall on dental morphologist to provide further hypotheses regarding the interaction between tooth cusps and crests, and the mechanisms responsible for crest formation.

Chapter 4 demonstrated that cusp patterning in macaque mandibular second molars was broadly consistent with the patterning cascade model, but that it did not explain all manifestations of accessory cusp expression seen in this sample. Interestingly, it was shown

that while lingual accessory cusp presence was associated with smaller primary cusps (matching the predictions of the PCM), cusp presence was also associated with more closely spaced cusps, which are thought to reduce the available space for cusp initiation and inhibit the formation of additional cusps. Whether the size of the surrounding cusps plays a greater role in inhibiting enamel knot initiation than cusp spacing highlights the difficulties in assessing these models in complex tooth shapes. A future challenge for studies of the patterning cascade model will be to tease apart the relative contribution of each presumed influencing variable. Testing this developmental model in taxa with notably different crown and cusp morphology, including representatives of the Strepsirrhini and Ceboidea clade, may improve our understanding of the developmental parameters (and relative contribution of them) responsible for cusp formation.

The proposed terms and clade-specific diagrams provided in Chapter 5 suggest a complete departure from all previous systems of nomenclature for accessory cusps. However, it is emphasised that with a better understanding of the development and history of a particular crown feature, the reintroduction or establishment of new, more appropriate terms is warranted. An exciting potential direction of research related to this may exist in the field of developmental genetics. Coin et al. (1999) have already shown that the secondary enamel knots form from non-proliferative or slowly cycling cells previously belonging to the primary enamel knot. As tooth and cusp development is highly iterative, it seems possible that non-proliferative or slowly cycling cells associated with secondary enamel knots may form or contribute to the initiation and folding of tertiary enamel knots (or accessory cusps). While this form of research would not be possible on human and non-human primates, it may

provide clues regarding the developmental relationship that exists between a metaconid and metaconulid for example, and whether these truly are interdependent structures.

A final consideration is that this dissertation and its findings were made possible through microtomography of a very large sample of teeth. Finding, scanning, and processing of teeth from museum collections around the world is extremely challenging, however, this dissertation has demonstrated that 1) the more teeth that are scanned the more variation in crown morphology is detected and 2) that this newly discovered variation is critically important for informing our models and hypotheses about odontogenesis. Not to forget that this dissertation focused, by necessities of time and funding, on mandibular molars and that considerable insights will be gained from the study of other tooth positions of both the deciduous and permanent dentitions. Similarly, very little work has been done on other mammalian taxa that have similarly complex tooth crowns to primates. Theoretically, a point should be reached when scanning additional teeth does not change these models, but we are currently a long way from that point.

BIBLIOGRAPHY

Aiello, L. and Dean, C., 1990. *An Introduction to Human Evolutionary Anatomy*. Academic Press.

Anemone, R.L., Skinner, M.M. and Dirks, W., 2012. Are there two distinct types of hypocone in Eocene primates? The 'pseudohypocone' of notharctines revisited. *Palaeontologia Electronica*, 15(15.3).

Bailey, S.E., 2000. Dental Morphological Affinities Among Late-Pleistocene and Recent Humans. *Dental Anthropology Journal*, 14(2), pp.1-8.

Bailey, S.E. 2002. A closer look at Neanderthal postcanine dental morphology: the mandibular dentition. *The Anatomical Record*, 269(3), pp.148-156.

Bailey, S.E. and Lynch, J.M., 2005. Diagnostic differences in mandibular P4 shape between Neandertals and anatomically modern humans. *American Journal of Physical Anthropology*, 126(3), pp.268-277.

Bailey, S.E., Skinner, M.M. and Hublin, J.J., 2011. What lies beneath? An evaluation of lower molar trigonid crest patterns based on both dentine and enamel expression. *American Journal of Physical Anthropology*, 145(4), pp.505-518.

Bailey, S.E. and Wood, B.A., 2007. Trends in postcanine occlusal morphology within the hominin clade: the case of *Paranthropus*. In *Dental perspectives on human evolution: state of the art research in dental paleoanthropology* (pp. 33-52). Springer, Dordrecht.

Bennejeant, C.B., 1936. *Anomalies et variations dentaires chez les primates*. Imprimeries P. Vallier, Paris.

Bermúdez de Castro, J.M., Modesto-Mata, M., García-Campos, C., Sarmiento, S., Martín-Francés, L., Martínez de Pinillos, M. and Martín-Torres, M., 2021. Testing the inhibitory cascade model in a recent human sample. *Journal of Anatomy*, 239(5), pp.1170-1181.

Bernal, V., Gonzalez, P.N. and Perez, S.I., 2013. Developmental processes, evolvability, and dental diversification of New World monkeys. *Evolutionary Biology*, 40(4), pp.532-541.

Billet, G. and Bardin, J., 2021. Segmental series and size: clade-wide investigation of molar proportions reveals a major evolutionary allometry in the dentition of placental mammals. *Systematic Biology*, 70(6), pp.1101-1109.

Bunn, J.M., Boyer, D.M., Lipman, Y., St. Clair, E.M., Jernvall, J. and Daubechies, I., 2011. Comparing Dirichlet normal surface energy of tooth crowns, a new technique of molar shape quantification for dietary inference, with previous methods in isolation and in combination. *American Journal of Physical Anthropology*, 145(2), pp.247-261.

Butler, P.M. 1939. Studies of the Mammalian Dentition.—Differentiation of the Post-canine Dentition. In *Proceedings of the Zoological Society of London*, vol. 109(1), pp. 1-36. Oxford, UK: Blackwell Publishing Ltd.

Butler, P.M., 1956. The ontogeny of molar pattern. *Biological Reviews*, 31(1), pp.30-69.

Butler, P.M., 1967. The prenatal development of the human first upper permanent molar. *Archives of Oral Biology*, 12(4), pp.551-563.

Butler, P.M. 1978. Molar cusp nomenclature and homology. *Development, Function and Evolution of Teeth*: 439-453.

Boughner, J.C., Marchiori, D.F. and Packota, G.V., 2021. Unexpected variation of human molar size patterns. *Journal of Human Evolution*, 161, p.103072.

Carter, K.E. and Worthington, S., 2016. The evolution of anthropoid molar proportions. *BMC Evolutionary Biology*, 16(1), pp.1-18.

Chapple, S.A. and Skinner, M.M., 2023. Primate tooth crown nomenclature revisited. *PeerJ*, 11, p.e14523.

Clark, W., 1971. *Antecedents of man*. Edinburgh University Press.

Cobourne, M.T. and Mitsiadis, T., 2006. Neural crest cells and patterning of the mammalian dentition. *Journal of Experimental Zoology Part B: Molecular and Developmental Evolution*, 306(3), pp.251-260.

Coin, R., 1999. Aspects of cell proliferation kinetics of the inner dental epithelium during mouse molar and incisor morphogenesis: a reappraisal of the role of the enamel knot area. *Int J. Dev. Biol.*, 43, pp.261-267.

Cooke, S.B., 2011. Paleodiet of extinct platyrrhines with emphasis on the Caribbean forms: three-dimensional geometric morphometrics of mandibular second molars. *The Anatomical Record: Advances in Integrative Anatomy and Evolutionary Biology*, 294(12), pp.2073-2091.

Cope, E.D., 1883. On the trituberculate type of molar tooth in the Mammalia. *Proceedings of the American Philosophical Society*, 21(114), pp.324-326.

Cope, E. 1888. On the tritubercular molar in human dentition. *Journal of Morphology*, 2, pp.7-26.

Corruccini, R.S., 1987. The dentinoenamel junction in primates. *International Journal of Primatology*, 8(2), pp.99-114.

Corruccini, R.S., 1998. The dentino-enamel junction in primate mandibular molars. *Human Dental Development, Morphology, and Pathology: A Tribute to Albert A. Dahlberg. University of Oregon Anthropological Papers, Portland*, pp.1-16.

Cuozzo, F.P., Rasoazanabary, E., Godfrey, L.R., Sauther, M.L., Yousouf, I.A. and LaFleur, M.M., 2013. Biological variation in a large sample of mouse lemurs from Amboasary, Madagascar: Implications for interpreting variation in primate biology and paleobiology. *Journal of Human Evolution*, 64(1), pp.1-20.

Cuozzo, F.P. and Yamashita, N., 2006. Impact of ecology on the teeth of extant lemurs: a review of dental adaptations, function, and life history. *Lemurs*, pp.67-96.

Dahlberg, A.A., 1950. The evolutionary significance of the protostylid. *American Journal of Physical Anthropology*, 8(1), pp.15-26.

Davies, T.W., Alemseged, Z., Gidna, A., Hublin, J.J., Kimbel, W.H., Kullmer, O., Spoor, F., Zanolli, C. and Skinner, M.M., 2021. Accessory cusp expression at the enamel-dentine junction of hominin mandibular molars. *PeerJ*, 9, p.e11415.

Davies, T.W., Deleuzene, L.K., Gunz, P., Hublin, J.J. and Skinner, M.M., 2019. Endostructural morphology in hominoid mandibular third premolars: Discrete traits at the enamel-dentine junction. *Journal of Human Evolution*, 136, p.102670.

Dean, C., 2004. 2D or not 2D, and other interesting questions about enamel: reply to Macho et al.(2003). *Journal of Human Evolution*, 46(5), pp.633-640.

Durand, K.R., Snow, M., Smith, D.G. and Durand, S.R., 2010. Discrete dental trait evidence of migration patterns in the Northern Southwest. *Human Variation in the Americas, Occasional Paper*, (38), pp.113-134.

Evans, A.R., Daly, E.S., Catlett, K.K., Paul, K.S., King, S.J., Skinner, M.M., Nesse, H.P., Hublin, J.J., Townsend, G.C., Schwartz, G.T. and Jernvall, J., 2016. A simple rule governs the evolution and development of hominin tooth size. *Nature*, 530(7591), pp.477-480.

Evans, A.R., Pollock, T.I., Cleuren, S.G., Parker, W.M., Richards, H.L., Garland, K.L., Fitzgerald, E.M., Wilson, T.E., Hocking, D.P. and Adams, J.W., 2021. A universal power law for modelling the growth and form of teeth, claws, horns, thorns, beaks, and shells. *BMC Biology*, 19(1), pp.1-14.

Feeney, R.N., Zermeno, J.P., Reid, D.J., Nakashima, S., Sano, H., Bahar, A., Hublin, J.J. and Smith, T.M., 2010. Enamel thickness in Asian human canines and premolars. *Anthropological Science*, 118(3), pp.191-198.

Frisch, J.E., 1965. Trends in the evolution of the hominoid dentition. *Bibliotheca Primatologica*, 3, pp.1-130.

Fortelius, M., 1985. Ungulate cheek teeth: developmental, functional, and evolutionary interrelations. *Acta Zoologica Fennica*, 180, pp.1-76.

Fraser, G.J., Graham, A. and Smith, M.M., 2006. Developmental and evolutionary origins of the vertebrate dentition: molecular controls for spatio-temporal organisation of tooth sites

in osteichthyans. *Journal of Experimental Zoology Part B: Molecular and Developmental Evolution*, 306(3), pp.183-203.

Gómez-Robles, A. and Polly, P.D., 2012. Morphological integration in the hominin dentition: evolutionary, developmental, and functional factors. *Evolution: International Journal of Organic Evolution*, 66(4), pp.1024-1043.

Gould, S.J., 1985. *Ontogeny and phylogeny*. Harvard University Press.

Gregory, W.K. 1916. Studies on the evolution of the primates. *Bulletin of the American Museum of Natural History*, 35, pp.239-355.

Gregory, W.K., 1920. The origin and evolution of the human dentition: a palaeontological review. *Journal of Dental Research*, 3(1), pp.87-228.

Guatelli-Steinberg, D. and Irish, J.D., 2005. Brief communication: early hominin variability in first molar dental trait frequencies. *American Journal of Physical Anthropology*, 128(2), pp.477-484.

Gunz, P., Mitteroecker, P. and Bookstein, F.L., 2005. Semilandmarks in three dimensions. In *Modern Morphometrics in Physical Anthropology* (pp. 73-98). Springer, Boston, MA.

Häkkinen, T.J., Sova, S.S., Corfe, I.J., Tjäderhane, L., Hannukainen, A. and Jernvall, J., 2019. Modeling enamel matrix secretion in mammalian teeth. *PLoS Computational Biology*, 15(5), p.e1007058.

Hall, B.K., 2003. Evo-Devo: evolutionary developmental mechanisms. *International Journal of Developmental Biology*, 47(7-8), pp.491-495.

Halliday, T.J. and Goswami, A., 2013. Testing the inhibitory cascade model in Mesozoic and Cenozoic mammaliaforms. *BMC Evolutionary Biology*, 13(1), pp.1-11.

Hardcastle, Z., Mo, R., Hui, C.C. and Sharpe, P.T., 1998. The Shh signalling pathway in tooth development: defects in Gli2 and Gli3 mutants. *Development*, 125(15), pp.2803-2811.

Harris, E.F., 2007. Carabelli's trait and tooth size of human maxillary first molars. *American Journal of Physical Anthropology*, 132(2), pp.238-246.

HersHKovitz, P., 1971. Basic crown patterns and cusp homologies of mammalian teeth. *Dental Morphology and Evolution*, pp.95-150.

Hendrikse, J.L., Parsons, T.E. and Hallgrímsson, B., 2007. Evolvability as the proper focus of evolutionary developmental biology. *Evolution & Development*, 9(4), pp.393-401.

Hlusko, L.J., 2002. Expression types for two cercopithecoid dental traits (interconulus and interconulid) and their variation in a modern baboon population. *International Journal of Primatology*, 23(6), pp.1309-1318.

Hlusko, L.J., 2004. Protostylid variation in *Australopithecus*. *Journal of Human Evolution*, 46(5), pp.579-594.

Hlusko, L.J., 2016. Elucidating the evolution of hominid dentition in the age of phenomics, modularity, and quantitative genetics. *Annals of Anatomy-Anatomischer Anzeiger*, 203, pp.3-11.

Hlusko, L.J. and Mahaney, M.C., 2007. Of mice and monkeys: Quantitative genetic analyses of size variation along the dental arcade. In *Dental perspectives on human evolution: State of the art research in dental Paleoanthropology* (pp. 237-245). Springer, Dordrecht.

Hlusko, L.J. and Mahaney, M.C., 2009. Quantitative genetics, pleiotropy, and morphological integration in the dentition of *Papio hamadryas*. *Evolutionary Biology*, 36(1), pp.5-18.

Hlusko, L.J., Do, N. and Mahaney, M.C., 2007. Genetic correlations between mandibular molar cusp areas in baboons. *American Journal of Physical Anthropology*, 132(3), pp.445-454.

Hlusko, L.J., Sage, R.D. and Mahaney, M.C., 2011. Modularity in the mammalian dentition: mice and monkeys share a common dental genetic architecture. *Journal of Experimental Zoology Part B: Molecular and Developmental Evolution*, 316(1), pp.21-49.

Hlusko, L.J., Schmitt, C.A., Monson, T.A., Brasil, M.F. and Mahaney, M.C., 2016. The integration of quantitative genetics, paleontology, and neontology reveals genetic underpinnings of primate dental evolution. *Proceedings of the National Academy of Sciences*, 113(33), pp.9262-9267.

Irish, J.D. and Guatelli-Steinberg, D., 2003. Ancient teeth and modern human origins: an expanded comparison of African Plio-Pleistocene and recent world dental samples. *Journal of Human Evolution*, 45(2), pp.113-144.

James, W.W., 1960. *The jaws and teeth of primates: photographs and commentaries*. Pitman Medical Publishing Company.

Järvinen, E., Salazar-Ciudad, I., Birchmeier, W., Taketo, M.M., Jernvall, J. and Thesleff, I., 2006. Continuous tooth generation in mouse is induced by activated epithelial Wnt/ β -catenin signaling. *Proceedings of the National Academy of Sciences*, 103(49), pp.18627-18632.

Järvinen, E., Tummers, M. and Thesleff, I., 2009. The role of the dental lamina in mammalian tooth replacement. *Journal of Experimental Zoology Part B: Molecular and Developmental Evolution*, 312(4), pp.281-291.

Järvinen, E., Välimäki, K., Pummila, M., Thesleff, I. and Jernvall, J., 2008. The taming of the shrew milk teeth. *Evolution & Development*, 10(4), pp.477-486.

Jernvall, J., 2000. Linking development with generation of novelty in mammalian teeth. *Proceedings of the National Academy of Sciences*, 97(6), pp.2641-2645.

Jernvall, J. and Jung, H.S., 2000. Genotype, phenotype, and developmental biology of molar tooth characters. *American Journal of Physical Anthropology* 113(S31), pp.171-190.

Jernvall, J. and Thesleff, I., 2000. Reiterative signaling and patterning during mammalian tooth morphogenesis. *Mechanisms of Development*, 92(1), pp.19-29.

Jernvall, J. and Thesleff, I., 2012. Tooth shape formation and tooth renewal: evolving with the same signals. *Development*, 139(19), pp.3487-3497.

Jernvall, J., Keränen, S.V. and Thesleff, I., 2000. Evolutionary modification of development in mammalian teeth: quantifying gene expression patterns and topography. *Proceedings of the National Academy of Sciences*, 97(26), pp.14444-14448.

Johanson, D.C. 1974. *An odontological study of the chimpanzee with some implications for hominoid evolution*. Ph.D. Dissertation, University of Chicago.

Kangas, A.T., Evans, A.R., Thesleff, I. and Jernvall, J., 2004. Nonindependence of mammalian dental characters. *Nature*, 432(7014), pp.211-214.

Kassai, Y., Munne, P., Hotta, Y., Penttilä, E., Kavanagh, K., Ohbayashi, N., Takada, S., Thesleff, I., Jernvall, J. and Itoh, N., 2005. Regulation of mammalian tooth cusp patterning by ectodin. *Science*, 309(5743), pp.2067-2070.

Kato, A., Tang, N., Borries, C., Papakyrikos, A.M., Hinde, K., Miller, E., Kunimatsu, Y., Hirasaki, E., Shimizu, D. and Smith, T.M., 2014. Intra-and interspecific variation in macaque molar enamel thickness. *American Journal of Physical Anthropology*, 155(3), pp.447-459.

Kavanagh, K.D., Evans, A.R. and Jernvall, J., 2007. Predicting evolutionary patterns of mammalian teeth from development. *Nature*, 449(7161), pp.427-432.

Kay, R.F., 1977. The evolution of molar occlusion in the Cercopithecidae and early catarrhines. *American Journal of Physical Anthropology*, 46(2), pp.327-352.

Keränen, S.V., Kettunen, P., Åberg, T., Thesleff, I. and Jernvall, J., 1999. Gene expression patterns associated with suppression of odontogenesis in mouse and vole diastema regions. *Development, Genes and Evolution*, 209(8), pp.495-506.

Kinzey, W.G., 1973. Reduction of the cingulum in Ceboidea. In *Symp 4th Int Congr Primat, Craniofacial Biology of Primates* (Vol. 3, pp. 101-127). S. Karger.

Koh, C., Bates, E., Broughton, E., Do, N.T., Fletcher, Z., Mahaney, M.C. and Hlusko, L.J., 2010. Genetic integration of molar cusp size variation in baboons. *American Journal of Physical Anthropology*, 142(2), pp.246-260.

Kondo, S. and Townsend, G.C., 2006. Associations between Carabelli trait and cusp areas in human permanent maxillary first molars. *American Journal of Physical Anthropology*, 129(2), pp.196-203.

Korenhof, C.A.W., 1960. Morphogenetical aspects of the human upper molar. *A comparative study of its enamel and dentine surfaces and their relationship to the crown pattern of fossil and recent primates*, Uitgeversmaatschappij Neerlandia, Utrecht.

Korenhof, C.A.W. 1961. The enamel-dentine border: a new morphological factor in the study of the (human) molar pattern. *Proc. Koninkl. Nederl. Acad. Wetensch*, 64, pp.639-664.

Korenhof, C.A.W., 1978. De evolutie van het ondermolaarpatroon en overblijfselen van het trigonid bij de mens (I). *Ned. Tijdschr. Tandheelkd*, 85, pp.456-495.

Korenhof, C.A.W., 1982. Evolutionary trends of the inner enamel anatomy of deciduous molars from Sangiran (Java, Indonesia). *Teeth; From, Function and Evolution*, pp.350-365.

Kraus, B.S., 1952. Morphologic relationships between enamel and dentin surfaces of lower first molar teeth. *Journal of Dental Research*, 31(2), pp.248-256.

Kraus, B.S. and Jordan, R.E., 1965. *The human dentition before birth*. Lea & Febiger.

Kraus, B.S. and Oka, S.W., 1967. Wrinkling of molar crowns: new evidence. *Science*, 157(3786), pp.328-329.

Kozitzky, E.A. and Shara E.B., 2019. Mixed support for the patterning cascade model in bears: Implications for understanding the evolution and development of hominoid molar morphology. *American Association of Physical Anthropologists Conference Poster*

Labonne, G., Laffont, R., Renvoise, E., Jebrane, A., Labruère, C., Chateau-Smith, C., Navarro, N. and Montuire, S., 2012. When less means more: evolutionary and developmental hypotheses in rodent molars. *Journal of Evolutionary Biology*, 25(10), pp.2102-2111.

Lieberman, D.E., 1999. Homology and hominid phylogeny: problems and potential solutions. *Evolutionary Anthropology: Issues, News, and Reviews: Issues, News, and Reviews*, 7(4), pp.142-151.

Lumsden, A., 1988. Spatial organization of the epithelium and the role of neural crest cells in the initiation of the mammalian tooth germ. *Development*, 103, pp.155-169.

Macchiarelli, R., Bondioli, L., Debénath, A., Mazurier, A., Tournepiche, J.F., Birch, W. and Dean, M.C., 2006. How Neanderthal molar teeth grew. *Nature*, 444(7120), pp.748-751.

Macho, G.A., Jiang, Y. and Spears, I.R., 2003. Enamel microstructure—a truly three-dimensional structure. *Journal of Human Evolution*, 45(1), pp.81-90.

Marchiori, D.F., Packota, G.V. and Boughner, J.C., 2016. Third-molar mineralization as a function of available retromolar space. *Acta Odontologica Scandinavica*, 74(7), pp.509-517.

Martin, R.M., Hublin, J.J., Gunz, P. and Skinner, M.M., 2017. The morphology of the enamel–dentine junction in Neanderthal molars: Gross morphology, non-metric traits, and temporal trends. *Journal of Human Evolution*, 103, pp.20-44.

Martínez de Pinillos, M., Martínón-Torres, M., Martín-Francés, L., Arsuaga, J.L. and de Castro, J.M.B., 2017. Comparative analysis of the trigonid crests patterns in Homo antecessor molars at the enamel and dentine surfaces. *Quaternary International*, 433, pp.189-198.

Mina, M. and Kollar, E.J., 1987. The induction of odontogenesis in non-dental mesenchyme combined with early murine mandibular arch epithelium. *Archives of Oral Biology*, 32(2), pp.123-127.

Miyado, M., Ogi, H., Yamada, G., Kitoh, J., Jogahara, T., Oda, S.I., Sato, I., Miyado, K. and Sunohara, M., 2007. Sonic hedgehog expression during early tooth development in *Suncus murinus*. *Biochemical and Biophysical Research Communications*, 363(2), pp.269-275.

Morita, W., Morimoto, N. and Ohshima, H., 2016. Exploring metameric variation in human molars: a morphological study using morphometric mapping. *Journal of Anatomy*, 229(3), pp.343-355.

Morita, W., Morimoto, N., Otsu, K. and Miura, T., 2022. Stripe and spot selection in cusp patterning of mammalian molar formation. *Scientific reports*, 12(1), pp.1-11.

Monson, T.A., 2012. Metameric Variation in the Expression of the Interconulus in Papio and Macaca (Doctoral dissertation, San Francisco State University).

Moustakas, J.E., Smith, K.K. and Hlusko, L.J., 2011. Evolution and development of the mammalian dentition: insights from the marsupial *Monodelphis domestica*. *Developmental Dynamics*, 240(1), pp.232-239.

Müller, G.B. and Wagner, G.P., 1996. Homology, Hox genes, and developmental integration. *American Zoologist*, 36(1), pp.4-13.

Mustonen, T., Ilmonen, M., Pummila, M., Kangas, A.T., Laurikkala, J., Jaatinen, R., Pispä, J., Gaide, O., Schneider, P., Thesleff, I. and Mikkola, M.L., Ectodysplasin A1 promotes placodal cell fate during early morphogenesis of ectodermal appendages. *Development*, 131, pp.4907-4919.

Nager, G., 1960. Der vergleich zwischen dem räumlichen verhalten des dentin-kronenreliefs und dem schmelzrelief der zahnkrone. *Cells Tissues Organs*, 42(3), pp.226-250.

Navarro, N. and Murat Maga, A., 2018. Genetic mapping of molar size relations identifies inhibitory locus for third molars in mice. *Heredity*, 121(1), pp.1-11.

Niswander, L. and Martin, G.R., 1992. Fgf-4 expression during gastrulation, myogenesis, limb and tooth development in the mouse. *Development*, 114(3), pp.755-768.

Olejniczak, A.J., Martin, L.B. and Ulhaas, L., 2004. Quantification of dentine shape in anthropoid primates. *Annals of Anatomy-Anatomischer Anzeiger*, 186(5-6), pp.479-485.

Olejniczak, A.J., Tafforeau, P., Smith, T.M., Temming, H. and Hublin, J.J., 2007. Compatibility of microtomographic imaging systems for dental measurements. *American Journal of Physical Anthropology*, 134(1), pp.130-134.

Orlosky, F., 1973. Comparative Dental Morphology of Extant and Extinct Cebidae. PhD Dissertation, University of Washington, Seattle.

Ortiz, A., Bailey, S.E., Hublin, J.J. and Skinner, M.M., 2017. Homology, homoplasy and cusp variability at the enamel–dentine junction of hominoid molars. *Journal of Anatomy*, 231(4), pp.585-599.

Ortiz, A., Bailey, S.E., Schwartz, G.T., Hublin, J.J. and Skinner, M.M., 2018. Evo-devo models of tooth development and the origin of hominoid molar diversity. *Science advances*, 4(4), p.eaar2334.

Ortiz, A., Skinner, M.M., Bailey, S.E. and Hublin, J.J., 2012. Carabelli's trait revisited: An examination of mesiolingual features at the enamel–dentine junction and enamel surface of Pan and Homo sapiens upper molars. *Journal of Human Evolution*, 63(4), pp.586-596.

Osborn, H.F., 1888. The evolution of mammalian molars to and from the tritubercular type. *The American Naturalist*, 22(264), pp.1067-1079.

Osborn, J.W., 1978. Morphogenetic gradients: fields versus clones. In: Butler PM, Joysey KA, editors. *Development, function and evolution of teeth*. London, New York and San Francisco: Academic Press, p.171-201

Oster, G. and Alberch, P., 1982. Evolution and bifurcation of developmental programs. *Evolution*, pp.444-459.

Patterson, B., 1956. Early Cretaceous mammals and the evolution of mammalian molar teeth. *Fieldiana-Geology*, 13, pp.1-105.

Pilbrow, V.C., 2003. *Dental variation in African apes with implications for understanding patterns of variation in species of fossil apes*. New York University.

Pilbrow, V., 2006. Lingual incisor traits in modern hominoids and an assessment of their utility for fossil hominoid taxonomy. *American Journal of Physical Anthropology*, 129(3), pp.323-338.

Plikus, M.V., Zeichner-David, M., Mayer, J.A., Reyna, J., Bringas, P., Thewissen, J.G.M., Snead, M.L., Chai, Y. and Chuong, C.M., 2005. Morphoregulation of teeth: modulating the number,

size, shape and differentiation by tuning Bmp activity. *Evolution & Development*, 7(5), pp.440-457.

Polly, P.D., 1998. Variability, selection, and constraints: development and evolution in viverravid (Carnivora, Mammalia) molar morphology. *Paleobiology*, 24(4), pp.409-429.

Polly, P.D., 2007. Development with a bite. *Nature*, 449(7161), pp.413-414.

Polly, P.D., 2008. Developmental dynamics and G-matrices: Can morphometric spaces be used to model phenotypic evolution? *Evolutionary Biology*, 35(2), pp.83-96.

Renvoisé, E., Evans, A.R., Jebrane, A., Labruère, C., Laffont, R. and Montuire, S., 2009. Evolution of mammal tooth patterns: new insights from a developmental prediction model. *Evolution: International Journal of Organic Evolution*, 63(5), pp.1327-1340.

Renvoisé, E., Kavanagh, K.D., Lazzari, V., Häkkinen, T.J., Rice, R., Pantalacci, S., Salazar-Ciudad, I. and Jernvall, J., 2017. Mechanical constraint from growing jaw facilitates mammalian dental diversity. *Proceedings of the National Academy of Sciences*, 114(35), pp.9403-9408.

Rodrigues, H.G., Renaud, S., Charles, C., Le Poul, Y., Solé, F., Aguilar, J.P., Michaux, J., Tafforeau, P., Headon, D., Jernvall, J. and Viriot, L., 2013. Roles of dental development and adaptation in rodent evolution. *Nature Communications*, 4(1), pp.1-8.

Roseman, C.C. and Delezene, L.K., 2019. The inhibitory cascade model is not a good predictor of molar size covariation. *Evolutionary Biology*, 46(3), pp.229-238.

Roth, V.L., 1984. On homology. *Biological Journal of the Linnean Society*, 22(1), pp.13-29.

Salazar-Ciudad, I. and Jernvall, J., 2002. A gene network model accounting for development and evolution of mammalian teeth. *Proceedings of the National Academy of Sciences*, 99(12), pp.8116-8120.

Salazar-Ciudad, I. and Jernvall, J., 2010. A computational model of teeth and the developmental origins of morphological variation. *Nature*, 464(7288), pp.583-586.

Schroer, K. and Wood, B., 2015. Modeling the dental development of fossil hominins through the inhibitory cascade. *Journal of Anatomy*, 226(2), pp.150-162.

Schulze, M.A. and Pearce, J.A., 1994, November. A morphology-based filter structure for edge-enhancing smoothing. In *Proceedings of 1st International Conference on Image Processing* (Vol. 2, pp. 530-534). IEEE.

Schwartz, J.H., 1984. What is a Tarsier?. In *Living Fossils* (pp. 38-49). Springer, New York, NY.

Schwartz, J.H. and Tattersall, I., 1985. *Evolutionary relationships of living lemurs and lorises (Mammalia, Primates) and their potential affinities with European Eocene Adapidae* (Vol. 60, No. 1). American Museum of Natural History.

Schwartz, G.T., Thackeray, J.F., Reid, C. and Van Reenan, J.F., 1998. Enamel thickness and the topography of the enamel–dentine junction in South African Plio-Pleistocene hominids with special reference to the Carabelli trait. *Journal of Human Evolution*, 35(4-5), pp.523-542.

Scott, G.R. and Dahlberg, A.A., 1982. Microdifferentiation in tooth crown morphology among Indians of the American Southwest. *Teeth: Form. Function and Evolution. New York*, pp.259-91.

Scott, G.R. and Turner, C.G., 1997. *Anthropology of modern human teeth* (p. 381). Cambridge: Cambridge University Press.

Seiffert, E.R., Simons, E.L., Clyde, W.C., Rossie, J.B., Attia, Y., Bown, T.M., Chatrath, P. and Mathison, M.E., 2005. Basal anthropoids from Egypt and the antiquity of Africa's higher primate radiation. *Science*, 310(5746), pp.300-304.

Selig, K.R., Khalid, W. and Silcox, M.T., 2021. Mammalian molar complexity follows simple, predictable patterns. *Proceedings of the National Academy of Sciences*, 118(1), p.e2008850118.

Seligsohn, D., and Szalay, F.S., 1978. Relationship between natural selection and dental morphology: tooth function and diet in *Lepilemur* and *Hapalemur*. *Development, Function and Evolution of Teeth*, pp.289-307.

Sharpe, P.T., 1995. Homeobox genes and orofacial development. *Connective Tissue Research*, 32(1-4), pp.17-25.

Shubin, N.H. and Wake, D., 1996. Phylogeny, variation, and morphological integration. *American Zoologist de Palaeontologie* 36, pp.51-60

Singleton, M., Rosenberger, A.L., Robinson, C. and O'Neill, R., 2011. Allometric and metameric shape variation in Pan mandibular molars: a digital morphometric analysis. *The Anatomical Record: Advances in Integrative Anatomy and Evolutionary Biology*, 294(2), pp.322-334.

Skinner, M.M., Evans, A., Smith, T., Jernvall, J., Tafforeau, P., Kupczik, K., Olejniczak, A.J., Rosas, A., Radovčić, J., Thackeray, J.F. and Toussaint, M., 2010. Brief communication: Contributions of enamel-dentine junction shape and enamel deposition to primate molar crown complexity. *American Journal of Physical Anthropology*, 142(1), pp.157-163.

Skinner, M.M. and Gunz, P., 2010. The presence of accessory cusps in chimpanzee lower molars is consistent with a patterning cascade model of development. *Journal of Anatomy*, 217(3), pp.245-253.

Skinner, M.F. and Skinner, M.M., 2017. Orangutans, enamel defects, and developmental health: A comparison of Borneo and Sumatra. *American Journal of Primatology*, 79(8), p.e22668.

Skinner, M.M., Wood, B.A., Boesch, C., Olejniczak, A.J., Rosas, A., Smith, T.M. and Hublin, J.J., 2008. Dental trait expression at the enamel-dentine junction of lower molars in extant and fossil hominoids. *Journal of Human Evolution*, 54(2), pp.173-186.

Skinner, M.M., Wood, B.A. and Hublin, J.J., 2009. Protostylid expression at the enamel-dentine junction and enamel surface of mandibular molars of *Paranthropus robustus* and *Australopithecus africanus*. *Journal of Human Evolution*, 56(1), pp.76-85.

Smith, T.M., Olejniczak, A.J., Zermeno, J.P., Tafforeau, P., Skinner, M.M., Hoffmann, A., Radovčić, J., Toussaint, M., Kruszynski, R., Menter, C. and Moggi-Cecchi, J., 2012. Variation in enamel thickness within the genus *Homo*. *Journal of Human Evolution*, 62(3), pp.395-411.

Soukup, V., Epperlein, H.H., Horáček, I. and Cerny, R., 2008. Dual epithelial origin of vertebrate oral teeth. *Nature*, 455(7214), pp.795-798.

Suwa, G., Wood, B.A. and White, T.D., 1994. Further analysis of mandibular molar crown and cusp areas in Pliocene and early Pleistocene hominids. *American Journal of Physical Anthropology*, 93(4), pp.407-426.

Swindler, D.R., 1976. *Dentition of living primates*. Academic Press, New York

Swindler, D.R., 2002. *Primate dentition: an introduction to the teeth of non-human primates* (Vol. 32). Cambridge University Press.

Szalay, F.S. and Delson, E., 2013. *Evolutionary history of the primates*. Academic Press, London.

Ten Cate, A.R., 1998. *Oral histology: development, structure, and function*. St. Louis; Toronto: Mosby.

Thesleff, I., 2003. Epithelial-mesenchymal signalling regulating tooth morphogenesis. *Journal of Cell Science*, 116(9), pp.1647-1648.

Thesleff, I. and Nieminen, P., 1996. Tooth morphogenesis and cell differentiation. *Current Opinion in Cell Biology*, 8(6), pp.844-850.

Thesleff, I., Vaahtokari, A. and Partanen, A.M., 1995. Regulation of organogenesis. Common molecular mechanisms regulating the development of teeth and other organs. *The International Journal of Developmental Biology*, 39(1), pp.35-50.

Tucker, A. and Sharpe, P., 2004. The cutting-edge of mammalian development; how the embryo makes teeth. *Nature Reviews Genetics*, 5(7), pp.499-508.

Tucker, A.S., Matthews, K.L. and Sharpe, P.T., 1998. Transformation of tooth type induced by inhibition of BMP signaling. *Science*, 282(5391), pp.1136-1138.

Tummers, M. and Thesleff, I., 2009. The importance of signal pathway modulation in all aspects of tooth development. *Journal of Experimental Zoology Part B: Molecular and Developmental Evolution*, 312(4), pp.309-319.

Turner, C.I., 1991. Scoring produces for key morphological traits of the permanent dentition: The Arizona State University dental anthropology system. *Advances in dental anthropology*, pp.13-31.

Uchida, A., 1996. *Craniodental Variation among the Great Apes*. Peabody Museum of Archaeology and Ethnology, Harvard University, Cambridge.

Ungar, P., 2004. Dental topography and diets of *Australopithecus afarensis* and early *Homo*. *Journal of Human Evolution*, 46(5), pp.605-622.

Ungar, P.S., 2015. Mammalian dental function and wear: a review. *Biosurface and Biotribology*, 1(1), pp.25-41.

Vaahtokari, A., Åberg, T., Jernvall, J., Keränen, S. and Thesleff, I., 1996. The enamel knot as a signaling center in the developing mouse tooth. *Mechanisms of Development*, 54(1), pp.39-43.

Vandebroek, G., 1961. The comparative anatomy of the teeth of lower and non-socialised mammals. *Kon. VI. Acad. Wetens. Lett. Sch. Kunst. Belgie*, 1, pp.215-313.

Vitek, N.S., Roseman, C.C. and Bloch, J.I., 2020. Mammal molar size ratios and the inhibitory cascade at the intraspecific scale. *Integrative Organismal Biology*, 2(1), p.obaa020.

Wakamatsu, Y., Egawa, S., Terashita, Y., Kawasaki, H., Tamura, K. and Suzuki, K., 2019. Homeobox code model of heterodont tooth in mammals revised. *Scientific reports*, 9(1), pp.1-13.

Wilson, G.P., Evans, A.R., Corfe, I.J., Smits, P.D., Fortelius, M. and Jernvall, J., 2012. Adaptive radiation of multituberculate mammals before the extinction of dinosaurs. *Nature*, 483(7390), pp.457-460.

Winchester, J.M., 2016. *Molar topographic shape as a system for inferring functional morphology and developmental patterning in extant cercopithecoid primates* (Doctoral dissertation, State University of New York at Stony Brook).

Wollny, G., Kellman, P., Ledesma-Carbayo, M.J., Skinner, M.M., Hublin, J.J. and Hierl, T., 2013. MIA-A free and open source software for gray scale medical image analysis. *Source Code for Biology and Medicine*, 8(1), pp.1-20.

Wood, B.A. and Abbott, S.A., 1983. Analysis of the dental morphology of Plio-pleistocene hominids. I. Mandibular molars: crown area measurements and morphological traits. *Journal of Anatomy*, 136(Pt 1), p.197.

Appendix A.

Primate species used in this thesis divided into clades relevant to their tooth crown morphology.

Strepsirrhini	n	Ceboidea	n	Cercopithecidae	n	Hominoidea	n
Lemuridae		Callitrichinae		Cercopithecini		Hominidae	
<i>Prolemur simus</i>	1	<i>Cebuella pygmaea</i>	1	<i>Erythrocebus patas</i>	2	<i>Pan troglodytes</i>	55
<i>Haplemur griseus</i>	2	<i>Callithrix jacchus</i>	3	<i>Chlorocebus aethiops</i>	4	<i>Pan paniscus</i>	22
<i>Eulemur fulvus</i>	2	<i>Leontopithecus rosalia</i>	2	<i>Miopithecus talapoin</i>	2	<i>Homo sapiens</i>	56
<i>Varecia variegata</i>	2	<i>Leontopithecus chrysopygus</i>	2	<i>Cercopithecus mitis</i>	6	<i>Gorilla gorilla</i>	12
		<i>Saguinus mystax</i>	2			<i>Pongo pygmaeus</i>	40
Lepilemuridae		<i>Saguinus oedipus</i>	2	Papionini		<i>Homo neanderthalensis</i>	4
<i>Lepilemur leucopus</i>	2			<i>Macaca fascicularis</i>	24	Hylobatidae	
<i>Lepilemur mustelinus</i>	1	Aotinae		<i>Macaca fuscata</i>	11	<i>Hylobates muelleri</i>	4
		<i>Aotus sp.</i>	10	<i>Macaca arctoides</i>	2	<i>Hylobates agilis</i>	2
Cheirogaleidae				<i>Macaca sylvanus</i>	2	<i>Hylobates lar</i>	1
<i>Phaner furcifer</i>	2	Cebinae		<i>Lophocebus albigena</i>	5	<i>Hoolock sp.</i>	1
<i>Microcebus sp.</i>	2	<i>Saimiri sp.</i>	2	<i>Papio anubis</i>	15		
<i>Cheirogaleus sp.</i>	3	<i>Cebus olivaceus</i>	1	<i>Theropithecus gelada</i>	2		
		<i>Cebus albifrons</i>	4	<i>Mandrillus sphinx</i>	3		
Indriidae		<i>Cebus capucinus</i>	1	<i>Mandrillus leucophaeus</i>	1		
<i>Propithecus diadema</i>	1	<i>Sapajus apella</i>	5	<i>Cercocebus torquatus</i>	2		
<i>Indri indri</i>	2						
<i>Avahi laniger</i>	2	Pitheciinae		Colobinae			
		<i>Cacajao calvus</i>	3	<i>Nasalis larvatus</i>	4		
Galagidae		<i>C. melanocephalus</i>	5	<i>Semnopithecus entellus</i>	2		
<i>Galago senegalensis</i>	3	<i>Chiropotes satanas</i>	9	<i>Trachypithecus cristatus</i>	5		
<i>Otolemur garnettii</i>	2	<i>Pithecia pithecia</i>	6	<i>Trachypithecus vetulus</i>	2		
<i>Euticus elegantulus</i>	2			<i>Presbytis comata</i>	1		
		Callicebinae		<i>Presbytis melalophos</i>	4		
Lorisidae		<i>Callicebus moloch</i>	4	<i>Ptilocolobus pennantii</i>	3		
<i>Loris tardigradus</i>	2			<i>Colobus guereza</i>	10		
<i>Nycticebus coucang</i>	3	Atelinae				Tarsioidea	n
<i>Perodicticus potto</i>	2	<i>Ateles geoffroyi</i>	9			<i>Tarsius spectrum</i>	2
<i>Arctocebus calabarensis</i>	2	<i>Alouatta seniculus</i>	8			<i>Tarsius syrichta</i>	1

Appendix B.

Example of the R code used in Chapter 4.

```
setwd("C:/Users/sac200/Desktop/3D GM R/molar test")
source("C:/Users/sac200/Desktop/3D GM R/evenPts.R")
source("C:/Users/sac200/Desktop/3D GM R/orp.R")

library(gtools);library(geomorph);library(Morpho);
library(tripack);library(klaR);
library(pca3d);library(princurve);
library(matlib);library(plot3D);
library(geometry);library(magick)

## use sessionInfo() to check whether the packages have successfully loaded.
sessionInfo()

filelist_EDJ_r <- list.files(path = "C:/Users/sac200/Desktop/3D GM R/molar
test/Landmarks_CEJ",pattern = ".EDJ_RIDGE.*.landmarkAscii")
sorted_EDJ_r <- mixedsort(sort(filelist_EDJ_r))
sorted_EDJ_r <- paste("Landmarks/",sorted_EDJ_r,sep="")

filelist_EDJ_m <- list.files(path = "C:/Users/sac200/Desktop/3D GM R/molar
test/Landmarks_CEJ",pattern = ".EDJ_MAIN.*.landmarkAscii")
sorted_EDJ_m <- mixedsort(sort(filelist_EDJ_m))
sorted_EDJ_m <- paste("Landmarks/",sorted_EDJ_m,sep="")

filelist_CEJ_r <- list.files(path = "C:/Users/sac200/Desktop/3D GM R/molar
test/Landmarks_CEJ",pattern = ".CEJ_RIDGE.*.landmarkAscii")
sorted_CEJ_r <- mixedsort(sort(filelist_CEJ_r))
sorted_CEJ_r <- paste("Landmarks/",sorted_CEJ_r,sep="")
```



```

filenames <- list.files(path = "C:/Users/sac200/Desktop/3D GM R/molar
test/Landmarks_CEJ",pattern = ".EDJ_MAIN.*.landmarkAscii")

sortednames <- mixedsort(sort(filenames))

spec_names<-strtrim(sortednames, nchar(sortednames)-23)

position <- "M2"

farbe<-
c("black","gray","chartreuse","orange","red","darkred","purple","darkorange","darkorange","darkgr
een","cyan","turquoise","brown","black","black")

farbetext<-
c("blue","magenta","chartreuse","orange","red","red","darkred","purple","darkorange","darkorang
e","darkgreen","cyan","turquoise","brown","black","black")

## checks if lists have same length
length(filelist_EDJ_r)==length(filelist_EDJ_m)
length(filelist_CEJ_r)==length(filelist_EDJ_m)
length(sortednames)==length(filelist_EDJ_m)

# load landmark files
data_list_EDJ_r = lapply((sorted_EDJ_r), read.table, fill = T, skip=14, sep = "")
datamat_EDJ_r <- sapply(data_list_EDJ_r, as.matrix, simplify=FALSE)

data_list_EDJ_m = lapply((sorted_EDJ_m), read.table, fill = T, skip=14, sep = "")
datamat_EDJ_m <- sapply(data_list_EDJ_m, as.matrix, simplify=FALSE)

data_list_CEJ_r = lapply((sorted_CEJ_r), read.table, fill = T, skip=14, sep = "")
datamat_CEJ_r <- sapply(data_list_CEJ_r, as.matrix, simplify=FALSE)

## fits splines
CEJ_curve<-list();EDJ_curve<-list()
EDJ_spline<-list();CEJ_spline<-list()

```

```

for(e in 1:length(datamat_EDJ_r)){

  EDJ_curve[[e]]<-rbind(datamat_EDJ_r[[e]],datamat_EDJ_r[[e]][1,])
  CEJ_curve[[e]]<-rbind(datamat_CEJ_r[[e]],datamat_CEJ_r[[e]][1,])

  xE<-spline(EDJ_curve[[e]][,1],method="natural")
  xC<-spline(CEJ_curve[[e]][,1],method="natural")

  yE<-spline(EDJ_curve[[e]][,2],method="natural")
  yC<-spline(CEJ_curve[[e]][,2],method="natural")

  zE<-spline(EDJ_curve[[e]][,3],method="natural")
  zC<-spline(CEJ_curve[[e]][,3],method="natural")

  EDJ_spline[[e]]<-cbind(xE$y,yE$y,zE$y)
  CEJ_spline[[e]]<-cbind(xC$y,yC$y,zC$y)
}

a<-11;clear3d("shapes");xmed<-median(EDJ_spline[[a]][,1]); ymed<-median(EDJ_spline[[a]][,2]);
zmed<-median(EDJ_spline[[a]][,3])

plot3d(EDJ_spline[[a]],type="",xlim=c(xmed-10,xmed+10),ylim=c(ymed-10,ymed+10),zlim=c(zmed-
10,zmed+10),aspect =T,xlab="",ylab="",zlab="",box=F,axes=F,main="Splines shown in black")

lines3d(CEJ_spline[[a]]);spheres3d(datamat_CEJ_r[[a]],radius=0.05,col="blue")

spheres3d(datamat_EDJ_m[[a]],radius=0.08,col="red")
spheres3d(datamat_EDJ_r[[a]],radius=0.05,col="blue")

# Project main landmarks on to curve

proj_pts<-list()

for(b in 1:length(datamat_EDJ_r)){

  proj <- project_to_curve(datamat_EDJ_m[[b]],EDJ_spline[[b]],stretch=0)

```

```

proj_pts[[b]] <- proj$s
}

# Splits EDJ ridge spline according to projections of fixed LMs

f1dist<-list();f1dism<-list();f1pos<-list();closestf1<-list()
f2dist<-list();f2dism<-list();f2pos<-list()
f3dist<-list();f3dism<-list();f3pos<-list()
f4dist<-list();f4dism<-list();f4pos<-list()
EDJ_spline_1<-list();EDJ_spline_2<-list();EDJ_spline_3<-list();EDJ_spline_4<-list()

for(i in 1:length(datamat_EDJ_r)){

  f1dist[[i]]<-as.matrix(dist(rbind(proj_pts[[i]][1,],EDJ_spline[[i]])))[1,]
  f1dism[[i]]<-matrix(f1dist[[i]][c(2:length(f1dist[[i]]))])
  row.names(f1dism[[i]])<-c(1:length(f1dism[[i]]))
  closestf1[[i]]<-as.numeric(names((f1dism[[i]][order(f1dism[[i]][,1]),])[c(1,2)]))
  if(abs(diff(closestf1[[i]]))==1){
    f1pos[[i]]<-min(closestf1[[i]])
  } else if(abs(diff(closestf1[[i]])>1){
    f1pos[[i]]<- 0
  }

  f2dist[[i]]<-as.matrix(dist(rbind(proj_pts[[i]][2,],EDJ_spline[[i]])))[1,]
  f2dism[[i]]<-matrix(f2dist[[i]][c(2:length(f2dist[[i]]))])
  row.names(f2dism[[i]])<-c(1:length(f2dism[[i]]))
  f2pos[[i]]<-min(as.numeric(names((f2dism[[i]][order(f2dism[[i]][,1]),])[c(1,2)])))

  f3dist[[i]]<-as.matrix(dist(rbind(proj_pts[[i]][3,],EDJ_spline[[i]])))[1,]
  f3dism[[i]]<-matrix(f3dist[[i]][c(2:length(f3dist[[i]]))])
  row.names(f3dism[[i]])<-c(1:length(f3dism[[i]]))

```

```

f3pos[[i]]<-min(as.numeric(names((f3distm[[i]][order(f3distm[[i]][,1]),,])[c(1,2)])))

f4dist[[i]]<-as.matrix(dist(rbind(proj_pts[[i]][4,],EDJ_spline[[i]]))[1,]
f4distm[[i]]<-matrix(f4dist[[i]][c(2:length(f4dist[[i]]))])
row.names(f4distm[[i]])<-c(1:length(f4distm[[i]]))
f4pos[[i]]<-min(as.numeric(names((f4distm[[i]][order(f4distm[[i]][,1]),,])[c(1,2)])))

if(f1pos[[i]]<f2pos[[i]]){
  EDJ_spline_1[[i]]<-EDJ_spline[[i]][c((f1pos[[i]]+1):f2pos[[i]]),]
  EDJ_spline_2[[i]]<-EDJ_spline[[i]][c((f2pos[[i]]+1):f3pos[[i]]),]
  EDJ_spline_3[[i]]<-EDJ_spline[[i]][c((f3pos[[i]]+1):f4pos[[i]]),]
  EDJ_spline_4[[i]]<-EDJ_spline[[i]][c((f4pos[[i]]+1):(length(EDJ_spline[[i]][,1])-1)),]
} else if(f1pos[[i]]>f2pos[[i]]){
  EDJ_spline_1[[i]]<-EDJ_spline[[i]][c(1:f2pos[[i]]),]
  EDJ_spline_2[[i]]<-EDJ_spline[[i]][c((f2pos[[i]]+1):f3pos[[i]]),]
  EDJ_spline_3[[i]]<-EDJ_spline[[i]][c((f3pos[[i]]+1):f4pos[[i]]),]
  EDJ_spline_4[[i]]<-EDJ_spline[[i]][c((f4pos[[i]]+1):f1pos[[i]]),]
}
}

#PLOT
a<-2;{clear3d("shapes");xmed<-median(CEJ_spline[[a]][,1]); ymed<-median(CEJ_spline[[a]][,2]);
zmed<-median(CEJ_spline[[a]][,3])

plot3d(CEJ_spline[[a]],type="l",xlab="", ylab="", zlab="", aspect =T,box=F,axes=F,xlim=c(xmed-
10,xmed+10),ylim=c(ymed-10,ymed+10),zlim=c(zmed-10,zmed+10))

lines3d(EDJ_spline_1[[a]],col="orange")
texts3d(c(EDJ_spline_1[[a]][as.integer(length(EDJ_spline_1[[a]][,1])/2),,],texts = "EDJ 1",font=2)
lines3d(EDJ_spline_2[[a]],col="red")
texts3d(c(EDJ_spline_2[[a]][as.integer(length(EDJ_spline_2[[a]][,1])/2),,],texts = "EDJ 2",font=2)
lines3d(EDJ_spline_3[[a]],col="blue")
texts3d(c(EDJ_spline_3[[a]][as.integer(length(EDJ_spline_3[[a]][,1])/2),,],texts = "EDJ 3",font=2)
lines3d(EDJ_spline_4[[a]],col="green")

```

```
texts3d(c(EDJ_spline_4[[a]][as.integer(length(EDJ_spline_4[[a]][,1])/2)],),texts = "EDJ 4",font=2)
spheres3d(datamat_EDJ_m[[a]],radius=0.05)}
```

```
# places main landmarks at end of each EDJ spline
```

```
EDJ_spline_1m<-list();EDJ_spline_2m<-list();EDJ_spline_3m<-list();EDJ_spline_4m<-list()
```

```
for(e in 1:length(datamat_EDJ_r)){
```

```
  EDJ_spline_1m[[e]]<-rbind(datamat_EDJ_m[[e]][1,],EDJ_spline_1[[e]],datamat_EDJ_m[[e]][2,])
```

```
  EDJ_spline_2m[[e]]<-rbind(datamat_EDJ_m[[e]][2,],EDJ_spline_2[[e]],datamat_EDJ_m[[e]][3,])
```

```
  EDJ_spline_3m[[e]]<-rbind(datamat_EDJ_m[[e]][3,],EDJ_spline_3[[e]],datamat_EDJ_m[[e]][4,])
```

```
  EDJ_spline_4m[[e]]<-rbind(datamat_EDJ_m[[e]][4,],EDJ_spline_4[[e]],datamat_EDJ_m[[e]][1,])
```

```
}
```

```
a<-1;clear3d("shapes");xmed<-median(CEJ_spline[[a]][,1]); ymed<-median(CEJ_spline[[a]][,2]);
zmed<-median(CEJ_spline[[a]][,3])
```

```
plot3d(CEJ_spline[[a]],type="l",xlab="", ylab="", zlab="",aspect =T,box=F,axes=F,xlim=c(xmed-10,xmed+10),ylim=c(ymed-10,ymed+10),zlim=c(zmed-10,zmed+10))
```

```
lines3d(EDJ_spline_1m[[a]],col="orange")
```

```
texts3d(c(EDJ_spline_1[[a]][as.integer(length(EDJ_spline_1[[a]][,1])/2)],),texts = "EDJ 1",font=2)
```

```
lines3d(EDJ_spline_2m[[a]],col="red")
```

```
texts3d(c(EDJ_spline_2[[a]][as.integer(length(EDJ_spline_2[[a]][,1])/2)],),texts = "EDJ 2",font=2)
```

```
lines3d(EDJ_spline_3m[[a]],col="blue")
```

```
texts3d(c(EDJ_spline_3[[a]][as.integer(length(EDJ_spline_3[[a]][,1])/2)],),texts = "EDJ 3",font=2)
```

```
lines3d(EDJ_spline_4m[[a]],col="green")
```

```
texts3d(c(EDJ_spline_4[[a]][as.integer(length(EDJ_spline_4[[a]][,1])/2)],),texts = "EDJ 4",font=2)
```

```
# places equidistant semi-landmarks along the splines
```

```
EDJ1<-18;EDJ2<-15;EDJ3<-15;EDJ4<-12
```

```
CEJ<-30
```

```

eq_EDJ1<-list();eq_EDJ2<-list();eq_EDJ3<-list();eq_EDJ4<-list();eq_CEJ<-list();combined<-list()

for(d in 1:length(EDJ_spline_1)){

  eq_EDJ1[[d]]<-digit.curves(start=EDJ_spline_1m[[d]][1,],curve=EDJ_spline_1m[[d]],nPoints=EDJ1,
closed = F)

  eq_EDJ2[[d]]<-digit.curves(start=EDJ_spline_2m[[d]][1,],curve=EDJ_spline_2m[[d]],nPoints=EDJ2,
closed = F)

  eq_EDJ3[[d]]<-digit.curves(start=EDJ_spline_3m[[d]][1,],curve=EDJ_spline_3m[[d]],nPoints=EDJ3,
closed = F)

  eq_EDJ4[[d]]<-digit.curves(start=EDJ_spline_4m[[d]][1,],curve=EDJ_spline_4m[[d]],nPoints=EDJ4,
closed = F)

  eq_CEJ[[d]]<-digit.curves(start=CEJ_spline[[d]][1,],curve=CEJ_spline[[d]],nPoints=CEJ,closed=T)

  combined[[d]]<-rbind(eq_EDJ1[[d]][1:(length(eq_EDJ1[[d]][1,])-
1),],eq_EDJ2[[d]][1:(length(eq_EDJ2[[d]][1,])-1),],eq_EDJ3[[d]][1:(length(eq_EDJ3[[d]][1,])-
1),],eq_EDJ4[[d]][1:(length(eq_EDJ4[[d]][1,])-1),],eq_CEJ[[d]][1:(length(eq_CEJ[[d]][1,])),])
}

```

```

NewCoordsArray <- array(as.numeric(unlist(combined)), dim=c(nrow(combined[[1]]),
ncol(combined[[1]]),length(combined)))

```

```

a<-1;{clear3d("shapes"); xmed<-median(CEJ_spline[[a]][1,]); ymed<-median(CEJ_spline[[a]][2,]);
zmed<-median(CEJ_spline[[a]][3,])

plot3d(CEJ_spline[[a]],type="l",xlab="", ylab="", zlab="",aspect =T,box=F,axes=F,xlim=c(xmed-
10,xmed+10),ylim=c(ymed-10,ymed+10),zlim=c(zmed-10,zmed+10),col="gray")

points3d(eq_CEJ[[a]])

lines3d(EDJ_spline_1[[a]],col="orange");points3d(eq_EDJ1[[a]])

texts3d(c(EDJ_spline_1[[a]][as.integer(length(EDJ_spline_1[[a]][1,])/2),]),texts = "EDJ 1",font=2)

lines3d(EDJ_spline_2[[a]],col="red");points3d(eq_EDJ2[[a]])

texts3d(c(EDJ_spline_2[[a]][as.integer(length(EDJ_spline_2[[a]][1,])/2),]),texts = "EDJ 2",font=2)

lines3d(EDJ_spline_3[[a]],col="blue");points3d(eq_EDJ3[[a]])

texts3d(c(EDJ_spline_3[[a]][as.integer(length(EDJ_spline_3[[a]][1,])/2),]),texts = "EDJ 3",font=2)

lines3d(EDJ_spline_4[[a]],col="green");points3d(eq_EDJ4[[a]])

```

```

texts3d(c(EDJ_spline_4[[a]][as.integer(length(EDJ_spline_4[[a]][,1])/2)],),texts = "EDJ 4",font=2)
spheres3d(datamat_EDJ_m[[a]],radius=0.05)}

# Load filled in template
classifierraw <-read.table(paste("xixi_M2_labels_CEJ_C6.txt",sep="_"),header=TRUE)
keep<-classifierraw$Exclude!="ex"
classifier<-classifierraw[keep,]

gp <- as.factor(paste(classifier$Class1))
dimnames(NewCoordsArray)[[3]] <- classifierraw$Name
SubCoordsArray<-NewCoordsArray[,keep]

fix<-c(1,(EDJ1+2),(EDJ1+EDJ2+3),(EDJ1+EDJ2+EDJ3+4))
slid<-c(1:length(SubCoordsArray[,1,1]))[-c(fix)]
curve1<-c(1:(EDJ1+2))
curve2<-c((EDJ1+2):(EDJ1+EDJ2+3))
curve3<-c((EDJ1+EDJ2+3):(EDJ1+EDJ2+EDJ3+4))
curve4<-c((EDJ1+EDJ2+EDJ3+4):(EDJ1+EDJ2+EDJ3+EDJ4+4),1)
curve5<-c((EDJ1+EDJ2+EDJ3+EDJ4+5):(EDJ1+EDJ2+EDJ3+EDJ4+CEJ+5),(EDJ1+EDJ2+EDJ3+EDJ4+5))
curves<-list(curve1,curve2,curve3,curve4,curve5)

### dropping landmarks
a<-11;clear3d("shapes"); xmed<-median(SubCoordsArray[,a][,1]); ymed<-
median(SubCoordsArray[,a][,2]); zmed<-median(SubCoordsArray[,a][,3])
plot3d(SubCoordsArray[curves[[5]],a),xlim=c(xmed-10,xmed+10),ylim=c(ymed-
10,ymed+10),zlim=c(zmed-10,zmed+10),aspect
=T,col="gray",type="l",xlab="",ylab="",zlab="",box=F,axes=F)
lines3d(SubCoordsArray[c(curves[[1]],curves[[2]],curves[[3]],curves[[4]]),a,col="gray")
texts3d(SubCoordsArray[,a],texts = c(1:length(SubCoordsArray[,a][,1])),font=2)

DROPLMs<-FALSE
if (DROPLMs==TRUE) {

```

```

todrop<- c(27:30,42:45)
total<-c(1:length(SubCoordsArray[,a][,1]))
tokeep<-total[-todrop]
} else {
  tokeep<-c(1:length(SubCoordsArray[,a][,1]))
}

### sliding and procrustes
include_size<-FALSE

Proc<-procSym(dataarray=SubCoordsArray,SMvector=slid,outlines=curves,iterations =
2,stepsize=0.5,use.lm=tokeep,center.part=F,sizeshape=include_size)

# sliding figure
a<-11;clear3d("shapes"); xmed<-median(CEJ_spline[[a]][,1]); ymed<-median(CEJ_spline[[a]][,2]);
zmed<-median(CEJ_spline[[a]][,3])

plot3d(CEJ_spline[[a]],type="l",xlab="", ylab="", zlab="",aspect =T,box=F,axes=F,xlim=c(xmed-
10,xmed+10),ylim=c(ymed-10,ymed+10),zlim=c(zmed-10,zmed+10),col="gray")

lines3d(rbind(EDJ_spline_1[[a]],EDJ_spline_2[[a]],EDJ_spline_3[[a]],EDJ_spline_4[[a]]),col="gray");
spheres3d(datamat_EDJ_m[[a]],radius=0.1)
pch3d(Proc$dataslide[,a],pch=19,cex=0.05,col="red")
pch3d(SubCoordsArray[,a],pch=19,cex=0.05,col="black")
n<-length(SubCoordsArray[,1,a])
X <- rbind(SubCoordsArray[,a],Proc$dataslide[,a])
OX <- X[as.vector(rbind(1:n, n + 1:n)), ]
try(arrows3d(OX,scale=c(1,1,1)),silent=T)

# compare specimens
as.matrix(classifier$Name)
specimens<-c(1,2,3,4,5,6,7,8,9,10,11)

```



```

clear3d("shapes");xmed<-median(Proc$rotated[,1,specimens[1]]); ymed<-
median(Proc$rotated[,2,specimens[1]]); zmed<-median(Proc$rotated[,3,specimens[1]]);

plot3d(Proc$rotated[,specimens[1]],type="n",xlab="", ylab="", zlab="",aspect
=T,box=F,axes=F,xlim=c(xmed-0.4,xmed+0.4),ylim=c(ymed-0.4,ymed+0.4),zlim=c(zmed-
0.4,zmed+0.4),col="red")

for(i in 1:length(specimens)){

  lines3d(Proc$rotated[c(curves[[1]],curves[[2]],curves[[3]],curves[[4]]),,specimens[i],col=farbe[i])

  lines3d(Proc$rotated[curves[[5]],,specimens[i],col=farbe[i])

  spheres3d(Proc$rotated[fix,,specimens[i]],radius=0.003, col=farbe[i])

}

```

```
# compare group means
```

```

cbind(levels(classifier$Class1),farbe[c(1:length(levels(classifier$Class1)))]))
groups<-c(1,2,3,4,5,6,7,8,9,10,11)

```

```

plot3d(Proc$rotated[,1],type="n",xlab="", ylab="", zlab="",aspect =T,box=F,axes=F,xlim=c(xmed-
0.4,xmed+0.4),ylim=c(ymed-0.4,ymed+0.4),zlim=c(zmed-0.4,zmed+0.4),col="red")

```

```

for(i in 1:length(groups)){

  sub<-gp==levels(gp)[groups[i]]

  X<-Proc$rotated[,1,sub]

  Y<-Proc$rotated[,2,sub]

  Z<-Proc$rotated[,3,sub]

  mean<-cbind(apply(X,1,mean),apply(Y,1,mean),apply(Z,1,mean))

  lines3d(mean[c(curves[[1]],curves[[2]],curves[[3]],curves[[4]]),,col=farbe[groups[i]],lwd=2)

  lines3d(mean[curves[[5]],,],col=farbe[groups[i]],lwd=2)

  spheres3d(mean[fix,,],radius=0.003, col=farbe[groups[i]])

}

```

```
### 2D PCA
```

```

plot(cbind(Proc$PCscores[,1],Proc$PCscores[,2]),xlim=c(-0.15,0.15),ylim=c(-
0.15,0.15),col=farbe[gp],pch=19,asp=1,cex=1,xlab="PC 1",ylab="PC 2",main=paste("PCA",sep=" "))

```

```

for(a in 1:length(levels(gp))){

  sub<-gp==levels(gp)[a]

```

```

tr <- NULL

try(tr<-tri.mesh(x=Proc$PCscores[sub,1],y=Proc$PCscores[sub,2],duplicate = "error"))

if(!is.null(tr)){
  convex.hull(tr,plot.it=TRUE,col=farbe[a],add=TRUE,lwd=1,lty=1)}
}

text(Proc$PCscores[,c(1,2)],label=classifier$Name,col=farbe[gp],pos=c(1,2),cex=0.6,offset=0.5)

### 3D PCA

clear3d("shapes");plot.range<-
1.02*max(abs(cbind(Proc$PCscores[,1],Proc$PCscores[,2],Proc$PCscores[,3])))

plot3d(cbind(Proc$PCscores[,1],Proc$PCscores[,2],Proc$PCscores[,3]),type="p",size=10,col=farbe[gp
],xlab="", ylab="", zlab="",aspect =T,axes=T,xlim=c(-plot.range,plot.range),ylim=c(-
plot.range,plot.range),zlim=c(-plot.range,plot.range))

for(a in 1:length(levels(gp))){
  sub<-gp==levels(gp)[a]
  PCsub<-cbind(Proc$PCscores[sub,1],Proc$PCscores[sub,2],Proc$PCscores[sub,3])
  if(length(PCsub[,1])>3){
    hull<-convhulln(PCsub)
    for(b in 1:length(hull[,1])){
      sub1<-PCsub[hull[b,],]
      triangles3d(sub1[,1],sub1[,2],sub1[,3],col=farbe[a],lit=F,alpha=0.1,fog=T)
    }
  } else if(length(PCsub[,1])==3){
    triangles3d(PCsub[,1],PCsub[,2],PCsub[,3],col=farbe[a],lit=F,alpha=0.1,fog=T)
  } else if(length(PCsub[,1])==2){
    lines3d(PCsub,col=farbe[a])
  }
}

## Centroid size boxplot

cs<- cbind(classifier,log(Proc$size))

```

```
boxplot(cs$log(Proc$size) ~ cs$Class1)
```

```
##REGENERATE PCA ON LM SUBSET
```

```
procrot <- orp(Proc$rotated[tokeep,,], mshape = Proc$mshape[tokeep,])
```

```
Symtan <- procrot
```

```
Symtan <- sweep(Symtan, 1:2, Proc$mshape[tokeep,])
```

```
tan <- vecx(Symtan)
```

```
princ <- prcompfast(tan)
```

```
values <- 0
```

```
eigv <- princ$sdev^2
```

```
values <- eigv[which(eigv > 1e-14)]
```

```
lv <- length(values)
```

```
PCs <- princ$rotation[, 1:lv]
```

```
PCscore_sym <- as.matrix(princ$x[, 1:lv])
```

```
Proc$PCscores_drop <- PCscore_sym
```

```
# save(Proc,file=paste("Procrustes_results_",position,".RData",sep=""))
```

```
### 2D PCA
```

```
plot.range <- max(abs(Proc$PCscores_drop))
```

```
plot(cbind(Proc$PCscores_drop[,1],Proc$PCscores_drop[,2]),xlim=c(-plot.range,plot.range),ylim=c(-plot.range,plot.range),col=farbe[gp],pch=19,asp=1,cex=1,xlab="PC 1",ylab="PC 2",main=paste("PCA",position,sep=" "))
```

```
for(a in 1:length(levels(gp))){
```

```
  sub <- gp == levels(gp)[a]
```

```
  tr <- NULL
```

```
  try(tr <- tri.mesh(x=Proc$PCscores_drop[sub,1],y=Proc$PCscores_drop[sub,2],duplicate = "error"))
```

```
  if(!is.null(tr)){
```

```
    convex.hull(tr,plot.it=TRUE,col=farbe[a],add=TRUE,lwd=1,lty=1)}
```

```
}
```

```
text(Proc$PCscores_drop[,c(1,2)],label=classifier$Name,col=farbe[gp],pos=c(1,2),cex=0.6,offset=0.5)
```

```
### 3D PCA
```

```
clear3d("shapes");plot.range<-  
1.05*max(abs(cbind(Proc$PCscores_drop[,1],Proc$PCscores_drop[,2],Proc$PCscores_drop[,3])))  
plot3d(cbind(Proc$PCscores_drop[,1],Proc$PCscores_drop[,2],Proc$PCscores_drop[,3]),type="p",siz  
e=10,col=farbe[gp],xlab="", ylab="", zlab="",aspect =T,axes=T,xlim=c(-plot.range,plot.range),ylim=c(-  
plot.range,plot.range),zlim=c(-plot.range,plot.range))  
texts3d(cbind(Proc$PCscores_drop[,1],Proc$PCscores_drop[,2],Proc$PCscores_drop[,3]),texts =  
rownames(Proc$PCscores),font=1,adj=1,cex=0.7)
```

```
for(a in 1:length(levels(gp))){  
  sub<-gp==levels(gp)[a]  
  PCsub<-cbind(Proc$PCscores_drop[sub,1],Proc$PCscores_drop[sub,2],Proc$PCscores_drop[sub,3])  
  if(length(PCsub[,1])>3){  
    hull<-convhulln(PCsub)  
    for(b in 1:length(hull[,1])){  
      sub1<-PCsub[hull[b,],]  
      triangles3d(sub1[,1],sub1[,2],sub1[,3],col=farbe[a],lit=F,alpha=0.1,fog=T)  
    }  
  } else if(length(PCsub[,1])==3){  
    triangles3d(PCsub[,1],PCsub[,2],PCsub[,3],col=farbe[a],lit=F,alpha=0.1,fog=T)  
  } else if(length(PCsub[,1])==2){  
    lines3d(PCsub,col=farbe[a])  
  }  
}
```

```
pos<-pcaplot3d(Proc, pcshow = c(1,2,3), mag = 2)
```

```
neg<-pcaplot3d(Proc, pcshow = c(1,2,3), mag = -2)
```

```
PC<-2
```

```
#plot positive and negative together
```

```
clear3d("shapes");xmed<-median(pos[,PC][,1]); ymed<-median(pos[,PC][,2]); zmed<-  
median(pos[,PC][,3])
```

```
plot3d(rbind(pos[c(1,2,3,4)],PC),pos[1,PC],type="l",xlab="",  
ylab="", zlab="",aspect =T,box=F,axes=F,xlim=c(xmed-0.4,xmed+0.4),ylim=c(ymed-  
0.4,ymed+0.4),zlim=c(zmed-0.4,zmed+0.4))
```

```
lines3d(pos[5,PC],col="black")
```

```
spheres3d(pos[fix,PC],radius=0.005)
```

```
lines3d(rbind(neg[c(1,2,3,4)],PC),pos[1,PC],col="gray")
```

```
lines3d(neg[5,PC],col="gray")
```

```
spheres3d(neg[fix,PC],radius=0.005,col="gray")
```